UNIVERSITY OF CALIFORNIA
SANTA CRUZ

STRUCTURAL AND IMMUNOGENIC STUDIES ON THE RESPIRATORY SYNCYITAL VIRUS G GLYCOPROTEIN

A dissertation submitted in partial satisfaction
of the requirements for the degree of

DOCTOR OF PHILOSOPHY

in

MOLECULAR, CELL, AND DEVELOPMENTAL BIOLOGY

by

Maria Guadalupe Juarez

September 2024

The Dissertation of Maria Guadalupe Juarez is approved:

_____
Professor Rebecca DuBois, thesis advisor

_____
Professor David Boyd

_____
Professor Sarah Loerch

_____
Peter F. Biehl
Vice Provost and Dean of Graduate Students

Table of Contents

List of Figures viii

List of Tables x

Abstract xi

Acknowledgements xiii

Significance xiv

Chapter 1 Immunogenicity and protective efficacy of an RSV G S177Q central conserved domain nanoparticle vaccine 1

1.1 Abstract 1

1.2 Introduction 2

1.3.1 Cells and virus 6

1.3.2 Nanoparticle construction 6

1.3.3 Mice 7

1.3.4 Serum ELISA 8

1.3.5 Microneutralization assay 8

1.3.6 CX3C-CX3CR1 blocking assay 9

1.3.7 Plaque assays 10

1.3.8 BAL cell phenotyping 10

1.3.9 Intracellular cytokine staining 11

1.3.10 Statistics 12

1.4 Results 12

1.4.1 Nanoparticle vaccine constructs 12

1.4.2 RSV NP vaccines induce Anti-RSV Abs 15

1.3.3 CX3C-CX3CR1 blocking 18

1.3.4 RSV neutralization 21

1.3.5 Immune response to RSV challenge 23

1.5 Discussion 24

1.6 Ethics statement 29

1.7 Author contributions 29

1.8 Funding 30

1.9 Acknowledgments 30

1.10 Conflict of interest 30

1.11 Publisher's note 30

1.12 Supplementary material 30

1.13 References 31

Chapter 2 Layer-by-Layer Microparticle Vaccines Containing Altered Sequences of the Central Conserved Domain of the RSV G Protein Induce Improved Immune Responses 39

2.1 Abstract 39

2.2 Introduction 39

2.3 Materials and Methods 45

2.3.1 Cells and viruses 45

2.3.2 Microparticle (MP) construction 45

2.3.3 ELISA analysis of MPs with mAb 2D10 45

2.3.4 Mice 46

2.3.5 ELISA 47

2.3.6 Virus neutralization 47

2.3.7 RSV plaque assays 48

2.3.8 Statistics 49

2.4 Results 49

2.4.1 S177Q vaccination improves immunogenicity and neutralization 49

2.4.2 Recall of anti-RSV antibody responses after RSV challenge 54

2.4.3 Vaccination reduces the lung viral load. 57

2.5.6 Vaccination modifies the cytokine and chemokine responses to RSV challenge 59

2.5 Discussion 61

2.6 Conflict of Interest 63

2.7 Author Contributions 63

2.8 Funding 64

2.9 Acknowledgment 64

2.10 Supplementary 64

2.11 References 66

Chapter 3 Structures of a Respiratory Syncytial Virus G Bound to Broadly-Reactive, High-Affinity Antibodies Reveal Novel Epitopes and Vaccine Insights 71

3.1 Abstract **71**

3.2 Author Summary **72**

3.3 Introduction **73**

3.4 Results **77**

3.4.1 mAb 1G1, 2B11, and 1G8 bind RSV G with high affinity 77

3.4.2 High-resolution structures of Fabs 1G1, 1G8, and 2B11 bound to RSV G CCD 78

3.4.3 Antibodies bound to similar RSV G CCD conformations and epitope amino acids utilize distinct molecular interactions 84

3.4.4 RSV G CCD has to two non-overlapping antigenic sites 86

3.4.5 Anti-RSV G antibodies have modest divergence from genomic precursors 88

3.5 Discussion **90**

3.6 Materials and Methods **93**

3.6.1 Production of bnmAbs 1G1, 3D3, 1G8, 2B11, 2D10, and 3G12 93

3.6.2 Antibody Germline Gene Sequence Identity Analysis 95

3.6.3 Expression and Purification of Fabs 3D3, 2D10, 1G1, 1G8, and 2B11 95

3.6.4 Expression and Purification of RSV Gecto 96

3.6.5 Binding Kinetics 98

3.6.6 Epitope Binning 99

3.6.7 Expression and Purification of RSV G157-197 100

3.6.8 Production and Structure Determination of Fab 1G1-RSV G157-197 Complex 102

3.6.9 Production and Structure Determination of Fab 1G8-RSV G157-197 Complex 103

3.6.10 Production and Structure Determination of Fab 2B11-RSV G157-197 Complex 104

3.6.11 Production and CryoEM Grid preparation of Fab 3D3-RSV Gecto-Fab 2D10 Complex 105

3.6.12 CryoEM Data Processing 106

3.7 Acknowledgements 106

3.8 References 107

Chapter 4 Implications for Respiratory Syncytial Virus G glycoprotein-based vaccines and monoclonal antibody prophylaxis: A Brief Review. 111

4.1 Review 111

4.2 References 119

Appendix 1 Crystal hits that yielded datasets for deposited structures..... 125

List of Figures

Figure 1.1 Production and Characterization of RSV G CCD coated nanoparticle immunogens 14

Figure 1.2 RSV G protein NP Vaccine Immunogenicity. 16

Figure 1.3 Serum Ab responses post-RSV challenge. 17

Figure 1.4 Ab Responses. 20

Figure 1.5 Lung Viral Titers. 23

Figure 2.1 mAb 2D10 binds its conformational epitope on WT, and S177Q MP constructs. 50

Figure 2.2 MP constructs are immunogenic, and S177Q improves immunogenicity. 52

Figure 2.3 S177Q induces neutralizing antibodies. 54

Figure 2.4 MP induces significant antibody recall responses during the RSV challenge. 56

Figure 2.5 MP vaccination reduces lung RSV titers. 59

Figure 2.6 Cytokine responses following RSV infection. 60

Figure 2.7 Antisera binding to RSV B. 64

Figure 2.8 25-plex cytokine/chemokine concentrations in the BALF of challenged animals. 66

Figure 3.1 Biolayer interferometry binding studies show that mAbs 1G1, 1G8, and 2B11 bind to RSV Gecto with high affinity. 78

Figure 3.2 Crystal structures of antibody - RSV G CCD complexes reveal novel conformational epitopes. 81

Figure 3.3 Comparative structural analyses of mAbs bound to similar RSV G CCD conformations reveal distinct interactions. 83

Figure 3.4 Broadly-reactive human mAbs use distinct interactions to bind to RSV G amino acids that are conserved across thousands of RSV genotypes 86

Figure 3.5 Biolayer interferometry epitope binning and cryo-EM reveal two non-overlapping antigenic sites on the RSV G CCD. 88

Figure 5.1 Pictures of Crystal Hits 125

List of Tables

Table 1.1 Nanoparticles. 7

Table 1.2 BAL Leukocytes. 24

Table 2.1 Microparticle vaccine peptides 45

Table 3.1 Data Collection and Refinement Statistics 82

Table 3.2 Germline Gene Sequence Identity 90

Abstract

Structural and Immunogenic Studies on the Respiratory Syncytial Virus G Glycoprotein

Maria Guadalupe Juarez

Respiratory syncytial virus (RSV) is a leading cause of bronchiolitis and pneumonia worldwide especially in infants, young children, immunocompromised individuals, and the elderly. In the United States alone, the economic burden to treat or prevent severe respiratory disease caused by RSV estimated 6.6 billion dollars in a study conducted with financial reports from 2021. Since its discovery in the late 1950's, the question of how to elicit a protective immunogenic response against RSV remained unclear, that is, until 2023 when the first FDA approved vaccines became commercially available. These vaccines serve to prevent severe RSV-associated respiratory disease with endpoints involving major economic and quality of life burdens like hospital visits. However, studies have shown that correlates of protection involve antibody responses against two major surface glycoproteins that are required for efficient viral entry: RSV F and RSV G. Currently, all commercially available vaccines and prophylactic monoclonal antibodies use RSV F as their antigenic target. To investigate RSV G as an antigenic target for protective immune responses, commercially unavailable correlates of protection, I develop structure guided RSV G based vaccine designs and determine novel RSV G conformational epitopes recognized by broadly reactive monoclonal antibodies. I begin by discussing our work to address the issue of RSV G's poor immunogenicity and its association to the

apparent immune modulating activity seen in natural infection and vaccination using a nanoparticle vaccine platform where my role was the design, production, and characterization of the vaccine constructs. Following this, I describe a synthetically produced microparticle vaccine design based on layer-by-layer technology where my role was to determine its reactivity with an antibody that relies heavily on correct CX3C folding to recognize the CCD. Finally, I present our structural studies involving five broadly reactive antibodies in complex with the CCD where we characterize three novel conformational epitopes and reveal two non-competing antigenic sites. This work serves as a blueprint for the generation of structure guided mutagenesis, structure guided vaccine design, and antibody therapeutic or prophylactic strategies to protect from and prevent RSV-associated respiratory disease.

Acknowledgements

I want to thank my advisor, Rebecca DuBois, for taking me on as her graduate student despite the challenges that might come with mentoring a young single mother. I hope I have shown endless gratitude for seeing something in me and choosing to invest in me. Because of her, I accomplished things that used to be a part of my wildest dreams. I show my utmost gratitude to my thesis committee, David Boyd and Sarah Loerch, for taking on this responsibility and helping me grow as a structural virologist. Thank you to our collaborators at Trellis Bioscience and the Tripp lab at University of Georgia for both laying the foundation of my work and for taking it an extra step with mouse models. I'd like to thank everyone in my lab for laughing at all my silly jokes. For their endless mentorship and guidance, I want to thank John Dziamanski and Sara O'Rourke. I appreciate your patience with me and your willingness to be there for me in the good times and the bad times. To my best friend, Sarah, I hope we became best friends in every other alternative universe. You made me stronger as a person and as a scientist and listened to all my problems endlessly, I don't know if I deserve this type of friendship but I will hold onto it forever! Thank you to my family for believing in me and especially my sister Kaylee for blazing a trail for me to follow, you amaze me. Thank you to my mom for taking all the risks to be in the U.S., I know it wasn't easy and I am grateful for your sacrifices. To my son Ezio, I am so glad things happened the way they did. I truly believe I would not be here without you. I hope I can start making it up to you for all the time I gave to school that should have been time spent with you.

Significance

Since its discovery in the late 1950's, RSV has become one the largest healthcare burdens in the world accounting for a 6.6 billion dollar economic burden in the United States alone. Vulnerable populations include infants, children under age five, the elderly, and immunocompromised individuals. Naïve or weakened immune systems of these populations has contributed towards RSV's successful infectivity and transmission. The first prophylactic to become commercially available was a monoclonal antibody, Palivizumab (Synagis), that targets one of two major surface glycoproteins required for efficient viral entry, RSV F. RSV F is a type I integral membrane protein that undergoes a series of conformational changes to mediate fusion to human airway epithelial cell membranes. After 60 years in the making, the first round of FDA approved vaccines became commercially available in 2023, all targeting the same antigen, RSV F. Discoveries paramount to the development of these highly effective vaccines were identifying correlates of protection, specifically, monoclonal antibodies (mAbs) targeting RSV F in its prefusion form and then using structure guided vaccine design to stabilize RSV F in this prefusion state. Vaccines using this design are up to 90% effective at reducing severe lower respiratory disease and are available to both elderly populations and pregnant mothers. However, studies have shown evidence for circulating escape mutants to monoclonal antibody therapies that target RSV F, highlighting the need to consider all correlates of protection in passive immunization and vaccination programs. Anti-G mAbs are associated to lower disease severity even while being present at $1/30^{th}$ the abundance to those that

target RSV F in a natural infection. Additionally, at least five broadly protective antibodies have been structurally characterized in complex with a highly conserved region of RSV G known as the central conserved domain (CCD). However, it is well known that RSV G is associated to immune modulating activity characterized by a dampened Th1 and enhanced Th2 cytokine profile. The result is suppression of anti-viral activity, lung inflammation, and mucus overproduction. Anti-RSV G antibodies have been shown to reduce these effects by blocking RSV G's interaction with its receptor, CX3CR1, expressed on a variety of myeloid cells. The receptor binding domain has yet to be structurally characterized, making a clear pathway or mechanism difficult to define. In this thesis, I aimed to use what we know about the epitopes recognized by protective monoclonal antibodies to generate mutations in the CCD that might abrogate CX3CR1 binding but maintain antigenicity. Thus, creating a safe and immunogenic vaccine. Another question we addressed is that of improving RSV G's poor immunogenicity using what we know about stimulating robust B-cell responses through multimerized antigenic designs.

In my first chapter, I describe the design, expression, and characterization a nanoparticle bearing 60 CCD antigens and results following mouse vaccination studies. Previous work for our lab included three structural studies revealing conformational epitopes on the CCD and served to establish new boundaries for its N- and C-terminal ends. Additionally, it served as a preliminary blueprint used in structure guided mutagenesis to produce a single amino acid substitution at position 177 (serine to glutamine) that showed increased safety profiles in mice, presumably

by introducing a bulky amino acid in the CX3CR1 binding domain. This mutant was used in our nanoparticle design due to its ability to properly fold during expression and purification and maintain its flexibility and conformational epitopes. Thus, we combined these two important discoveries to not only generate a safe vaccine, but to use the newly established N- and C-terminal boundaries (a 157-197) in hopes of optimizing the immune response towards a region that encompasses all known epitopes recognized by broadly reactive antibodies. It is well known that nanoparticle vaccine designs can increase immunogenic responses as seen in Influenza, SARS-CoV2, and RSV. To control the expression of the nanoparticle platform independently of the CCD and conjugate them thereafter, we used a SpyTag/SpyCatcher system where SpyTag and SpyCatcher are proteins that form a spontaneous isopeptide bond when mixed. We used molecular cloning to fuse a SpyTag protein to the N-terminus of the CCD and a SpyCatcher protein that we fused to the C-terminus of a self-assembling 60-mer nanoparticle subunit, lumazine synthase. To confirm the formation of the isopeptide bond, we used a gel shift assay where we loaded either sample into different wells and the combined sample in a subsequent well. We also assessed self-assembly using negative stain cryo-EM and reconstructed 2D classes showing roughly 10 nm wide circular particles. Additionally, representative micrographs showed little heterogeneity. Results from mouse vaccination studies showed increased antibody titers compared to vehicle control and WT-CCD bearing nanoparticles. Sera from mice vaccinated with S177Q-CCD nanoparticles was also found to be

neutralizing in the presence of complement, highlighting the efficacy of focusing immune responses towards the CCD alone without the mucin-like domains.

A limitation from this study was that the nanoparticles had the tendency to aggregate, making it difficult to biochemically characterize its antigenicity. In chapter two, I describe a synthetically produced microparticle bearing CCD antigens fused to a poly-lysine tail. The positively charged tail is added as the last layer on the negatively charged microparticle surface. My role was to use an enzyme-linked immunosorbet assay (ELISA) to test its reactivity with a monoclonal antibody that recognizes a conformational epitope on the cysteine loop, mAb 2D10. In this assay, we saw reactivity across the same dilutions as WT RSV G^{ecto}, our positive control. Results from mouse vaccination studies revealed a more balanced Th1/Th2 response, a feature of reduced RSV G-induced immune modulating activity, in the S177Q microparticle vaccine group. Collectively, these vaccine studies serve as a proof-of-principle for multimerized vaccine designs and lay the foundation for future RSV-G based vaccines that elicit robust neutralizing antibody titers.

In my final chapter, I discuss structural studies involving five monoclonal antibodies in complex with RSV G CCD where we define three novel conformational epitopes and two non-competing antigenic sites. In these studies, we pulled mAb sequences from a panel of broadly reactive anti-RSV G antibodies discovered by our collaborators at Trellis Biosciences. Previous work in our lab structurally defined the first three from this panel. As mentioned previously, this worked served as a blueprint for structure guided mutagenesis to produce the S177Q mutant. To expand this

blueprint and generate newer generations of RSV G CCD mutants, we examined three additional antibodies from the panel and found that each antibody recognizes unique conformational epitopes. We described the unique molecular interactions that each antibody uses to elicit similar conformations. Interestingly, some antibodies have the tendency to from extensive hydrogen bond networks with the backbone of the CCD while other antibodies interact with the same amino acid position in a residue-residue fashion. This is important because it opens the possibility that the panel might collectively resist mutations in RSV G if subjected to selective pressure. Highlighting the importance of a large antibody panel that is diverse. We also used an epitope binning assay to test two hypothesized antigenic sites on the CCD in real time and found that mAb 2D10 binds non-competitively to all other mAbs. Using cryoEM, we structurally visualize two non-competing antibodies, mAb 2D10 and mAb 3D3, bound to RSV G^{ecto} simultaneously for the first time. A feature we think might have an implication for synergistic neutralization. We wrapped up this work by assessing the genomic precursors for structurally characterized anti-G mAbs and found that they come from diverse lineages, explaining the nuances in their paratopes, and high sequence identities that might make natural stimulation of anti-G mAbs feasible. Ultimately, we think this work serves as a more cohesive blueprint for the development of RSV G based vaccines and strategies for prophylactic/therapeutic monoclonal antibody treatment.

Chapter 1 Immunogenicity and protective efficacy of an RSV G S177Q central conserved domain nanoparticle vaccine

Harrison C. Bergeron[1], Jackelyn Murray[1], Maria G. Juarez[2], Samuel J. Nangle[2], Rebecca M. DuBois[2], and Ralph A. Tripp[1*]
[1]Department of Infectious Diseases, College of Veterinary Medicine, University of Georgia, Athens, GA
[2] Department of Biomolecular Engineering, University of California Santa Cruz, Santa Cruz, CA
* Correspondence: Ralph A Tripp, PhD; ratripp@uga.edu

Preface
This publication was accepted in June 2023, however, it was written and submitted before the first wave of RSV F vaccines were FDA approved (May-June 2023). Therefore, information in this chapter regarding RSV vaccines does not reflect current FDA approved prophylactics.

1.1 Abstract

Introduction: Respiratory syncytial virus (RSV) can cause lower respiratory tract disease in infants and elderly populations. Despite decades of research, there remains no safe and approved RSV vaccine. Previously, we showed that an RSV G glycoprotein subunit vaccine candidate with a single point mutation within the central conserved domain (CCD), i.e. S177Q, considerably improved immunogenicity. Here, we examine the development of nanoparticle (NP) vaccines having either an RSV G protein CCD with wild-type sequence (NPWT) or an S177Q mutation (NP-S177Q). The NP vaccine immunogens were adjuvanted with monophosphoryl lipid A (MPLA), a TLR4 agonist to improve Th1- type responses. BALB/c mice were primed with 10 μg of NP-WT vaccine, NPS177Q, or vehicle, rested, and then boosted with a high (25 μg) or low (10 μg) dose of the NP-WT or NP-S177Q homologous candidate and subsequently challenged with RSV A2, a well-characterized RSV laboratory

strain. The results showed that mice boosted with NP-S177Q developed superior immunogenicity and neutralizing antibodies compared to NP-WT boosting. IgG from either NP-S177Q or NP-WT vaccinated mice did not interfere with fractalkine (CX3CL1) binding to CX3CR1 and effectively blocked G protein CX3C-CX3CR1 binding. Both NP-WT and NP-S177Q vaccination induced similar neutralizing antibodies to RSV in challenged mice compared to vehicle control. NP-S177Q boosting improved correlates of protection including reduced BAL cell infiltration following RSV challenge. However, the NP vaccine platform will require improvement due to the poor solubility and the unexpectedly weaker Th1-type IgG2a response. The results from this study support further NP-S177Q vaccine candidate development.

1.2 Introduction

RSV is the leading cause of lower respiratory tract disease in infants and the elderly (1, 2). By age 2, nearly all infants have experienced RSV infection (3). RSV typically causes a mild upper respiratory tract infection, however severe respiratory disease presenting as bronchiolitis, pneumonia, and wheezing may require hospitalization (4). Infants <12 months of age are at the greatest risk for hospitalization (5). While preexisting conditions including preterm birth and cardiopulmonary abnormalities significantly increase susceptibility to RSV disease (6) previously healthy infants are also at risk for hospitalization (5, 7). Synagis® (palivizumab) is an antibody against the RSV F protein that helps decrease the risk of serious lung infections and is restricted for use in at-risk infants (8). Its use in healthy infants is excluded thus

countermeasures are currently unavailable in the United States (9–11). RSV infection may predispose infected infants to asthma and/or chronic wheezing later in life (12). Further, RSV infection does not induce robust antibody responses as reinfections are common (13). Maternal antibodies (Abs) provide protection against RSV, however, this protection wanes shortly after birth and the level of protection may vary (14, 15). Gaps remain in understanding the mechanisms of RSV disease, but it is understood that severe disease is linked to immunopathology (16). Thus, RSV vaccines that prevent immune-mediated pathology are needed to prevent severe RSV disease (17). RSV has two major surface proteins, i.e. the F and G proteins. The F protein is indispensable for virus infection and is the antigen targeted by palivizumab and nirsevimab therapeutic antibodies (18, 19). While therapeutic anti-F protein antibodies (Abs) and serum anti-F protein Abs induced by RSV vaccine candidates are neutralizing and may provide some protection from disease (20), these Abs are insufficient at blocking RSV disease linked to the RSV G protein (17, 21–23). The RSV G protein is a heavily glycosylated surface protein comprised of three domains, i.e. the cytoplasmic (CT), transmembrane (TM), and ectodomain (ecto) domains. Importantly, the G protein ectodomain contains a central conserved domain (CCD) and CX3C motif that are highly conserved among RSV subtypes and strains (24). CX3C is the attachment motif for CX3CR1, or fractalkine receptor, that is expressed on human airway epithelial cells (hAECs) and some immune cells (25–30). G protein CX3C binding to CX3CR1 has been shown to induce aberrant CX3CR1+ T cell trafficking, modify host miRNA profiles, dampen antibody maturation, reduce

antiviral cytokine and IFN responses, and potentiate Th2-type immune response during RSV infection (24, 31–37). Thus, the G protein affects RSV attachment and modifies host immune response to infection, and Abs that block the CX3C motif may prevent CX3C-mediated attachment and immune dysregulation (38, 39).

Anti-G protein Abs targeting the CCD and/or CX3C are protective, reduce Th2-type immune responses, increase antiviral IFN and T cell responses, and prevent lung pathology but the G protein itself is poorly immunogenic (40–43). The G protein has been implicated in vaccine-enhanced respiratory disease as early RSV vaccine trials with formalin-inactivated RSV (FI-RSV) resulted in vaccine-enhanced disease and two infant deaths following natural infection of FI-RSV vaccinees (44–46). Several studies have shown that G protein may prime for enhanced RSV disease (23, 32, 47, 48). Importantly, ablation of the CX3C motif to CX4C eliminates vaccine-enhanced disease showing that proper modifications to G protein can induce a protective response following vaccination while preventing disease (49, 50). Recently, we showed that the G protein with a single point mutation, i.e., S177Q, improved immunogenicity compared to wild-type G protein or CX4C G protein vaccination (51). A key finding was that the S177Q mutant, similar to CX4C, did not mediate CX3CR1+ immune cell trafficking illuminating how the S177Q mutant may resist the development of enhanced disease (52). Notably, unlike the CX4C mutant, the S177Q mutant was found to be structurally intact and display conformational epitopes for high-affinity anti-G Abs (52).

In this study, we made and evaluated nanoparticle (NP) immunogens displaying the CCD of the RSV G protein. We hypothesized that the self-assembling NPs would improve vaccine immunogenicity by presenting multiple copies of CCD antigens in a repetitive manner that is similar to natural infection. NPs displaying wild-type CCD (NP-WT), CCD containing the S177Q mutation (NP-S177Q), or no antigen (vehicle control) were used to immunize mice, followed by RSV challenge. NP-WT and NP-S177Q vaccine candidates were adjuvanted with MPLA to induce a Th1-type response (53, 54). Mice were intramuscularly (i.m.) primed with 10 μg of vehicle, NP-WT, or NP-S177Q vaccines and subsequently boosted with either 10 μg (low dose) or 25 μg (high dose) of the homologous NP vaccine candidates. Subsequently, mice were intranasally (i.n.) challenged with 106 PFU RSV A2, and on day 5 post-challenge, lung viral loads and immune correlates were determined.

The results show the NP-S177Q vaccination induced greater immunogenicity compared to NP-WT or vehicle control. While both NP-WT and NP-S177Q vaccination reduced lung viral titers, NP-S177Q vaccination led to improved viral neutralization compared to NP-WT. IgG from NP-WT or NP-S177Q vaccinated mice did not interfere with FKN binding to CX3CR1, and the IgG blocked G protein binding to CX3CR1. Importantly, NP-S177Q vaccination was able to significantly reduce BAL cell infiltration following the RSV challenge compared to vehicle-vaccinated mice. This study shows that RSV G protein CCD nanoparticle vaccines have promise in the development of precision RSV vaccines, however as expected with novel vaccine development, will require optimization such as improving vaccine

solubility. However, the findings of this study support improved NP platforms in developing the next generation of RSV G protein vaccines expressing the S177Q mutant.

1.3 Methods

1.3.1 Cells and virus

Vero E6 (CRL-1586), A549 (CCL-185), HEp-2 (CCL-23), and HEK-293 (CRL-1573) (all from American Type Culture Collection (ATCC), Manassas, VA) were maintained in 10% fetal bovine serum (FBS)/DMEM (Hyclone, Logan, UT). CX3CR1.293 cells (>90% CX3CR1+) were maintained in selection media (10% FBS/DMEM + 1.0 μg/mL puromycin) as previously described (51). RSV A2 and B1 were propagated in HEp-2 cells as described (55). RSV A2 expressing green fluorescent protein (GFP) was propagated in HEp-2 cells as described (56).

1.3.2 Nanoparticle construction

Nanoparticle (NP) vaccines were constructed using self-assembling Aquifex aeolicus lumazine synthase (57) fused to a next-generation SpyCatcher domain (54, 58, 59). To generate the NPs, a pET28a plasmid encoding an N-terminal 6-histidine tag, the Aquifex aeolicus lumazine synthase protein (UniProtKB entry O66529), and SpyCatcher003 (58) (Table 1) was transformed into T7 Express E. coli and recombinant LumazineSynthase-SpyCatcher003 was expressed overnight at 18C. Cells were lysed by ultrasonication in wash buffer (10 mM Tris-Cl pH 8.0, 10 mM imidazole, 150 mM NaCl) with 1 mM MgCl2, protease inhibitors, benzonase, and DTT. E. coli lysates were clarified by centrifugation and 0.22 um filtered. LumazineSynthase-SpyCatcher003 was purified from clarified lysates by affinity

chromatography using a HisPur Nickel-NTA Resin and eluted using wash buffer with 250 mM imidazole. LumazineSynthase-SpyCatcher003 was dialyzed into PBS (pH 7.4) overnight at 4°C, resulting in empty vehicle control NPs. For negative stain imaging, LumazineSynthase-SpyCatcher003 protein was deposited onto glow-discharged, carbon-coated 400 mesh copper grids, stained with 2% (w/v) uranyl-formate, and viewed on a 200 kV FEI Glacios transmission electron microscope.

LS-NP (empty)	*6xHis*-Lumazine Synthase Nanoparticle-SpyCatcher	MGSS*HHHHHH*SSGLVPRGSHMQIYEGKLTAEGLRFGIVASRFNHALVDRLVEGAIDCIVRHGGREEDITLVRVPGSWEIPVAAGELARKE DIDAVIAIGVLIRGATPHFDYIASEVSKGLANLSLELRKPITFGVITADTLEQAIERAGTKHGNKGWEAALSAIEMANLFKSLRSGGSGGGG MVTTLSGLSGEQGPSGDMTTEEDSATHIKFSKRDEDGRELAGATMELRDSSGKTISTWISDGHVKDFYLYPGKYTFVETAAPDGYEVATP IEFTVNEDGQVTVDGEATEGDAHT
CCD-WT	***SpyTag***-CCD-*6xHis-tag*	M***RGVPHIVMVDAYKRYK***GSKPNNDFHFEVFNFVPCSICSNNPTCWAICKRIPNKKPGKK*HHHHHH*
CCD-S177Q	>**SpyTag**-CCD-S177**Q**-*6xHis-tag*	M**RGVPHIVMVDAYKRYK**GSKPNNDFHFEVFNFVPCSIC**Q**NNPTCWAICKRIPNKKPGKK*HHHHHH**

Nanoparticle construction of empty nanoparticle (LS-NP), CCD-WT (NP-WT), and CCD-S177Q (NP-S177Q); italicized = His-Tag, underline = lumazine synthase NP, CCD, or CCD-S117Q, capitalized normal = SpyCatcher003, bold = SpyTag003.

Table 1.1 Nanoparticles.

1.3.3 Mice

Female BALB/c mice (10-to-12-weeks old; Jackson Laboratories, Bar Harbor, ME) were housed in micro isolator cages with 12h light/dark cycle, and fed ad libitum. The mice received a priming dose of 10 µg NP-WT, NP-S177Q, or empty NPs. All vaccines were adjuvanted with 10 µg monophosphoryl Lipid A (MPLA; VacciGrade™ from S. Minnesota R595, InvivoGen, San Diego, CA), a TLR4 agonist, diluted in PBS. Similar to a related study that used using SpyCatcher multimerization of a SARS-CoV-2 spike vaccine candidate to induce a potent neutralizing antibody response at 21 days post-priming (62), vaccinated mice were boosted with either 10 µg or 25 µg of homologous vaccine or empty NPs and 10 µg MPLA diluted in PBS. Mice were i.m. vaccinated in the left and right and left quadriceps with 0.05

mL/quadriceps. Sera were collected on days 0, 14, 28, and 35 post-boosts. On day 21 post-boost, mice were i.n. anesthetized with Avertin (2, 2, 2-Tribromoethanol), and i.n. and challenged with 0.05 mL 10^6 PFU RSV A2 diluted in PBS. Mice were monitored daily and euthanized on day 5 pi. Sera, BAL, lungs, and spleen were collected and stored on ice during organ processing for assays described below.

1.3.4 Serum ELISA

Sera were evaluated for anti-RSV IgG levels as described (51). Briefly, high-binding ELISA plates (Corning, Corning, NY) were coated with 5 μg/mL RSV A2 or B1 lysate overnight at 4°C. The next day, wells were washed 3x with KPL wash buffer (1x KPL in distilled water (diH2O) (SeraCare, Milford, MA) and blocked with Blotto (5% non-fat dry milk) overnight at 4°C. Blotto was removed and sera (in 3-fold dilutions starting at 1:50) was diluted in Blotto and added to wells overnight at 4°C. Wells were washed 3x with KPL wash buffer and 2° goat-anti-mouse IgG-HRP (ThermoFisher, Waltham, MA), or secondary subtype IgG1 or IgG2a antibodies (Southern Biotech, Birmingham, AL) were added. Plates were incubated overnight at 4°C, washed 3x with KPL wash buffer, and developed with 1-Step™ Ultra 3,3',5,5'-tetramethylbenzidine (TMB; ThermoFisher) for 20 min, and stopped with Stop Solution (ThermoFisher), then read immediately using a BioTek plate reader (BioTek, Winooski, VT) at OD450.

1.3.5 Microneutralization assay

To determine the level of RSV antibody neutralization in the mouse sera, a microneutralization assay was used as described with minor modifications (63). Briefly, sera were pooled and heat-inactivated at 55°C for 30 min. Diluted sera in 2%

FBS/DMEM (1:40) were co-incubated with 200 FFU RSV A2-GFP +/- 10% guinea pig complement (C') (Sigma-Aldrich, St. Louis, MO) for 1 h at 37°C. Following pre-incubation, the virus/sera mixture was added to 95% confluent A549 cells for 48 h. Fluorescent focus units (FFUs) were visualized using Cellomics ArrayScan (ThermoFisher), enumerated with HTS software, and mean FFUs of replicate wells were determined. Neutralization was determined as the percent reduction in mean FFUs compared to empty NP antisera.

1.3.6 CX3C-CX3CR1 blocking assay

A CX3C-CX3CR1 blocking assay was performed as described (24). Briefly, 500 nM RSV G ectodomain (Gecto) was incubated +/- 5/mL heparin sulfate (HS) (Sigma) to prevent non-specific binding and +/- 20 µg/mL IgG (isolated from vaccinated mice by Protein G beads (Invitrogen) for 1 h on ice. CX3CR1.293 and HEK-293 cells were harvested, and 4 x 106 cells/mL were blocked with 1 µg/mL Fc block diluted in FACS buffer (0.8% FBS/PBS) for 15 min on ice followed by incubation with 500 nM RSV Gecto +/- 5 µg/mL HS +/- 10 µg/mL IgG for 1 h on ice. Cells were washed and resuspended in 20 µg/mL anti-G protein mAb (clone 130-5F) for 45 min on ice. Cells were washed and resuspended in goat-anti-mouse Alexa488 (1:200) (ThermoFisher) for 45 min on ice and protected from light. Cells were washed 3x with FACS buffer, resuspended in FACS buffer, and analyzed by flow cytometry. To determine FKN blocking, the assay was followed similarly except cells were incubated with 2 µg/mL biotinylated-FKN (Acro Biosystems, Newark, DE) +/- 5 µg/mL HS and +/- 10 µg/mL IgG. To detect CX3CR1-bound FKN, cells were incubated with Streptavidin-PE (1:200) (ThermoFisher). Identical times and temperatures were used for both ligands.

Percent inhibition was determined as the difference of CX3CR1+ binding (G or FKN +HS + vehicle IgG) – (G or FKN +HS +NP IgG or mAb control bound to) x 100 as previously described (51). At least 20,000 events were collected using BD LSR II (BD Bioscience, Franklin Lakes, NJ).

1.3.7 Plaque assays

Lungs were harvested at day 5 pi and homogenized in 1 mL DMEM using GentleMACS tissue homogenizer (Miltenyi Biotec, Gaithersburg, MD) as described (55). Homogenates were centrifuged at 500 xG at 4°C for 8 min, supernatant was 10-fold diluted in DMEM (Hyclone) and overlaid onto 90% confluent Vero E6 cells in 24-well plates. After 2h of absorption, cells were overlaid with 2% methylcellulose (Sigma Aldrich) and incubated at 37°C for 6 days. Following incubation, methylcellulose was aspirated, wells were washed with PBS, fixed with acetone: methanol (60:40, Sigma-Aldrich), and air-dried overnight. Wells were washed 3x with KPL wash buffer and blocked with Blotto overnight at 4°C. The next day, Blotto was removed and a mAb cocktail against RSV F and G proteins (clones 131-2A, 131-2G) was diluted in blotto was added overnight at 4°C. Wells were washed 3x with KPL wash buffer and goat anti-mouse-AP (ThermoFisher) was added overnight at 4°C. Wells were washed 3x with KPL wash buffer and virus plaques were developed with 1-Step™ NBT/BCIP substrate solution (ThermoFisher) for 5 min, rinsed with diH2O, and enumerated using a dissection microscope.

1.3.8 BAL cell phenotyping

Bronchioalveolar leucocytes (BAL) were collected by i.p. anesthetizing (Avertin) mice and terminally bleeding by severing the left axillary artery. The trachea was

exposed and a small incision was made. The lungs were flushed 3x with 1 mL PBS and collected in 1.5 mL snap-cap tubes and BAL was centrifuged for 10 min at 500 xG at 4°C. The supernatant (BAL fluid) was separated and stored at -80°C until cytokine/chemokine analysis. BAL cells were resuspended in FACS buffer (0.8% FBS/PBS) and enumerated using a hemocytometer and Trypan blue. Cells were washed with FACS buffer and resuspended in Fc Block for 15 min on ice followed by the addition of anti-CD3, anti-CD8, and anti-CD11b, or isotype control Abs (all from BD Bioscience) for 1h on ice (Supplementary Figure 2). Cells were washed, fixed with 2% PFA (Ted Pella, Redding, CA) for 20 min at room temperature, washed, and resuspended with FACS buffer. At least 10,000 events were collected with BD LSR II (BD).

1.3.9 Intracellular cytokine staining

Spleens from mice were collected at day 5 pi. Single-cell suspensions of spleen cells were made by dissociation through a 100 uM cell strainer (Corning), washed with Hanks Balanced Salt Solution (HBSS) (HyClone), and red blood cells were lysed with Gey's solution (Sigma-Aldrich) for 5 min. Splenocytes were washed 2x with HBSS, resuspended in media containing 10% FBS + RPMI-1640, and enumerated using a hemocytometer, and 2 x 107 cells/mL were plated in a round bottom 96-well plate (Corning). Splenocytes were stimulated with 10 µg/mL RSV G (183WAICKRIPNKKPGKK197) and M2 peptides (82SYIGSINNI90) (42) or control (GFP, aa 200-208), phorbol 12-myristate 13-acetate (PMA)/ionomycin (Sigma), or left unstimulated and were treated with GolgiPlug (Brefeldin A) (BD) to retain cytokines and incubated at 37°C for 6h. After 6 h, cells were washed 3x with FACS

buffer, blocked with 1 μg/mL Fc block (BD), and stained with anti-CD3 and anti-CD4 or isotype controls (all from BD Bioscience) for 1 h on ice. Cells were fixed with 2% PFA for 20 min at room temperature, washed with permeabilization buffer (BD Bioscience), and incubated with anti-IFNγ and anti-IL-4 or isotype controls diluted in permeabilization buffer for 1 h at 4°C (Supplementary Figure 2). Cells were washed 3X with permeabilization buffer, resuspended in FACS buffer, and analyzed with BD LSR II (BD Bioscience) with at least 10,000 events collected.

1.3.10 Statistics

Data were analyzed by one-way ANOVA with Dunnett's multiple comparison test. $p<0.05$ was considered significant. Data are represented as mean +/- SEM. A vaccination study was performed once. Experiments were performed at least in duplicate with representative data shown.

1.4 Results

1.4.1 Nanoparticle vaccine constructs

NP immunogens were constructed using SpyTag/SpyCatcher technology (54, 58) (Figure 1.1). Briefly, a construct of lumazine synthase, which self-assembles into 60-mer spherical particles, was fused to a SpyCatcher domain. Recombinant lumazine synthase – SpyCatcher protein was purified and confirmed by negative stain electron microscopy to self-assemble into NPs (Figure 1.1D). To generate CCD-coated NPs, the lumazine synthase – SpyCatcher NPs were incubated with recombinant RSV G CCD protein fused to a SpyTag, allowing for the formation of the covalent isopeptide bond between the SpyCatcher and SpyTag and display of the CCD antigen on the surface of the NPs (Figure 1.1B). Covalent linking of the SpyTagged CCD to the

lumazine synthase – SpyCatcher was verified by SDS-PAGE and a change in molecular weight of the bands (Figure 1.1C). We previously identified that a point mutation at site 177 (serine to glutamine) improved immunogenicity in a G glycoprotein vaccine compared to wild-type G protein adjuvanted with MPLA (51). Thus, in addition to wild-type CCD antigen loaded onto NPs (NP-WT), the S177Q CCD antigen was also generated and loaded onto NPs (NP-S177Q). Notably, upon overnight incubation of CCD antigens with NPs, precipitation was observed. Pelleting of the precipitate by centrifugation and evaluation by SDS-PAGE revealed that the precipitate is the NP-WT and NP-S177Q nanoparticle samples (Figure 1.1C). No precipitation is observed by incubation of empty NPs or CCD alone, suggesting that the loading of the CCD, which contains many hydrophobic amino acids, promoted insolubility of the NPs. To generate samples for immunization, pellets were resuspended in PBS.

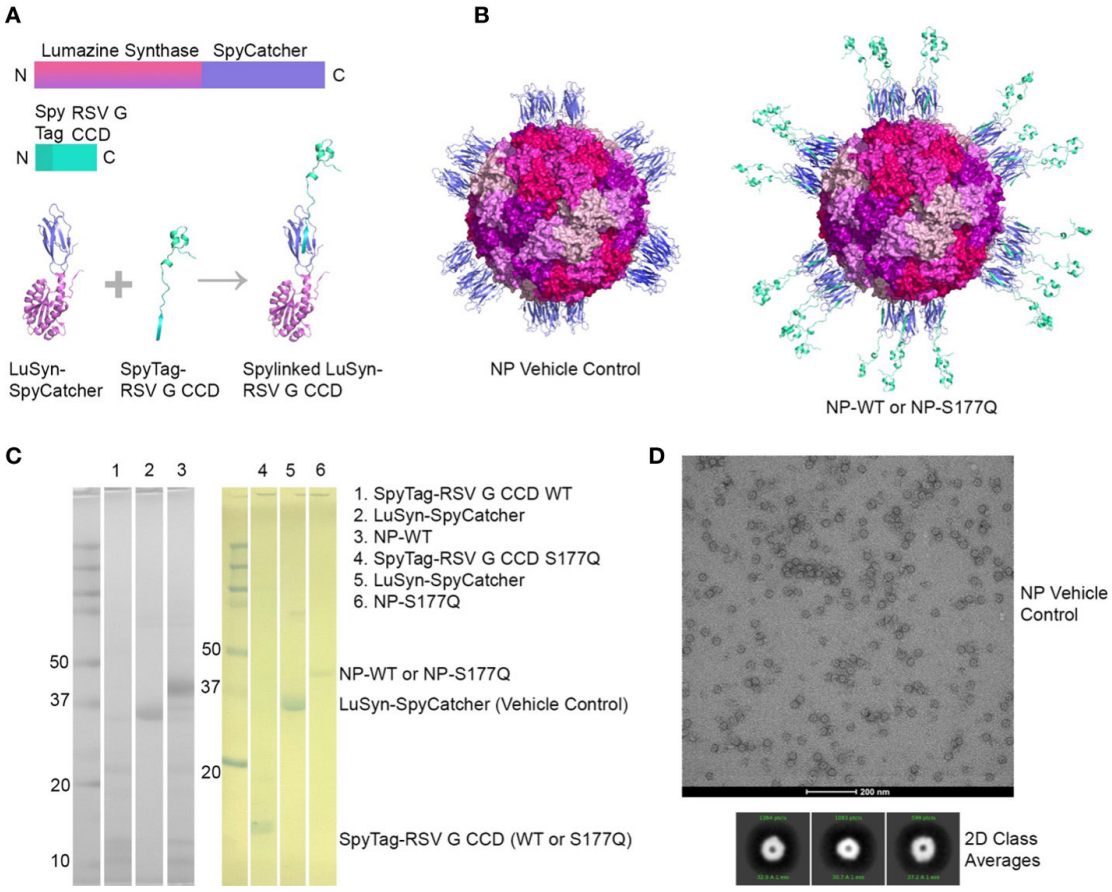

Figure 1.1 Production and Characterization of RSV G CCD coated nanoparticle immunogens

Production and characterization of RSV G CCD coated nanoparticle immunogens. (A) Schematic of lumazine synthase (LuSyn) (gradient purple/pink) and RSV G CCD (green cyan) expression constructs. SpyCatcher (periwinkle) is C-terminally fused to lumazine synthase. SpyTag (teal) is N-terminally fused to RSV G CCD constructs (WT or S177Q mutant). LuSyn-SpyCatcher and SpyTag-RSV G CCD are incubated together and are covalently linked via a spontaneous isopeptide bond formed between SpyTag and SpyCatcher proteins. (B) Representation of expected nanoparticle structures (prepared with PyMol version 2.5): Lumazine Synthase – SpyCatcher (empty NP, vehicle control) and Lumazine Synthase – RSV G CCD (NP-WT or NP-S177Q). 60 copies of lumazine synthase self-assemble to create 12 pentameric interfaces via their C-terminal ends thereby displaying 60 copies of spylinked RSV G CCD antigens. (C) SDS-PAGE of gel shift assay showing SpyTag - RSV G CCD (7.6 kDa), Lumazine Synthase-SpyCatcher (31 kDa), and NP-CCD WT or NP-CCD S177Q (38.6 kDa as a monomer) constructs after pelleting and resuspending in 1xPBS, pH 7.4. Multiple bands are likely due to contaminating proteins after Ni-NTA purification of bacterial lysates. (D) Negative stain electron microscopy micrographs

(upper panel) and 2D class averages (lower panel) of empty NP's show expected self-assembly and size.

1.4.2 RSV NP vaccines induce Anti-RSV Abs

Mice received a priming dose of 10 μg NP-WT, NP-S177Q, or empty NPs adjuvanted with 10 μg MPLA. On day 21 post-prime, mice were boosted with either 10 μg or 25 μg of homologous vaccine or 10μg empty NP, all adjuvanted with 10 μg MPLA. At day 7 post-boost, the mice were bled, and anti-RSV Abs were detected by ELISA (Figure 1.2, Supplementary Figure 1). NP-WT and NP-S177Q vaccination induced anti-RSV Ab responses. Abs generated by NP-S177Q were significantly increased ($p < 0.05$), and NP-WT 25μg and NP-WT 10μg Abs were increased ($p = 0.28$, $p = 0.06$, respectively) compared to empty NP vaccination. NP-S177Q vaccination induced moderately higher serum IgG titers than NP-WT (Figure 1.2), although the IgG responses did not statistically differ between vaccine doses. At day 21 post-boost, the NP-vaccinated mice were challenged with RSV A2, and on day 5 the serum Ab responses were determined. Similar to pre-challenge IgG titers, all vaccinated mice had greater anti-RSV A2 IgG compared to vehicle control (Figure 1.3A). Mice boosted with 25 μg of NP-S177Q vaccine had significantly ($p<0.05$) increased Ab titers compared to vehicle control, however, NP-S177Q vaccination was not statistically improved over NP-WT boosted mice. Contrary to our previous study demonstrating improved Ab recall responses (51), these data show a less robust recall response as sera Ab levels were roughly 1 log3 lower in each group on days 7 post boost and 5 post-challenge. Previous constructs utilized full-length G protein as opposed to restricting antibody responses to the CCD, which may partially explain

this phenomenon. It is also possible Abs were present in the lung during infection and would not be detected in sera. It is also notable that serum Ab titers against RSV B1 were markedly lower than RSV A2 (Figure 1.3B). This finding was similar to a previous report suggesting anti-G Abs generated against A2 G protein bind with lower affinity to RSV B compared to RSV A2, likely due to variable residues encompassing the CCD between subtypes, despite conservation of the CX3C motif (40). NP-S177Q vaccination induced greater Abs compared to vehicle control. NP-WT also induced anti-B1 Abs although the titers were lower compared to NP-S177Q.

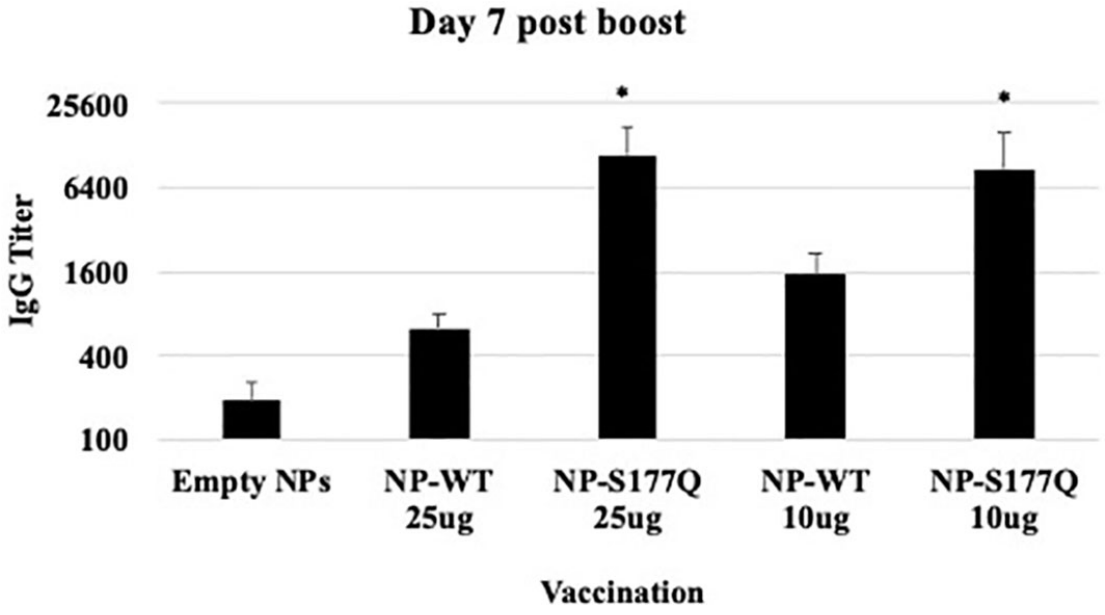

Figure 1.2 RSV G protein NP Vaccine Immunogenicity.

Mice received a priming dose of 10 µg NP-WT, NP-S177Q, or empty NPs, all adjuvanted with 10 µg MPLA. On day 21 post prime, mice were boosted with either 10 µg or 25 µg of homologous vaccine or 10 µg empty NP, all adjuvanted with 10 µg MPLA. On day 7 post-boost, serum IgG responses were determined by ELISA. IgG titer determined as the highest dilution OD450 value above background plus two standard deviations. Bars represent mean IgG titer + SEM (n = 5 mice/group). *$p<0.05$ by one-way ANOVA with Dunnett's multiple comparison test compared to empty NPs.

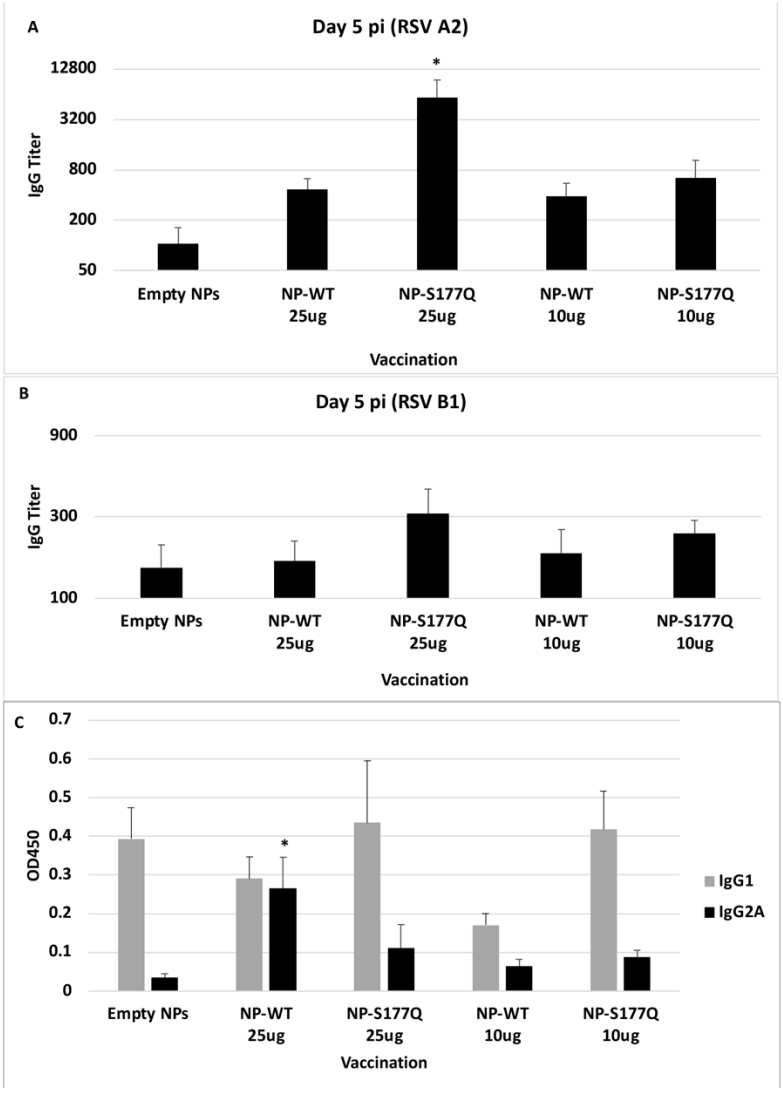

Figure 1.3 Serum Ab responses post-RSV challenge.

Mice received a priming dose of 10 µg NP-WT, NP-S177Q, or empty NPs, all adjuvanted with 10 µg MPLA. On day 21 post prime, mice were boosted with either 10 µg or 25 µg of homologous vaccine or 10 µg empty NP, all adjuvanted with 10 µg MPLA. On day 21 post boost, mice were challenged with 106 PFU RSV A2, and sera collected on day 5 pi. Ab responses were determined for (A) RSV A2 and (B) RSV B1. IgG titer determined as the highest dilution OD450 value above background plus two standard deviations. (C) OD450 values of IgG1 (gray) and IgG2A (black) responses against RSV A2. Bars represent mean IgG titer (A, B) or OD450 (C) +/- SEM (n=5 mice/group). *$p<0.05$ by one-way ANOVA with Dunnett's multiple comparison test compared to empty NPs.

To determine if the serum Ab response were Th1- or Th2-like, ELISAs were performed to determine the specific IgG subclass (Figure 1.3C). It is established that IgG2a corresponds to a Th1-type response, while IgG1 corresponds to a Th2-type in response (64) and determines Fc effector function (e.g., complement-dependent cytotoxicity) (65, 66). There were no significant changes in Th2-type Ab responses between vehicle and NP-WT or NP-S177Q vaccinated mice. Further, Th1-type responses were only significantly ($p<0.05$) increased in the 25 μg NP-WT vaccinated mice, while there were no significant IgG2a responses in NP-S177Q vaccinated mice. These findings do not recapitulate the increased Th1-type responses which were previously observed with G protein immunogen (51). Conformationally designed epitopes such as those in the NP vaccines may require adjuvants that do not denature or emulsify the antigens, and or the insolubility of NP-WT and NP-S177Q vaccines may have contributed to these differences (67).

1.3.3 CX3C-CX3CR1 blocking

Blocking CX3C-CX3CR1 interaction or ablating the CX3C motif is correlated with protection against RSV disease in mice and cotton rats (43, 49, 50, 68). To evaluate the efficacy of G protein CX3C-CX3CR1 blocking Abs generated in response to NP-WT or NP-S177Q vaccination, serum IgG from NP-vaccinated mice was isolated and tested. Similar to the G protein vaccinated mice (51), vaccination with NP-WT or NP-S177Q candidates induced significant ($p<0.05$) CX3C-CX3CR1 blocking Abs compared to vehicle IgG (Figure 1.4A), and Ab from NP-S177Q vaccination induced slightly higher blocking Abs (35%) than NP-WT vaccination (20%). As expected, mAb 131-2G which binds to a conserved epitope in the G

protein blocked up to 90% G protein binding to CX3CR1. Contrary to our previous report showing that G protein induced greater CX3C-CX3CR1 blocking Abs compared to vaccination with an S177Q G protein mutant, in this study, we observed a slight improvement in G protein CX3C-CX3CR1 blocking, and in agreement with previous reports, 131-2G blocked G protein binding more effectively than polyclonal IgG from vaccinated mice. These Abs did not cross-react and block FKN binding to CX3CR1 (data not shown). This is not unexpected as there are structural differences that may preclude anti-G protein binding (69). Thus, this NP-S177Q vaccine platform induces G protein CX3C-CX3CR1 blocking Abs which have been shown to protect against RSV disease and are not implicated in modifying endogenous FKN signaling.

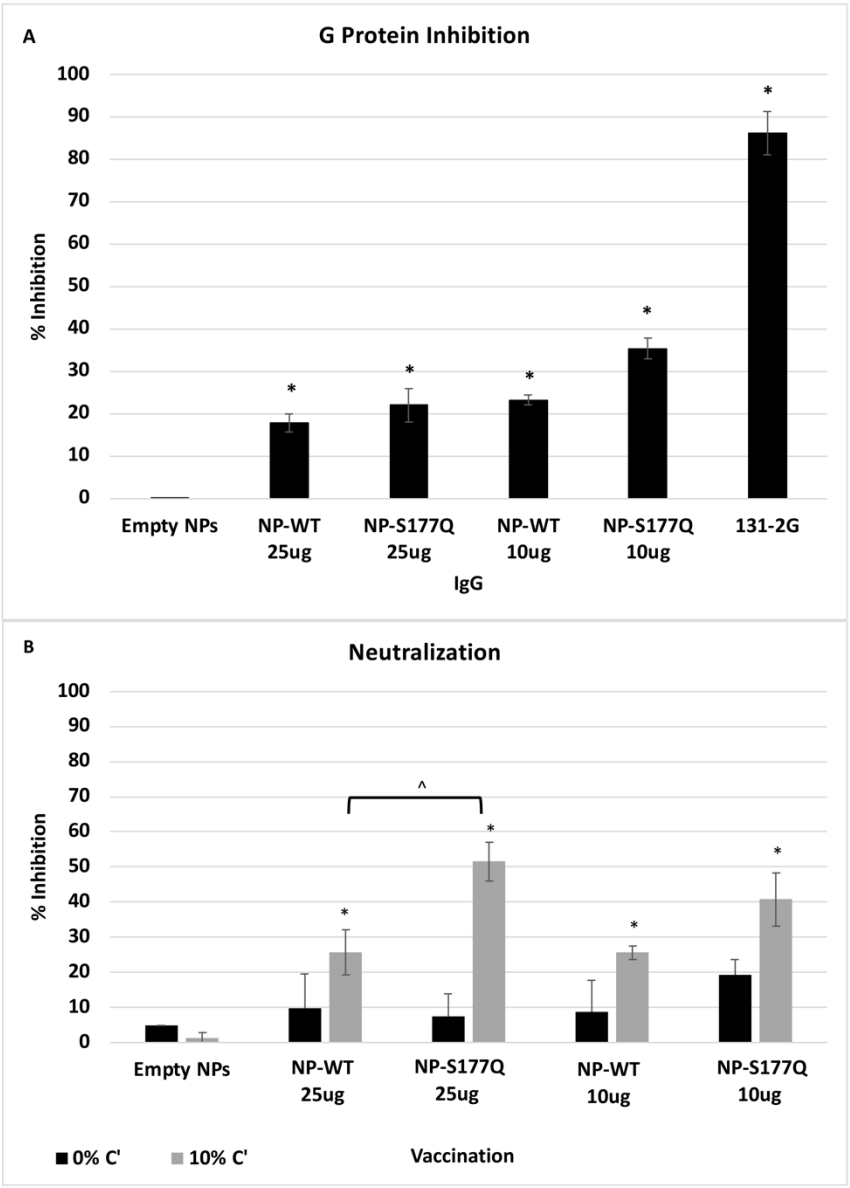

Figure 1.4 Ab Responses.

Mice received a priming dose of 10 µg NP-WT, NP-S177Q, or empty NPs, all adjuvanted with 10 µg MPLA. On day 21 post prime, mice were boosted with either 10 µg or 25 µg of homologous vaccine or 10 µg empty NP, all adjuvanted with 10 µg MPLA. On day 21 post boost, mice were challenged with 106 PFU RSV A2, and sera were collected on day 5 pi. (A) G protein CX3C-CX3CR1 blocking by IgG from challenged mice was determined by flow cytometry. (B) Pooled antisera were heat inactivated and diluted (1:40) for microneutralization assay in A549 cells with 0% (black) or 10% (grey) Guinea pig complement (C'). FFUs were collected on Cellomics ArrayScan and enumerated automatically with HTS Software

(ThermoFisher). Bars represent mean + SEM (n=5 mice/group). (A) *p<0.05 by one-way ANOVA with Dunnett's multiple comparison test compared to empty NP. For panel B, p <0.05 by one-way ANOVA with Tukey's multiple comparison test to compare equally dosed NPs (^) and empty NPs (*).

1.3.4 RSV neutralization

Anti-G protein Abs are neutralizing in human airway epithelial cells infected with RSV and in vivo (27). The addition of complement aids the neutralization of some anti-G protein Abs including the highly potent 3D3 and 3G12 anti-G protein mAbs that can be detected in immortalized cell lines (69, 70). To determine if serum from NP-WT or NP-S177Q vaccinated mice was neutralizing, heat-inactivated sera +/- 10% guinea pig complement (C') were co-incubated with RSV-GFP (56) and added to RSV-infected human A549 cells for 48 h (Figure 1.4B). In the absence of complement, there was no significant (p>0.05) neutralization for any vaccine groups, however, serum plus complement from NP-WT and NP-S177Q vaccinated mice significantly (p<0.05) neutralized infected A549 cells compared to empty NP vaccination. Moreover, serum from 25 μg S177Q induced significantly (p<0.05) greater neutralization compared to NP-WT at the same dose. These data suggest neutralization is complement-dependent and not CX3C:CX3CR1-mediated neutralization.

Lung viral titers showed that NP-WT and NP-S177Q vaccination reduces lung titers in vivo (Figure 1.5). On day 5 pi, corresponding to peak lung viral titers (71), 10 μg NP-WT or 25 μg NP-S177Q vaccination resulted in significantly (p<0.05) reduced viral titers in the lungs of RSV A2 challenged mice. 25 μg NP-WT vaccinated mice and 10 μg NP-S177Q vaccinated mice also reduced lung titers compared to empty NP

vaccination (p=0.16, p=0.15, respectively). These findings are consistent with other G protein vaccines that reduce lung titers and induce anti-G protein neutralizing Abs (nAbs), however, others have reported that Abs to G protein are non-neutralizing but this was determined in the absence of complement, an effect which has caused misunderstanding (40, 41, 72, 73). There may be mechanisms aside from nAbs that result in reduced viral titers after NP vaccination including a cytotoxic T lymphocyte (CTL) response or improved macrophage activity, however these were not examined here. Moreover, while *in vivo* and *in vitro* neutralization data suggest 25 µg NP-S177Q vaccination resulted in the greatest levels of nAbs and reduced lung titers, the lack of significant in vivo reduction for 25 µg NP-WT and 10 µg NP-S177Q does not correlate with our findings in vitro. The findings from this study show that G protein immunogens are capable of inducing nAbs that are detectable in vitro with additional complement and vaccination may reduce lung viral titers in mice.

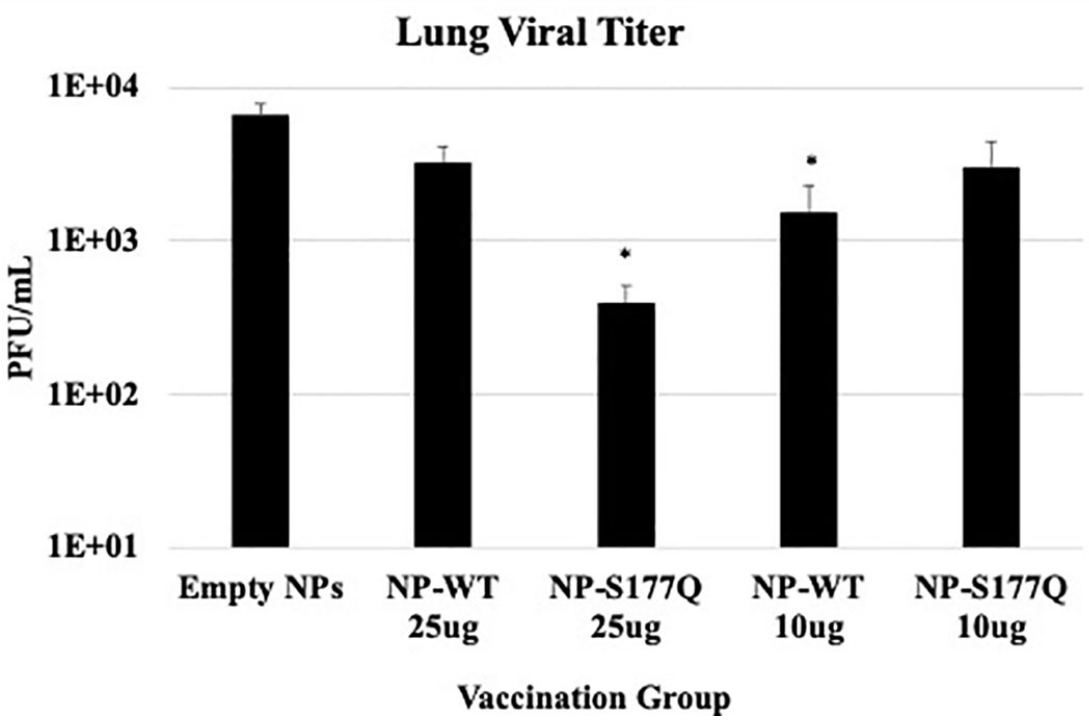

Figure 1.5 Lung Viral Titers.

Mice received a priming dose of 10 µg NP-WT, NP-S177Q, or empty NPs, all adjuvanted with 10 µg MPLA. On day 21 post prime, mice were boosted with either 10 µg or 25 µg of homologous vaccine or 10 µg empty NP, all adjuvanted with 10 µg MPLA. On day 21 post boost, mice were challenged with 106 PFU RSV A2, and at day 5 pi, lungs were harvested to determine virus loads. The bars represent the mean +/- SEM of plaque forming units (PFU)/mL of lung homogenate. *$p<0.05$ by one-way ANOVA with Dunnett's multiple comparison test compared to empty NPs.

1.3.5 Immune response to RSV challenge

Aspects of RSV disease are connected with the expression of the G protein CX3C motif (50). Blocking G protein CX3C-CX3CR1 interaction with mAbs specific to this motif or the CCD domain is correlated with reduced RSV disease in vivo (40, 41, 73). To determine if NP-WT or NP-S177Q vaccination is protective against G protein-mediated disease, vaccinated mice were challenged with RSV A2 and BAL leukocytes were evaluated (Table 1.2). A significant ($p<0.05$) reduction in

BAL cell numbers (3.9 x 10^4 cells) in RSV-challenged mice that were vaccinated with 10 µg of NP-S177Q vaccine was evident compared to the empty NP control vaccinated mice (7.5 x 10^4 cells). Interestingly, no other vaccination group including mice vaccinated with 25 µg of NP-S177Q vaccine had substantially reduced BAL cells following RSV challenge. Consistent with an overall reduction in BAL cell infiltration, RSV-challenged 10 µg NP-S177Q mice vaccinated had reduced CD11b+ cell numbers (2.3 x 10^3) and a trend toward lower in CD8+ T cell numbers (2.0 x 10^3) compared to RSV-challenged empty NP vaccinated mice (5.4 x 10^3 and 3.3 x 10^3 cells, respectively). Taken together, these support lung disease protection in mice vaccinated with NP-S177Q vaccine compared to vehicle control vaccinated mice. We also examined intracellular cytokine production by splenocytes stimulated with RSV G peptide encompassing the CCD and M2 as previously described (42, 68), however, there were no statistical differences detected in the production of IFNγ+ or IL-4+ by CD3+/CD4+ T cells between groups (data not shown).

	Empty NPs	NP-WT 25µg	NP-S177Q 25µg	NP-WT 10µg	NP-S177Q 10µg
Total BAL Cells	7.5 x 10^4 *(± 4.7 x 10^3)*	8.4 x 10^4 *(± 12.0 x 10^3)*	6.6 x 10^4 *(± 14.0 x 10^3)*	6.2 x 10^4 *(± 6 x 10^3)*	3.9 x 10^4 * *(± 6.2 x 10^3)*
CD8+	3.3 x 10^3 *(± 5.5 x 10^2)*	3.1 x 10^3 *(± 4.3 x 10^2)*	3.7 x 10^3 *(± 8.2 x 10^2)*	2.5 x 10^3 *(± 5.2 x 10^2)*	2.0 x 10^3 *(± 1.0 x 10^2)*
CD11b+	5.4 x 10^3 *(± 6.0 x 10^2)*	4.7 x 10^3 *(± 6.8 x 10^2)*	5.0 x 10^3 *(± 17.0 x 10^2)*	2.9 x 10^3 *(± 4.8 x 10^2)*	2.3 x 10^3 *(± 2.4 x 10^2)*

Mice received a priming dose of 10 µg NP-WT, NP-S177Q, or empty NPs, all adjuvanted with 10 µg MPLA. On day 21 post prime, mice were boosted with either 10 µg or 25 µg of homologous vaccine or 10 µg empty NP, all adjuvanted with 10 µg MPLA. On day 21 post boost, vaccinated mice were challenged with 10^6 PFU RSV A2, and on day 5 pi the BAL cells were collected and enumerated (total BAL cells). CD8+ T cells and CD11b+ cells were determined by flow cytometry with at least 10,000 events collected. Mean total cells ± SEM (shown in italics) are presented. *p<0.05 by one-way ANOVA with Dunnett's multiple comparison test compared to empty NPs within the same row.

Table 1.2 BAL Leukocytes.

1.5 Discussion

RSV is a major cause of respiratory disease in the very young and old with no safe and approved vaccine available despite decades of research. The landscape of RSV vaccine research started with a failed formalin-inactivated RSV (FI-RSV) vaccine tested in the early 1960s (74). In those studies, FI-RSV vaccinated infants naturally infected with RSV infection resulted in a majority of infants requiring hospitalization where two infants died (44). Further investigation revealed that the FI-RSV vaccine caused enhanced disease (75). Moreover, it was later shown that Abs generated against RSV correlate with some but incomplete protection from disease, and that reinfection with identical RSV strains could occur, and that viral loads did not consistently correlate with disease severity in hospitalized infants (76–78). Thus, a safe and effective RSV vaccine has been elusive (20).

The RSV F protein has historically been the focus for RSV vaccine development as it is more conserved than G protein, and F protein is indispensable for in vitro infection (79). However, the G protein has a highly conserved CX3C chemokine mimic motif within its central conserved domain (CCD) (24, 60). Abs which bind the CCD and/or CX3C motif may be protective by preventing viral attachment to host cells as well as blocking G protein CX3C-CX3CR1 responses and G protein chemokine mimicry. Importantly, Abs induced by RSV G protein, including anti-G protein mAbs, that target the CCD and/or CX3C motif will neutralize RSV A and B strains, prevent Th2-type immune biasing due to G protein, reduce many of the immune correlates of severe RSV disease (e.g., eosinophilia), improve respiratory efforts, rescue protective IFN responses, and reduce lung pathology (17, 37, 80–85).

At least two findings have stalled RSV G protein-based vaccine development, one being that the CCD region is poorly immunogenic compared to epitopes on F protein (86–88), and the G protein has been linked to the development of enhanced RSV disease (17, 22, 39).

To address these impediments, we have investigated the function and immunogenicity of various G protein mutants (49, 51, 68). Specifically, we examined the G protein S177Q mutant as a vaccine candidate because our studies showed that the mutation S177Q increased immunogenicity and improved Th1-type responses compared to G protein (51). The findings were predicted as immunogen was derived by structurally-guided vaccine development and knowing that a single point mutation in the CCD would alter the conformation of the G protein likely affecting its immunogenicity and safety profile. Structural and conformational validation showed that the CCD S177Q mutant retains high affinity when binding to mAbs and human anti-RSV reference sera and was substantially improved compared to the CX4C G protein mutant (52). In this study, mice were vaccinated with NP-WT or NP-S177Q generated with SpyTag/SpyCatcher technology (54, 58). Recently, a pre-F ferritin NP (pre-F-NP) with modified glycans was evaluated in mice and nonhuman primates (NHPs) (89). It was shown that pre-F-NP vaccination induced greater neutralizing antibody responses compared to DS-Cav1 trimer, suggesting the NP vaccine platform may offer superior characteristics compared to protein or subunit vaccination.
In this study, the NP-WT or NP-S177Q vaccine candidates were immunogenic in a prime/boost scheme, and consistent with our previous work, the NP-S117Q candidate

showed improved immunogenicity. We sought to determine if these vaccines were protective, and to this end, the NP-vaccinated mice were i.n. challenged with RSV A2 and the serum antibody and BAL cell responses were determined. The sera responses after the RSV challenge were similar to the 25 μg NP-S177Q vaccinated mice, being significantly ($p<0.05$) more immunogenic than vehicle control, and NP-S177Q vaccinated mice also trended towards increased IgG titers compared to NP-WT for binding to RSV A2 and B1. As the CX3C motif is conserved between RSV subtypes and strains, these data suggest that Abs induced by NP-WT or NP-S177Q vaccination may be cross-reactive (40). The serum Ab isotypes were evaluated to determine if NP vaccination induced a Th1-dependent IgG2 response, or a Th2-dependent IgG1 response (64). Serum from NP-WT vaccinated mice indicated a predominantly Th1-type response, however, mice vaccinated with NP-S177Q predominantly had a Th2-type response (Figure 3C), which was inconsistent with our previous results. However, sera from both NP-WT and NP-S177Q vaccinated mice blocked G protein CX3C-CX3CR1 and did not interfere with FKN binding to CX3CR1 (Figure 4). Sera from 25 μg NP-S177Q vaccinated mice had significantly greater ($p<0.05$) complement-dependent neutralization activity in A549 cells compared to empty NP and 25 μg NP-WT. Thus, the Ab response to NP vaccination suggests NP-S177Q improves immunogenicity and induces greater nAbs, and that Abs that block G protein binding to CX3CR1.

Neutralizing the virus can contribute to reducing virus-mediated disease, however disease severity does not faithfully correlate with viral load or neutralizing

Ab responses (77, 78, 80, 90–92). RSV disease is understood to be affected by both virus and host factors, and interventions that do not address G protein-mediated immune dysregulation may provide incomplete protection (22). While we noted significant reductions in lung viral loads in vaccinated mice, modalities that neutralize viruses and block G protein mediated disease are of great interest.

BAL cell influx during RSV infection is a correlate of immune-mediated disease (93). Initial vaccination with NP-WT did not prime for enhanced respiratory disease when the mice were boosted with NP-WT or NP-S117Q vaccines likely because of the MPLA adjuvant precluding non-neutralizing Th2-type responses and/or restriction of responses to the CCD. Mice receiving the 10 μg NP-S177Q vaccination resulted in significantly ($p<0.05$) fewer total BAL cells where CD11b+ and CD8+ BAL cells were substantially reduced while 25 μg vaccination did not have this result. It is possible that the 10 μg vaccine dose was suboptimal in terms of the robustness of BAL cell recruitment when the vaccinated mice were challenged. However, these findings show the NP-S177Q boosting effectively induces CX3C-CX3CR1 blocking and neutralizing Abs which can provide protection against RSV challenge and disease. Our previous study (51) evaluated various full-length mutant G proteins in a prime/boost/boost scheme, and we discovered significant Ab responses in mice vaccinated with S177Q mutations. Here, we describe the next iteration of this platform, an NP containing CCD with or without the S177Q mutation in a prime/boost scheme. Consistent with our previous studies, the NP-S177Q vaccine improves immunogenicity, however these studies do not demonstrate superiority to

our previous full-length constructs. This may be due to the vaccination scheme (i.e., one versus two boosts), antigen delivery quality and/or presentation (e.g. poor solubility of NP constructs), or other differences. It will be important in future studies to compare various NP and microparticle (MP) vaccine platforms that improve solubility and immunogenicity and protect from disease. Our ongoing studies using these improved candidates will fully elucidate immune responses to this vaccine and show robust protection from disease.

1.5 Data availability statement

The original contributions presented in the study are included in the article/Supplementary Material. Further inquiries can be directed to the corresponding author.

1.6 Ethics statement

Mice studies were performed in compliance with all national and institutional guidelines and guidelines from the Human Care and Use of Laboratory Animals (American Association for Laboratory Animal Science) and performed according to a protocol approved by the University of Georgia Institutional Animal Care and Use Committee (IACUC) (A2022 04-023-Y1-A0, approval date 05/19/2022). All efforts were made to minimize animal pain and discomfort.

1.7 Author contributions

HB designed and carried out experiments, wrote and edited the manuscript. JM data acquisition. MJ provided reagents. SN provided reagents. RD and RT secured funding

and guided project, wrote and edited the manuscript. All authors contributed to the article and approved the submitted version.

1.8 Funding

Funding was provided by the Georgia Research Alliance (GRA) and from NIH 1R01AI166066.

1.9 Acknowledgments

We would like to thank Les Jones (University of Georgia) for purifying RSV G protein. We thank Vitor and UCSC CryoEM Facility.

1.10 Conflict of interest

RD is an inventor on US patent filing No. 62/588,022.

The remaining authors declare that the research was conducted in the absence of any commercial or financial relationships that could be construed as a potential conflict of interest.

1.11 Publisher's note

1.12 Supplementary material

The Supplementary Material for this article can be found online at:

https://www.frontiersin.org/articles/10.3389/fimmu.2023.1215323/full#supplementary-material

1.13 References

1. Nguyen-Van-Tam JS, O'Leary M, Martin ET, Heijnen E, Callendret B, Fleischhackl R, et al. Burden of respiratory syncytial virus infection in older and high-risk adults: a systematic review and meta-analysis of the evidence from developed countries. Eur Respir Rev (2022) 31(166). doi: 10.1183/16000617.0105-2022
2. Baraldi E, Checcucci Lisi G, Costantino C, Heinrichs JH, Manzoni P, Ricco M, et al. RSV Disease in infants and young children: can we see a brighter future? Hum Vaccin Immunother (2022) 18(4):2079322. doi: 10.1080/21645515.2022.2079322
3. Borchers AT, Chang C, Gershwin ME, Gershwin LJ. Respiratory syncytial virus–a comprehensive review. Clin Rev Allergy Immunol (2013) 45(3):331–79. doi: 10.1007/s12016-013-8368-9
4. Henderson FW, Collier AM, Clyde WA Jr., Denny FW. Respiratory-syncytial-virus infections, reinfections and immunity. a prospective, longitudinal study in young children. New Engl J Med (1979) 300(10):530–4. doi: 10.1056/NEJM197903083001004
5. Hall CB, Weinberg GA, Iwane MK, Blumkin AK, Edwards KM, Staat MA, et al. The burden of respiratory syncytial virus infection in young children. New Engl J Med (2009) 360(6):588–98. doi: 10.1056/NEJMoa0804877
6. Thorburn K. Pre-existing disease is associated with a significantly higher risk of death in severe respiratory syncytial virus infection. Arch Dis Child. (2009) 94(2):99–103. doi: 10.1136/adc.2008.139188
7. Rha B, Curns AT, Lively JY, Campbell AP, Englund JA, Boom JA, et al. Respiratory syncytial virus-associated hospitalizations among young children: 2015-2016. Pediatrics (2020) 146(1). doi: 10.1542/peds.2019-3611
8. Garegnani L, Styrmisdottir L, Roson Rodriguez P, Escobar Liquitay CM, Esteban I, Franco JV. Palivizumab for preventing severe respiratory syncytial virus (RSV) infection in children. Cochrane Database Syst Rev (2021) 11(11):CD013757. doi: 10.1002/14651858.CD013757.pub2
9. Luna MS, Manzoni P, Paes B, Baraldi E, Cossey V, Kugelman A, et al. Expert consensus on palivizumab use for respiratory syncytial virus in developed countries. Paediatr Respir Rev (2020) 33:35–44. doi: 10.1016/j.prrv.2018.12.001
10. Chatterjee A, Mavunda K, Krilov LR. Current state of respiratory syncytial virus disease and management. Infect Dis Ther (2021) 10(Suppl 1):5–16. doi: 10.1007/s40121-020-00387-2
11. American Academy of Pediatrics Committee on Infectious D, American Academy of Pediatrics Bronchiolitis Guidelines C. Updated guidance for palivizumab prophylaxis among infants and young children at increased risk of hospitalization for

respiratory syncytial virus infection. Pediatrics. (2014) 134(2):e620–38. doi: 10.1542/peds.2014-1665
12. Garcia-Garcia ML, Calvo Rey C, Del Rosal Rabes T. Pediatric asthma and viral infection. Arch Bronconeumol. (2016) 52(5):269–73. doi: 10.1016/j.arbres.2015.11.008
13. Lambert L, Sagfors AM, Openshaw PJ, Culley FJ. Immunity to RSV in early-life. Front Immunol (2014) 5:466. doi: 10.3389/fimmu.2014.00466
14. Reicherz F, Xu RY, Abu-Raya B, Majdoubi A, Michalski C, Golding L, et al. Waning immunity against respiratory syncytial virus during the COVID-19 pandemic. J Infect Dis (2022) 226(12):2064–8. doi: 10.1093/infdis/jiac192
15. Ogilvie MM, Vathenen AS, Radford M, Codd J, Key S. Maternal antibody and respiratory syncytial virus infection in infancy. J Med Virol (1981) 7(4):263–71. doi: 10.1002/jmv.1890070403
16. Bergeron HC, Tripp RA. Immunopathology of RSV: an updated review. Viruses. (2021) 13(12). doi: 10.3390/v13122478
17. Tripp RA, Power UF, Openshaw PJM, Kauvar LM. Respiratory syncytial virus: targeting the G protein provides a new approach for an old problem. J Virol (2018) 92(3). doi: 10.1128/JVI.01302-17
18. Bergeron HC, Tripp RA. Breakthrough therapy designation of nirsevimab for the prevention of lower respiratory tract illness caused by respiratory syncytial virus infections (RSV). Expert Opin Investig Drugs (2022) 31(1):23–9. doi: 10.1080/13543784.2022.2020248
19. Griffin MP, Yuan Y, Takas T, Domachowske JB, Madhi SA, Manzoni P, et al. Single-dose Nirsevimab for prevention of RSV in preterm infants. New Engl J Med (2020) 383(5):415–25. doi: 10.1056/NEJMoa1913556
20. Mazur NI, Higgins D, Nunes MC, Melero JA, Langedijk AC, Horsley N, et al. The respiratory syncytial virus vaccine landscape: lessons from the graveyard and promising candidates. Lancet Infect Dis (2018) 18(10):e295–311. doi: 10.1016/S1473-3099(18)30292-5
21. Anderson LJ, Jadhao SJ, Paden CR, Tong S. Functional features of the respiratory syncytial virus G protein. Viruses. (2021) 13(7). doi: 10.3390/v13071214
22. Bergeron HC, Tripp RA. RSV Replication, transmission, and disease are influenced by the RSV G protein. Viruses. (2022) 14(11). doi: 10.3390/v14112396
23. Kauvar LM, Harcourt JL, Haynes LM, Tripp RA. Therapeutic targeting of respiratory syncytial virus G-protein. Immunotherapy. (2010) 2(5):655–61. doi: 10.2217/imt.10.53
24. Tripp RA, Jones LP, Haynes LM, Zheng H, Murphy PM, Anderson LJ. CX3C chemokine mimicry by respiratory syncytial virus G glycoprotein. Nat Immunol (2001) 2(8):732–8. doi: 10.1038/90675
25. Green G, Johnson SM, Costello H, Brakel K, Harder O, Oomens AG, et al. CX3CR1 is a receptor for human respiratory syncytial virus in cotton rats. J Virol (2021) 95(16):e0001021. doi: 10.1128/JVI.00010-21
26. Anderson CS, Chirkova T, Slaunwhite CG, Qiu X, Walsh EE, Anderson LJ, et al. CX3CR1 engagement by respiratory syncytial virus leads to induction of nucleolin

and dysregulation of cilia-related genes. J Virol (2021) 95(11). doi: 10.1128/JVI.00095-21
27. Johnson SM, McNally BA, Ioannidis I, Flano E, Teng MN, Oomens AG, et al. Respiratory syncytial virus uses CX3CR1 as a receptor on primary human airway epithelial cultures. PLoS pathogens. (2015) 11(12):e1005318. doi: 10.1371/journal.ppat.1005318
28. Jeong KI, Piepenhagen PA, Kishko M, DiNapoli JM, Groppo RP, Zhang L, et al. CX3CR1 is expressed in differentiated human ciliated airway cells and Co-localizes with respiratory syncytial virus on cilia in a G protein-dependent manner. PLoS One (2015) 10(6):e0130517. doi: 10.1371/journal.pone.0130517
29. Kim S, Joo DH, Lee JB, Shim BS, Cheon IS, Jang JE, et al. Dual role of respiratory syncytial virus glycoprotein fragment as a mucosal immunogen and chemotactic adjuvant. PLoS One (2012) 7(2):e32226. doi: 10.1371/journal.pone.0032226
30. Zhivaki D, Lemoine S, Lim A, Morva A, Vidalain PO, Schandene L, et al. Respiratory syncytial virus infects regulatory b cells in human neonates via chemokine receptor CX3CR1 and promotes lung disease severity. Immunity. (2017) 46(2):301–14. doi: 10.1016/j.immuni.2017.01.010
31. Harcourt JL, Karron RA, Tripp RA. Anti-G protein antibody responses to respiratory syncytial virus infection or vaccination are associated with inhibition of G protein CX3C-CX3CR1 binding and leukocyte chemotaxis. J Infect diseases. (2004) 190(11):1936–40. doi: 10.1086/425516
32. Haynes LM, Jones LP, Barskey A, Anderson LJ, Tripp RA. Enhanced disease and pulmonary eosinophilia associated with formalin-inactivated respiratory syncytial virus vaccination are linked to G glycoprotein CX3C-CX3CR1 interaction and expression of substance p. J Virol (2003) 77(18):9831–44. doi: 10.1128/JVI.77.18.9831-9844.2003
33. Bakre AA, Harcourt JL, Haynes LM, Anderson LJ, Tripp RA. The central conserved region (CCR) of respiratory syncytial virus (RSV) G protein modulates host miRNA expression and alters the cellular response to infection. Vaccines. (2017) 5(3). doi: 10.3390/vaccines5030016
34. Li XQ, Fu ZF, Alvarez R, Henderson C, Tripp RA. Respiratory syncytial virus (RSV) infects neuronal cells and processes that innervate the lung by a process involving RSV G protein. J Virol (2006) 80(1):537–40. doi: 10.1128/JVI.80.1.537-540.2006
35. Tripp RA, Dakhama A, Jones LP, Barskey A, Gelfand EW, Anderson LJ. The G glycoprotein of respiratory syncytial virus depresses respiratory rates through the CX3C motif and substance p. J Virol (2003) 77(11):6580–4. doi: 10.1128/JVI.77.11.6580-6584.2003
36. Polack FP, Irusta PM, Hoffman SJ, Schiatti MP, Melendi GA, Delgado MF, et al. The cysteine-rich region of respiratory syncytial virus attachment protein inhibits innate immunity elicited by the virus and endotoxin. Proc Natl Acad Sci U S A. (2005) 102(25):8996–9001. doi: 10.1073/pnas.0409478102

37. Bergeron HC, Kauvar LM, Tripp RA. Anti-G protein antibodies targeting the RSV G protein CX3C chemokine region improve the interferon response. Ther Adv Infect Dis (2023) 10:20499361231161157. doi: 10.1177/20499361231161157
38. Tripp RA. Respiratory syncytial virus (RSV) modulation at the virus-host interface affects immune outcome and disease pathogenesis. Immune network. (2013) 13(5):163–7. doi: 10.4110/in.2013.13.5.163
39. Jorquera PA, Anderson L, Tripp RA. Understanding respiratory syncytial virus (RSV) vaccine development and aspects of disease pathogenesis. Expert Rev Vaccines (2016) 15(2):173–87. doi: 10.1586/14760584.2016.1115353
40. Choi Y, Mason CS, Jones LP, Crabtree J, Jorquera PA, Tripp RA. Antibodies to the central conserved region of respiratory syncytial virus (RSV) G protein block RSV G protein CX3C-CX3CR1 binding and cross-neutralize RSV a and b strains. Viral Immunol (2012) 25(3):193–203. doi: 10.1089/vim.2011.0094
41. Jorquera PA, Oakley KE, Powell TJ, Palath N, Boyd JG, Tripp RA. Layer-By-Layer nanoparticle vaccines carrying the G protein CX3C motif protect against RSV infection and disease. Vaccines. (2015) 3(4):829–49. doi: 10.3390/vaccines3040829
42. Jorquera PA, Choi Y, Oakley KE, Powell TJ, Boyd JG, Palath N, et al. Nanoparticle vaccines encompassing the respiratory syncytial virus (RSV) G protein CX3C chemokine motif induce robust immunity protecting from challenge and disease. PLoS One (2013) 8(9):e74905. doi: 10.1371/journal.pone.0074905
43. Zhang W, Choi Y, Haynes LM, Harcourt JL, Anderson LJ, Jones LP, et al. Vaccination to induce antibodies blocking the CX3C-CX3CR1 interaction of respiratory syncytial virus G protein reduces pulmonary inflammation and virus replication in mice. J Virol (2010) 84(2):1148–57. doi: 10.1128/JVI.01755-09
44. Fulginiti VA, Eller JJ, Sieber OF, Joyner JW, Minamitani M, Meiklejohn G. Respiratory virus immunization. i. a field trial of two inactivated respiratory virus vaccines; an aqueous trivalent parainfluenza virus vaccine and an alum-precipitated respiratory syncytial virus vaccine. Am J Epidemiol. (1969) 89(4):435–48. doi: 10.1093/oxfordjournals.aje.a120956
45. Chin J, Magoffin RL, Shearer LA, Schieble JH, Lennette EH. Field evaluation of a respiratory syncytial virus vaccine and a trivalent parainfluenza virus vaccine in a pediatric population. Am J Epidemiol. (1969) 89(4):449–63. doi: 10.1093/oxfordjournals.aje.a120957
46. Kim HW, Canchola JG, Brandt CD, Pyles G, Chanock RM, Jensen K, et al. Respiratory syncytial virus disease in infants despite prior administration of antigenic inactivated vaccine. Am J Epidemiol. (1969) 89(4):422–34. doi: 10.1093/oxfordjournals.aje.a120955
47. Elliott MB, Pryharski KS, Yu Q, Boutilier LA, Campeol N, Melville K, et al. Characterization of recombinant respiratory syncytial viruses with the region responsible for type 2 T-cell responses and pulmonary eosinophilia deleted from the attachment (G) protein. J Virol (2004) 78(16):8446–54. doi: 10.1128/JVI.78.16.8446-8454.2004

48. Castilow EM, Olson MR, Varga SM. Understanding respiratory syncytial virus (RSV) vaccine-enhanced disease. Immunol Res (2007) 39(1-3):225–39. doi: 10.1007/s12026-007-0071-6
49. Boyoglu-Barnum S, Todd SO, Meng J, Barnum TR, Chirkova T, Haynes LM, et al. Mutating the CX3C motif in the G protein should make a live respiratory syncytial virus vaccine safer and more effective. J Virol (2017) 91(10). doi: 10.1128/JVI.02059-16
50. Ha B, Chirkova T, Boukhvalova MS, Sun HY, Walsh EE, Anderson CS, et al. Mutation of respiratory syncytial virus G protein's CX3C motif attenuates infection in cotton rats and primary human airway epithelial cells. Vaccines (2019) 7(3). doi: 10.3390/vaccines7030069
51. Bergeron HC, Murray J, Nunez Castrejon AM, DuBois RM, Tripp RA. Respiratory syncytial virus (RSV) G protein vaccines with central conserved domain mutations induce CX3C-CX3CR1 blocking antibodies. Viruses. (2021) 13(2). doi: 10.3390/v13020352
52. Nunez Castrejon AM, O'Rourke SM, Kauvar LM, DuBois RM. Structure-based design and antigenic validation of respiratory syncytial virus G immunogens. J Virol (2022) 96(7):e0220121. doi: 10.1128/jvi.02201-21
53. Komai-Koma M, Ji Y, Cao H, Liu Z, McSharry C, Xu D. Monophosphoryl lipid a directly regulates Th1 cytokine production in human CD4(+) T-cells through toll-like receptor 2 and 4. Immunobiology. (2021) 226(5):152132. doi: 10.1016/j.imbio.2021.152132
54. Zakeri B, Fierer JO, Celik E, Chittock EC, Schwarz-Linek U, Moy VT, et al. Peptide tag forming a rapid covalent bond to a protein, through engineering a bacterial adhesin. Proc Natl Acad Sci U S A. (2012) 109(12):E690–7. doi: 10.1073/pnas.1115485109
55. Murray J, Bergeron HC, Jones LP, Reener ZB, Martin DE, Sancilio FD, et al. Probenecid inhibits respiratory syncytial virus (RSV) replication. Viruses (2022) 14(5). doi: 10.3390/v14050912
56. Villenave R, Broadbent L, Douglas I, Lyons JD, Coyle PV, Teng MN, et al. Induction and antagonism of antiviral responses in respiratory syncytial virus-infected pediatric airway epithelium. J Virol (2015) 89(24):12309–18. doi: 10.1128/JVI.02119-15
57. Zhang X, Meining W, Fischer M, Bacher A, Ladenstein R. X-Ray structure analysis and crystallographic refinement of lumazine synthase from the hyperthermophile aquifex aeolicus at 1.6 a resolution: determinants of thermostability revealed from structural comparisons. J Mol Biol (2001) 306(5):1099–114. doi: 10.1006/jmbi.2000.4435

58. Keeble AH, Turkki P, Stokes S, Khairil Anuar INA, Rahikainen R, Hytonen VP, et al. Approaching infinite affinity through engineering of peptide-protein interaction. Proc Natl Acad Sci U S A. (2019) 116(52):26523–33. doi: 10.1073/pnas.1909653116
59. Malonis RJ, Georgiev GI, Haslwanter D, VanBlargan LA, Fallon G, Vergnolle O, et al. A powassan virus domain III nanoparticle immunogen elicits neutralizing and

protective antibodies in mice. PLoS pathogens. (2022) 18(6):e1010573. doi: 10.1371/journal.ppat.1010573
60. Fedechkin SO, George NL, Nunez Castrejon AM, Dillen JR, Kauvar LM, DuBois RM. Conformational flexibility in respiratory syncytial virus G neutralizing epitopes. J Virol (2020) 94(6). doi: 10.1128/JVI.01879-19
61. Fedechkin SO, George NL, Wolff JT, Kauvar LM, DuBois RM. Structures of respiratory syncytial virus G antigen bound to broadly neutralizing antibodies. Sci Immunol (2018) 3(21). doi: 10.1126/sciimmunol.aar3534
62. Tan TK, Rijal P, Rahikainen R, Keeble AH, Schimanski L, Hussain S, et al. A COVID-19 vaccine candidate using SpyCatcher multimerization of the SARS-CoV-2 spike protein receptor-binding domain induces potent neutralising antibody responses. Nat Commun (2021) 12(1):542. doi: 10.1038/s41467-020-20654-7
63. Shambaugh C, Azshirvani S, Yu L, Pache J, Lambert SL, Zuo F, et al. Development of a high-throughput respiratory syncytial virus fluorescent focus-based microneutralization assay. Clin Vaccine Immunol (2017) 24(12). doi: 10.1128/CVI.00225-17
64. Snapper CM, Paul WE. Interferon-gamma and b cell stimulatory factor-1 reciprocally regulate ig isotype production. Sci (New York NY). (1987) 236(4804):944–7. doi: 10.1126/science.3107127
65. Bruhns P. Properties of mouse and human IgG receptors and their contribution to disease models. Blood. (2012) 119(24):5640–9. doi: 10.1182/blood-2012-01-380121
66. Valenzuela NM, Schaub S. The biology of IgG subclasses and their clinical relevance to transplantation. Transplantation. (2018) 102(1S Suppl 1):S7–S13. doi: 10.1097/TP.0000000000001816
67. Malonis RJ, Lai JR, Vergnolle O. Peptide-based vaccines: current progress and future challenges. Chem Rev (2020) 120(6):3210–29. doi: 10.1021/acs.chemrev.9b00472
68. Powell TJ, Jacobs A, Tang J, Cardenas E, Palath N, Daniels J, et al. Microparticle RSV vaccines presenting the G protein CX3C chemokine motif in the context of TLR signaling induce protective Th1 immune responses and prevent pulmonary eosinophilia post-challenge. Vaccines (2022) 10(12). doi: 10.3390/vaccines10122078
69. Jones HG, Ritschel T, Pascual G, Brakenhoff JPJ, Keogh E, Furmanova-Hollenstein P, et al. Structural basis for recognition of the central conserved region of RSV G by neutralizing human antibodies. PLoS pathogens. (2018) 14(3):e1006935. doi: 10.1371/journal.ppat.1006935
70. Kishko M, Catalan J, Swanson K, DiNapoli J, Wei CJ, Delagrave S, et al. Evaluation of the respiratory syncytial virus G-directed neutralizing antibody response in the human airway epithelial cell model. Virology. (2020) 550:21–6. doi: 10.1016/j.virol.2020.08.006
71. Ruckwardt TJ, Malloy AM, Gostick E, Price DA, Dash P, McClaren JL, et al. Neonatal CD8 T-cell hierarchy is distinct from adults and is influenced by intrinsic T cell properties in respiratory syncytial virus infected mice. PLoS pathogens. (2011) 7(12):e1002377. doi: 10.1371/journal.ppat.1002377

72. Jo YM, Kim J, Chang J. Vaccine containing G protein fragment and recombinant baculovirus expressing M2 protein induces protective immunity to respiratory syncytial virus. Clin Exp Vaccine Res (2019) 8(1):43–53. doi: 10.7774/cevr.2019.8.1.43
73. Cheon IS, Shim BS, Park SM, Choi Y, Jang JE, Jung DI, et al. Development of safe and effective RSV vaccine by modified CD4 epitope in G protein core fragment (Gcf). PLoS One (2014) 9(4):e94269. doi: 10.1371/journal.pone.0094269
74. Acosta PL, Caballero MT, Polack FP. Brief history and characterization of enhanced respiratory syncytial virus disease. Clin Vaccine Immunol (2015) 23(3):189–95. doi: 10.1128/CVI.00609-15
75. Collins PL, Graham BS. Viral and host factors in human respiratory syncytial virus pathogenesis. J Virol (2008) 82(5):2040–55. doi: 10.1128/JVI.01625-07
76. Hall CB, Walsh EE, Long CE, Schnabel KC. Immunity to and frequency of reinfection with respiratory syncytial virus. J Infect diseases. (1991) 163(4):693–8. doi: 10.1093/infdis/163.4.693
77. Souza AP, Leitao LA, Luisi F, Souza RG, Coutinho SE, Silva JR, et al. Lack of association between viral load and severity of acute bronchiolitis in infants. J Bras Pneumol (2016) 42(4):261–5. doi: 10.1590/s1806-37562015000000241
78. Uusitupa E, Waris M, Heikkinen T. Association of viral load with disease severity in outpatient children with respiratory syncytial virus infection. J Infect diseases. (2020) 222(2):298–304. doi: 10.1093/infdis/jiaa076
79. Biacchesi S, Skiadopoulos MH, Yang L, Lamirande EW, Tran KC, Murphy BR, et al. Recombinant human metapneumovirus lacking the small hydrophobic SH and/or attachment G glycoprotein: deletion of G yields a promising vaccine candidate. J Virol (2004) 78(23):12877–87. doi: 10.1128/JVI.78.23.12877-12887.2004
80. Caidi H, Miao C, Thornburg NJ, Tripp RA, Anderson LJ, Haynes LM. Anti-respiratory syncytial virus (RSV) G monoclonal antibodies reduce lung inflammation and viral lung titers when delivered therapeutically in a BALB/c mouse model. Antiviral Res (2018) 154:149–57. doi: 10.1016/j.antiviral.2018.04.014
81. Lee HJ, Lee JY, Park MH, Kim JY, Chang J. Monoclonal antibody against G glycoprotein increases respiratory syncytial virus clearance In vivo and prevents vaccine-enhanced diseases. PLoS One (2017) 12(1):e0169139. doi: 10.1371/journal.pone.0169139
82. Boyoglu-Barnum S, Todd SO, Chirkova T, Barnum TR, Gaston KA, Haynes LM, et al. An anti-G protein monoclonal antibody treats RSV disease more effectively than an anti-f monoclonal antibody in BALB/c mice. Virology. (2015) 483:117–25. doi: 10.1016/j.virol.2015.02.035
83. Boyoglu-Barnum S, Chirkova T, Todd SO, Barnum TR, Gaston KA, Jorquera P, et al. Prophylaxis with a respiratory syncytial virus (RSV) anti-G protein monoclonal antibody shifts the adaptive immune response to RSV rA2-line19F infection from Th2 to Th1 in BALB/c mice. J Virol (2014) 88(18):10569–83. doi: 10.1128/JVI.01503-14
84. Boyoglu-Barnum S, Gaston KA, Todd SO, Boyoglu C, Chirkova T, Barnum TR, et al. A respiratory syncytial virus (RSV) anti-G protein F(ab')2 monoclonal antibody

suppresses mucous production and breathing effort in RSV rA2-line19F-infected BALB/c mice. J Virol (2013) 87(20):10955–67. doi: 10.1128/JVI.01164-13
85. Radu GU, Caidi H, Miao C, Tripp RA, Anderson LJ, Haynes LM. Prophylactic treatment with a G glycoprotein monoclonal antibody reduces pulmonary inflammation in respiratory syncytial virus (RSV)-challenged naive and formalin-inactivated RSV-immunized BALB/c mice. J Virol (2010) 84(18):9632–6. doi: 10.1128/JVI.00451-10
86. Higgins D, Trujillo C, Keech C. Advances in RSV vaccine research and development - a global agenda. Vaccine. (2016) 34(26):2870–5. doi: 10.1016/j.vaccine.2016.03.10987. Collarini EJ, Lee FE, Foord O, Park M, Sperinde G, Wu H, et al. Potent high-affinity antibodies for treatment and prophylaxis of respiratory syncytial virus derived from b cells of infected patients. J Immunol (Baltimore Md 1950). (2009) 183(10):6338–45. doi: 10.4049/jimmunol.0901373
88. Fuentes S, Coyle EM, Golding H, Khurana S. Nonglycosylated G-protein vaccine protects against homologous and heterologous respiratory syncytial virus (RSV) challenge, while glycosylated G enhances RSV lung pathology and cytokine levels. J Virol (2015) 89(16):8193–205. doi: 10.1128/JVI.00133-15
89. Swanson KA, Rainho-Tomko JN, Williams ZP, Lanza L, Peredelchuk M, Kishko M, et al. A respiratory syncytial virus (RSV) f protein nanoparticle vaccine focuses antibody responses to a conserved neutralization domain. Sci Immunol (2020) 5(47). doi: 10.1126/sciimmunol.aba6466
90. Garcia-Maurino C, Moore-Clingenpeel M, Thomas J, Mertz S, Cohen DM, Ramilo O, et al. Viral load dynamics and clinical disease severity in infants with respiratory syncytial virus infection. J Infect diseases. (2019) 219(8):1207–15. doi: 10.1093/infdis/jiy655
91. Jafri HS, Wu X, Makari D, Henrickson KJ. Distribution of respiratory syncytial virus subtypes a and b among infants presenting to the emergency department with lower respiratory tract infection or apnea. Pediatr Infect Dis J (2013) 32(4):335–40. doi: 10.1097/INF.0b013e318282603a
92. Mejias A, Hall MW, Ramilo O. Immune monitoring of children with respiratory syncytial virus infection. Expert Rev Clin Immunol (2013) 9(5):393–5. doi: 10.1586/eci.13.20
93. Waris ME, Tsou C, Erdman DD, Zaki SR, Anderson LJ. Respiratory synctial virus infection in BALB/c mice previously immunized with formalin-inactivated virus induces enhanced pulmonary inflammatory response with a predominant Th2-like cytokine pattern. J Virol (1996) 70(5):2852–60. doi: 10.1128/jvi.70.5.2852-2860.1996

Chapter 2 Layer-by-Layer Microparticle Vaccines Containing Altered Sequences of the Central Conserved Domain of the RSV G Protein Induce Improved Immune Responses

Harrison C. Bergeron[1], Jackelyn Murray[1], Maria G. Juarez[2], Les P. Jones[1], Rebecca M. DuBois[2], Thomas J. Powell[3], Ralph A. Tripp[1,*]
[1] University of Georgia College of Veterinary Medicine, Department of Infectious Diseases, Athens, GA, 30605, USA
[2] University of California, Santa Cruz, Department of Biomolecular Engineering, Santa Cruz, CA, 95064, USA
[3] Artificial Cell Technologies, 5 Science Park, New Haven, CT, 06511, USA
*** Correspondence:** Ralph A Tripp, PhD; ratripp@uga.edu

2.1 Abstract

We previously showed that an RSV G protein central conserved domain (CCD) nanoparticle vaccine containing an S177Q mutation (NP-S177Q) induced superior immunogenicity and RSV-neutralizing antibodies compared to RSV G protein vaccination alone in mice. Boosting BALB/c mice with NP-S177Q vaccines improved correlates of protection and reduced markers of immunopathology following RSV challenge. This study examined microparticle vaccines displaying the CCD with an RSV G S177Q mutation (MP-S177Q) adjuvanted with monophosphoryl lipid A (MPLA) in BALB/c mice. Our findings show that adjuvanted MP-S177Q vaccination has preclinical promise toward developing an effective and safe precision RSV vaccine.

2.2 Introduction

Vaccination can reduce diseases associated with viral infection. However, effective vaccination can be difficult as not all vaccine platforms are suitable for all vaccinees, and there are issues with temperature stability and other factors required

by the vaccine, as well as costs or access to vaccines in lower-income countries. These concerns have driven the development of new vaccine strategies and novel vaccine platforms such as mRNA. Precision vaccination, or the ability to optimize vaccines specific to vulnerable populations, particularly those at greatest risk of infection (e.g., young, elderly, and the immunocompromised), has become reachable based on customized platforms that provide new vaccines and immunization strategies for different populations. For example, the recent approval of RSV vaccines is based on vaccination recommendations for specific risk groups to provide the safest and most effective use of vaccines (1). The FDA approval of Abrysvo™ was the first RSV vaccine approved for use in pregnant individuals to prevent lower respiratory tract disease (LRTD) caused by RSV in infants from birth through 6 months of age, and Abrysvo™ was approved for use at 32 through 36 weeks gestational age of pregnancy. Later, the FDA approved Abrysvo™ for preventing LRTD caused by RSV in individuals 60 years of age and older (2). Another advancement in RSV vaccine development has been the layer-by-layer (LbL) method of vaccine fabrication, which offers simplicity in the assembly of vaccine platforms and allows for the rapid development of synthetic vaccine components, providing the foundation for optimizing vaccine antigens needed for precision vaccine development. Additionally, LbL vaccines offer versatility and modularity, opening new paths for designing vaccination platforms with high efficiency and specific targeting and minimizing the economic impact associated with their fabrication. MP vaccines utilizing LbL constructs can be used to develop the RSV vaccine (3). Importantly, LbL particles

facilitate how the antigen payloads are presented to the immune system by antigen-presenting cells (APCs), enhance antigen uptake by APCs, act as an antigen depot, and modulate the Th1/Th2 immune response when engineered to include an innate immune agonist (4, 5). Importantly, LbL-MP carrying the RSV G protein CX3C motif and an RSV M2 CD8+ epitope promoted both humoral and cellular immune responses and protected the mice from RSV challenge (6).

It is necessary to develop safe and effective RSV vaccines because RSV is a leading cause of respiratory disease in infants, young children, the elderly, and the immunocompromised (7-9). Childhood RSV disease has a substantial global health and economic burden (8), and RSV is the primary cause of hospitalization due to lower respiratory tract disease among infants worldwide (10). Recently, new RSV countermeasures have been approved by the FDA. Specifically, Beyfortus™ (nirsevimab) was approved for the prevention of RSV in neonates and infants born during or entering their first RSV season and in children up to 24 months of age (11). Nirsevimab is a human monoclonal antibody administered as a 1-dose intramuscular injection shortly before or during the RSV season, typically during spring in the US. It is an extended half-life prophylactic monoclonal antibody targeting the pre-fusion RSV F protein (12). Presently, the development of RSV vaccines and monoclonal antibody therapy appears to have addressed the significant need to control and prevent RSV disease, the consequences of potential antibodies against the F protein and viral escape remain unknown. Complex issues related to global distribution, manufacturing, and potential off-target effects of monoclonal antibodies (mAbs) with

an extended half-life emphasize the need to consider new vaccine platforms for RSV, as high therapeutic dosing can affect efficacy, clearance, tissue bioavailability, or toxicity.

The RSV G protein is a 298 aa viral surface protein that contains cytosolic, transmembrane, and ectodomain regions (13). The intact G protein is heavily glycosylated and diverse. However, the central conserved domain (CCD; aa 157-198) is highly conserved between RSV A and B types, lacks glycosylation, and contains a CX3C chemokine mimic motif (aa 182–186) that binds to the fractalkine receptor, CX3CR1, and can trigger fractalkine-like host cell responses that contribute to inflammatory mechanisms (14-16). The G protein CX3C motif interacts with CX3CR1 on ciliated respiratory epithelia and some immune cells (17-20). Interestingly, the RSV G protein has an alternative translation site (Met 48), which results in an unstable transmembrane domain and the release of a soluble form of G protein (sG) protein (21, 22). sG contains the CX3C motif and, like membrane-bound G (mG), functions to interfere with host immunity (23). Previous work by our group and others has shown the CX3C motif of RSV G protein impacts immunity by biasing the pathogenic Th2-type cytokine response, reducing IFNγ and IL-6, altering trafficking of CX3CR1+ CTL and NK cells and pulmonary eosinophils to the virus-infected lung, modifying host miRNAs, dampening type I IFN responses, impacting TLR4 signaling, and reducing antibody production (24-26). Importantly, several studies have shown antibodies against RSV G protein to be protective by interfering

with RSV-mediated immune antagonism, improving the protective Th1-type immunity, and blocking CX3C-CX3CR1 mediation (27-34).

When considering RSV vaccine platforms, vaccine safety is important as it has been shown that some viral vaccines may induce vaccine-enhanced respiratory disease (VERD), which is atypical but can occur when vaccination promotes aberrant immune responses that exacerbate the disease caused by subsequent infection with the associated pathogen. VERD has been observed in humans in three vaccine trials against RSV, dengue, and measles (35-37). In 1966, RSV vaccine studies in infants and young children using a formalin-inactivated vaccine against RSV (FI-RSV) found that immunized children who were subsequently exposed to environmental RSV experienced an enhanced disease, and two immunized infants died (35). It was subsequently shown that the FI-RSV vaccine stimulated an unbalanced immune response in which the induced antibodies were directed against nonprotective epitopes concomitant with substantial Th2-type immune responses (38-41). The RSV G protein is attractive for vaccine development because the G protein CCD is essential for infectivity in vivo, it mediates attachment to airway epithelial cells, and the CCD has a conserved CX3C chemokine motif implicated in the alteration of the host immune response (33). It has been shown that mAb TRL3D3, which binds with low picomolar affinity to an epitope within the CCD, can neutralize sG and has antiviral activity (29, 33, 42-44). Thus, safety and the ability to induce a balanced Th1/Th2 cytokine response and reduce G protein reactogenicity are important considerations in RSV vaccine development.

We showed that immunizing mice with LbL-NP vaccines containing a G peptide having a CX3C chemokine motif (aa 169-198) and a CD8+ epitope from the RSV M2 protein induced antibodies that block CX3CL1 (fractalkine) chemotactic activity of RSV G protein and protected from infection replication post-RSV challenge (4, 5). Importantly, structural studies revealed conformational epitopes in a larger region of RSV G, i.e. between aa 157-198 (43-45). This study investigated the next iteration of RSV G protein MP vaccines using a larger RSV G peptide with a G protein S177Q mutation and a Th1-biasing adjuvant, i.e., monophosphoryl lipid A (MPLA) (46). Previously, we showed that RSV G with an S177Q mutation does not alter conformational epitopes but increases anti-G protein antibody responses and Th1-type cytokine responses, improves RSV neutralization, and does not mediate enhanced disease compared to wild-type G (47-49). This study compared rationally designed G protein mutants to wild-type G protein immune responses in both male and female BALB/c mice as it is known there are sex-dependent immune responses to vaccinations and infections (47), and elucidating these similarities and differences improves preclinical modeling. The results showed that mice boosted with MP-S177Q developed superior immunogenicity and neutralizing antibodies compared to MP-WT boosting. Importantly, MP-S177Q vaccination led to strong viral neutralization compared to MP-WT, and MP-S177Q vaccination improved bronchoalveolar lavage fluid (BALF) Th1-type cytokine concentrations following the RSV challenge compared to MP-WT and vehicle-vaccinated mice. This study shows

that a rationally mutated RSV G protein microparticle vaccine is safe, effective, and can advance precision RSV vaccines.

2.3 Materials and Methods

2.3.1 Cells and viruses

Vero E6 cells (CRL-1586), A549 cells (CCL-185), and HEp-2 cells (CCL-23), all from American Type Culture Collection (ATCC, Manassas, VA), were maintained in 10% fetal bovine serum (FBS) in DMEM (Hyclone, Logan, UT). RSV A2 (ATCC VR-1540) and RSV A2 expressing GFP (a kind gift from Dr. Marty Moore, Meissa Vaccines) were propagated in HEp-2 cells (ATCC CCL-23) as described (48).

2.3.2 Microparticle (MP) construction

LbL-MP were fabricated as previously described (6). Poly-L-glutamic acid (PGA) and poly-L-lysine (PLL) were alternately layered on 3 μm diameter CaCO3 cores to build up a non-crosslinked, seven-layer base film and capped with designed peptide (DP) containing RSV G CCD epitopes. MPs were evaluated by amino acid analysis (DP content), Limulus amebocyte assay (endotoxin levels), and dynamic light scattering (particle size dispersity). Peptide sequences are clarified in Table 1.

Construct	Peptide sequence
WT	SKPNNDFHFEVFNFVPCSIC**S**NNPTCWAICKRIPNKKPGKKK$_{20}$
S177Q	SKPNNDFHFEVFNFVPCSIC**Q**NNPTCWAICKRIPNKKPGKKK$_{20}$

Table 2.1 Microparticle vaccine peptides

2.3.3 ELISA analysis of MPs with mAb 2D10

All antigens (MP-WT, MP-S177Q, MP-Empty, and recombinant RSV G ectodomain) were examined using high-binding ELISA plates (Costar 3590, Corning, NY) at 10

µg/ml in PBS. Recombinant RSV G ectodomain was generated as described previously (49). PBS was plated for negative control wells. Plates were left at 4°C overnight. Plates were washed four times with PBS-T (PBS+0.1% Tween). Blocking buffer (PBS-T+5% milk) was added to all wells and incubated for 2 h at room temperature. mAb 2D10 was diluted to 5 µg/ml in blocking buffer and serially diluted 1:3 with blocking buffer. The blocking solution was decanted, and 150 µl of serially diluted mAb 2D10 was added to wells. Plates were incubated for 1 h at room temperature and then washed four times with PBS-T. 50 µl of goat anti-human IgG Fc secondary antibody conjugated to horseradish peroxidase (HRP) (Invitrogen A18817, Carlsbad, CA) diluted 1:3,000 in PBS-T+1% milk was added to all wells. Plates were incubated for 1 h at room temperature and then washed four times with PBS-T. Each well was added 100 µl of TMB substrate (Sigma T0440, Burlington, MA). Plates were developed for 10 min, at which point the reaction was quenched by adding 100 µl 1N sulfuric acid. Absorbance at 450 nm was quantified using a plate reader. Plotting with SEM values was carried out using Excel.

2.3.4 Mice

Male and female BALB/c mice (10 - 12 weeks old; Jackson Laboratories, Bar Harbor, ME) were housed in microisolator cages with 12 h light/dark cycle and fed ad libitum. The mice received a priming dose of 10 µg MP-WT, MP-S177Q, or empty MPs. All vaccines were adjuvanted with 10 µg MPLA (VacciGrade™ from S. Minnesota R595, InvivoGen, San Diego, CA, (a TLR4 agonist) diluted in PBS. Mice were i.m. vaccinated in the left and right rear quadriceps with 0.05 mL/quadriceps. On day 21 post-prime, mice were boosted with the same dose of the homologous

vaccine. Mice were bled on day 28 post-prime (day 7 post-boost). On day 14 post-boost (or day 35 post-prime), mice were i.p. anesthetized with 2, 2, 2-tribromoethanol (T48402; Sigma-Aldrich St. Louis, MO), and i.n. challenged with 10^6 PFU RSV A2 diluted in PBS. Mice were monitored daily and euthanized on day five pi. Sera, BALF, and lungs were collected and stored in serum-free-DMEM on ice during organ processing.

2.3.5 ELISA

Sera were evaluated for anti-RSV IgG levels. Briefly, high-binding ELISA plates (Corning, Corning, NY) were coated with RSV A2 or B1 (5 μg/mL) overnight at 4°C. The next day, the wells were washed three times with 1x KPL wash buffer in distilled water (SeraCare, Milford, MA) and blocked with Blotto (5% non-fat dry milk) for 1 h at 37°C. Blotto was removed, and the sera were 1:3 diluted (starting at 1:50) in Blotto and added to wells for 1 h at 37°C. The wells were washed 3x with KPL wash buffer, and secondary goat-anti-mouse IgG-AP (ThermoFisher, Waltham, MA) or secondary subtype IgG1 or IgG2a antibodies (Southern Biotech, Birmingham, AL) were added. Plates were incubated for 1 h at 37°C, washed 3x with KPL wash buffer, and developed with p-Nitrophenyl Phosphate (pNPP; ThermoFisher) for 45 min, and read using a BioTek plate reader (BioTek, Winooski, VT) at OD405. The area under the curve (AUC) was calculated using Prism 10 (GraphPad, La Jolla, CA).

2.3.6 Virus neutralization

To determine the level of antisera neutralization, a reporter-based microneutralization protocol was performed as previously described (50). Briefly, sera were pooled and heat-inactivated at 56°C for 30 min. Sera were two-fold diluted (starting at 1:40) and

pre-incubated with RSV A2/GFP (MOI = 0.1) for 1 h at 37°C +/- 10% guinea pig complement (C') (NovusBio, Centennial, CO). After pre-incubation, the mixture was added to confluent A549 cells in a 96-well plate for 24 h. At 24 hpi, cells were gently washed, fixed with 4% PFA (Ted Pella, Redding, CA) for 20 min at room temperature, and counterstained with 1 ug/mL 4',6-diamidino-2-phenylindole (DAPI) (ThermoFisher, Waltham, MA). Plates were read using Cellomics ArrayScan (ThermoFisher), and fluorescent focus units (FFUs) were automatically enumerated. The area under the curve (AUC) was calculated using Prism 10 (GraphPad, La Jolla, CA).

2.3.7 RSV plaque assays

Lungs were harvested on day 5 pi and homogenized in 1 mL DMEM using a GentleMACS tissue homogenizer (Miltenyi Biotec, Gaithersburg, MD). Homogenates were centrifuged at 500 xG at 4°C for 8 min, the supernatant diluted 10-fold in DMEM (Hyclone), and overlaid onto 90% confluent Vero E6 cells in 24 well plates. After 2 h of absorption, cells were overlaid with 2% methylcellulose (Sigma Aldrich, St. Louis, MO) and incubated at 37°C for 7 days. Following incubation, methylcellulose was aspirated, the cells washed with PBS, fixed with acetone:methanol (60:40, Sigma-Aldrich), and air-dried overnight. Wells were washed 3x with KPL wash buffer (VWR, Radnor, PA) and blocked with Blotto (ThermoFisher) overnight at 4°C. The next day, Blotto was removed, and a mAb cocktail against RSV F and G proteins (clones 131-2A, 131-2G) was diluted in Blotto (ThermoFisher) and added overnight at 4°C. Wells were washed 3x with KPL wash buffer (VWR), and goat anti-mouse-AP (ThermoFisher) was added overnight at 4°C.

Wells were washed 3x with KPL wash buffer (VWR), and RSV plaques were developed with KPL TrueBlue substrate solution (VWR) for 5 min, rinsed with distilled H2O, and enumerated using a dissection microscope (VWR).

Bronchoalveolar lavage fluid (BALF) cytokine/chemokine analysis

BALF was collected from terminally bled mice. The trachea was exposed, and the lungs were flushed 3x with 1 mL 0.5% BSA/PBS collected and centrifuged for 10 min at 500 xG at 4°C to isolate cell-free fluid. The BALF was stored at -80°C until analysis. BALF was analyzed in the Milliplex MAP Mouse Cytokine/Chemokine Immunology Multiplex Assay as described by the manufacturer (Millipore Sigma, Rockville, MD) using standards and quality controls included in the kit. Individual BALF samples were run in duplicate from n = 4-5 mice/group/sex in one experiment. Samples were analyzed on a Luminex 200 instrument (Luminex Corporation, Austin, TX) using Luminex xPONENT 3.1 software.

2.3.8 Statistics

Data were analyzed by one-way ANOVA with Dunnett's multiple comparison test, or Kruskal-Wallis was performed for non-parametric tests. $p<0.05$ was considered significant. Data are presented as mean +/- SEM. The vaccination study was performed once for male and female mice, while experiments were performed at least in duplicate with representative data shown.

2.4 Results

2.4.1 S177Q vaccination improves immunogenicity and neutralization

Previous results from our lab and others have shown that while the antibody response to RSV G protein is protective, vaccination with G protein containing an

unmodified CX3C motif and central conserved domain (CCD), may not be optimal for inducing peak immunogenicity, a feature linked to the CX3C motif (15, 51). We previously identified the serine-to-glutamine point mutation at aa177 (i.e., S177Q), which improves humoral responses to vaccination in intact G protein and G nanoparticle formulations (50, 52). We first evaluated MPs for proper folding and display of CCDs using an ELISA with mAb 2D10, which recognizes a conformational epitope that requires native disulfide linkages in the CCD (Figure 2.1A) (44). We found that mAb 2D10 bound to MP + wildtype G CCD (WT) and MP + G CCD S177Q (S177Q) but not empty MP (Figure 1B). These data support that MPs display correctly folded and disulfide-bonded CCDs and that the S177Q mutation does not disrupt this folding.

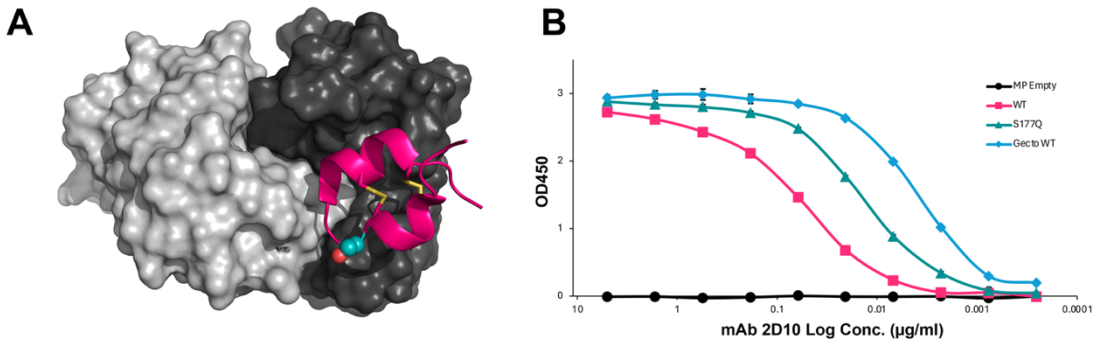

Figure 2.1 mAb 2D10 binds its conformational epitope on WT, and S177Q MP constructs.

(A) The crystal structure of antibody 2D10 (heavy chain in dark gray and light chain in light gray) is bound to the CCD (magenta) (PDB entry: 5wn9)(44). Disulfide bonds are colored in yellow. Serine 177 (cyan colored spheres) is outside the binding epitope and was used in structure-guided mutagenesis to produce the S177Q mutant rationally. The image was generated using PyMol. (B) ELISA showing MP construct reactivity to serial dilutions of mAb 2D10 (starting at a concentration of 5 µg/ml). mAb 2D10 binds to MP constructs displaying WT and S177Q CCDs but not empty MP. Recombinant RSV G ectodomain (GectoWT) was used as a positive control. ELISA was performed as technical triplicates, with shapes indicating mean +/- SEM.

To determine if this mutation improves immunogenicity in a LbL-MP platform (MP), male and female BALB/c mice were immunized on days 0 and 21 with 10 ug of either empty MP, MP + wildtype G CCD (WT) or MP + G CCD S177Q (S177Q), all adjuvanted with 10 ug MPLA. Sera from vaccines were examined for antibody responses on day 28 post-prime (day 7 post-boost). WT and S177Q vaccination induce robust antibody responses to RSV compared to empty MP or naïve controls (Figure 2.2). Importantly, S177Q vaccination resulted in increased antibody responses compared to WT in female ($p=0.12$) (Figure 2.2A and 2.2B) and male ($p = 0.074$) mice (Figure 2.2C and 2.2D) to near statistical ($p<0.05$) significance. These findings are consistent with our previous study (50). Although the magnitude of the serum antibody response was lower compared to responses to RSV A2 vaccination, S177Q antisera also reacted to RSV B1 by ELISA (Supplementary Figure 1) from male ($p=0.0574$) and female ($p=0.1954$) vaccinees, while WT sera did not ($p=0.42$ for males and $p=0.99$ for females) compared to naïve control sera.

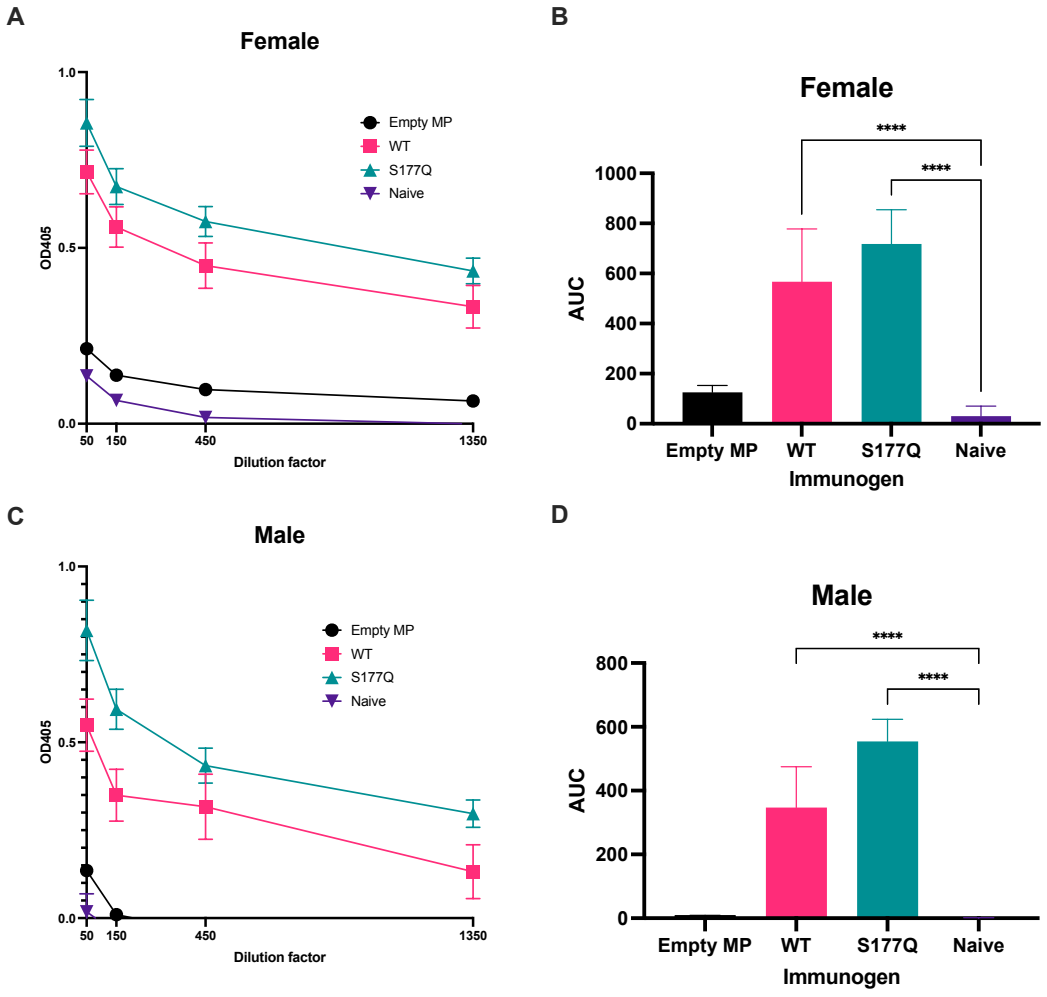

Figure 2.2 MP constructs are immunogenic, and S177Q improves immunogenicity.

Female (A, B) and male (C, D) BALB/c mice were immunized with 10 μg empty MP, WT, or S177Q, all adjuvanted with 10 μg MPLA on days 0 and 21. On day 28 (day 7 post-boost), sera were collected and analyzed for antibody responses against RSV A2 by ELISA. A and C show ½ log dilution of sera (starting at 1:50) with shapes indicating mean +/- SEM. B and D show the area under curve (AUC) +/- SEM. Data were analyzed by one-way ANOVA with Dunnett's multiple comparison test where * $p < 0.05$, ** $p < 0.01$, *** $p < 0.001$, and **** $p < 0.0001$.

We next determined the neutralizing capacity of antisera generated by MP vaccination (Figure 2.3). Sera from each group were heat-inactivated, pooled, and pre-incubated

with RSV A2-GFP (MOI 0.1) for 1h in the presence or absence of 10% guinea pig C'. Sera/virus mixture was then added to A549 cells for 24 h to determine neutralization. Remarkably, S177Q vaccination induced neutralizing antibodies regardless of C' addition in both female (Figure 2.3A, 2.3C) and male (Figure 2.3B, 2.3D) mice. WT G induced neutralizing antibodies in female mice in the absence or presence of C' ($p=0.054$, $p=0.062$, respectively), although to a lower extent than S177Q. While empty MP vaccination did not induce significant neutralizing antibody responses, it did elicit low levels of virus neutralization compared to naïve sera in the presence of complement. This result may be due to the induction of non-specific antibody responses that functioned with C' or other effector mechanisms, resulting in low levels of a non-specific neutralization activity. These data suggest the S177Q is more immunogenic and induces a greater neutralizing response than WT.

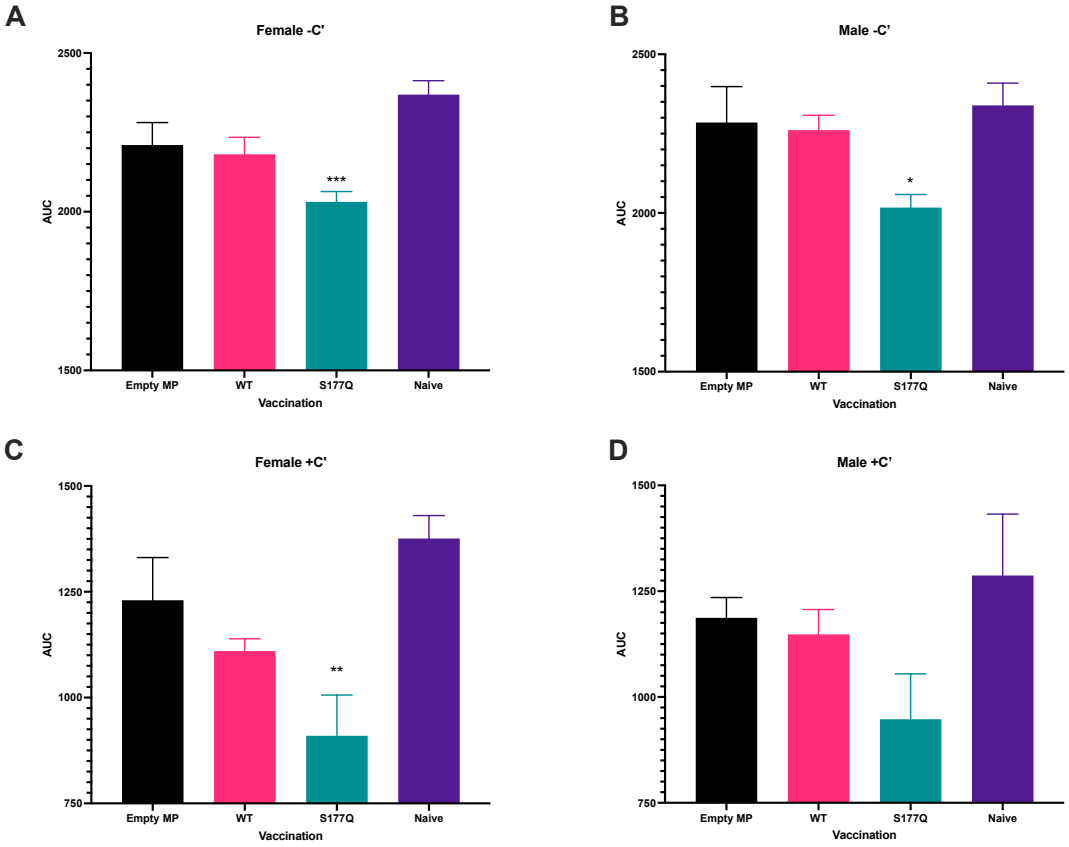

Figure 2.3 S177Q induces neutralizing antibodies.

Female (A, C) and male (B, D) BALB/c mice were immunized with 10 ug empty MP, WT, or S177Q, all adjuvanted with 10 μg MPLA on days 0 and 21. On day 28 (day 7 post-boost), sera were pooled (n = 5 mice/group/sex), 2-fold diluted (1:40 – 1:640), and analyzed for neutralization in the presence (A, C) or absence (B, D) of 10% guinea pig complement (C'). The area under the curve (AUC) was calculated, and the bars represent AUC's mean +/- SEM. Data were analyzed by one-way ANOVA with Dunnett's multiple comparison test where * $p < 0.05$, ** $p < 0.01$, *** $p < 0.001$, and **** $p < 0.0001$ compared to naïve.

2.4.2 Recall of anti-RSV antibody responses after RSV challenge

As expected, the WT and S177Q vaccines were immunogenic after prime and boost (Figure 2.2). We sought to evaluate the antibody response after RSV infection. WT and S177Q vaccinated mice were i.n. challenged with 10^6 PFU RSV A2, and on day 5 pi sera were collected and analyzed (Figure 2.4). Male and female mice

vaccinated with WT or S177Q vaccines had noteworthy and robust increases in serum IgG compared to empty MP vehicle control or WT vaccines (Figure 2.4 A – D), with no significant ($p<0.5$) differences between WT and S177Q vaccination. One metric for a safe RSV G vaccine is avoiding a Th2-type biased immune response following RSV infection, which has been correlated with enhanced pulmonary RSV disease (24). Antisera were analyzed for IgG subtypes to determine the Th1-type (IgG1) and Th2-type (IgG2a) antibody responses in vaccinated and challenged mice. IgG1 levels were significantly increased in both WT and S177Q vaccinations, with no significant ($p<0.05$) differences between WT and S177Q (Figure 2.4E and 2.4G). Interestingly, IgG2a levels were significantly ($p<0.05$) increased in S177Q compared to all other groups of vaccinated male mice (Figure 2.4H). While there were significant ($p<0.05$) but modest increases in female IgG2a responses in S177Q responses compared to controls, there were no significant ($p<0.05$) antibody increases compared to WT vaccinated mice (Figure 2.4F). These data suggest that S177Q vaccination drives a substantial recall and balanced Th1/2-type antibody response.

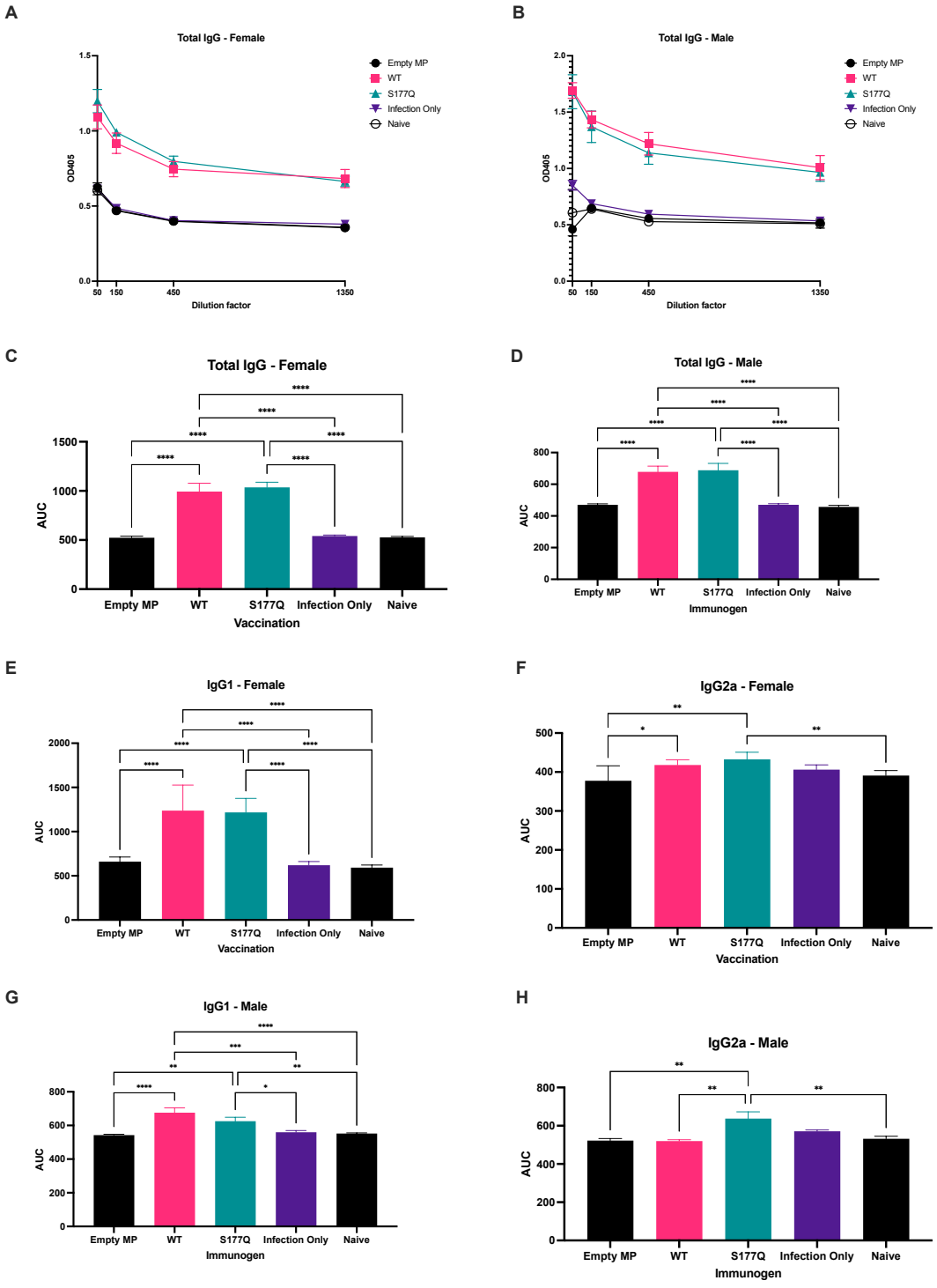

Figure 2.4 MP induces significant antibody recall responses during the RSV challenge.

Female (A, C, E, F) and male (B, D, G, H) BALB/c mice were immunized with 10 μg empty MP, WT, or S177Q all adjuvanted with 10 μg MPLA on days 0 and 21. 14 days post boost mice were i.n. challenged with 106 PFU RSV A2 or unchallenged as naïve control, and on day 5 pi, sera were collected and analyzed for total IgG, IgG1, and IgG2a. A and B show ½ log dilution of sera (starting at 1:50) with shapes indicating mean +/- SEM. C - H shows the area under the curve (AUC) +/- SEM. A - D show total IgG, E and G show IgG1, and F and H show IgG2a. Data were analyzed by one-way ANOVA with Dunnett's multiple comparison test where * $p<0.05$, ** $p<0.01$, *** $p<0.001$, and **** $p<0.0001$.

2.4.3 Vaccination reduces the lung viral load.

To determine the capacity of vaccination to protect against RSV challenge, immunized mice were challenged with 106 PFU RSV A2 on day 5 pi, the lungs were collected, and viral titers were determined by plaque assay. Significant ($p<0.05$) reductions in lung viral titers were observed in female (Figure 2.5A) and male (Figure 2.5B) mice vaccinated with WT or S177Q. Interestingly, vaccinated male mice demonstrated lower lung virus titer than female mice. At the same time, WT and S177Q vaccination was associated with reduced lung viral titers in both sexes. WT and S177Q vaccination in female mice reduced viral titers >2 logs compared to controls. Male mice vaccinated with WT had ~ 2 log reduction of lung titers compared to controls. However, S117Q vaccinated mice had >4 log reduction, and no detectable infectious virus was recovered.

A

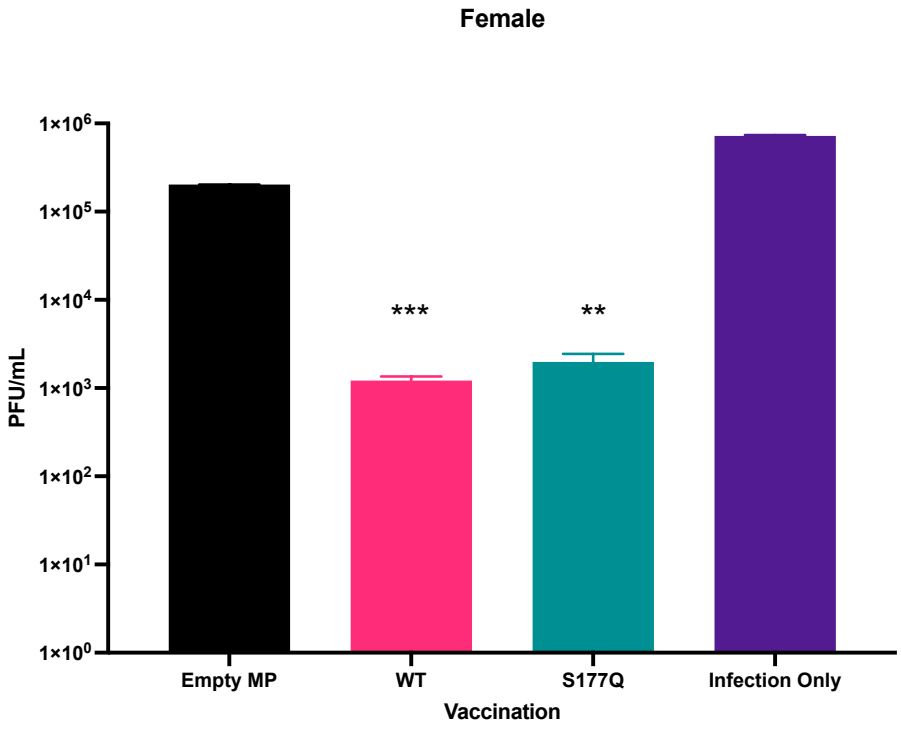
Female
1×10^6
1×10^5
1×10^4
1×10^3
1×10^2
1×10^1
1×10^0
PFU/mL
***
**
Empty MP
WT
S177Q
Infection Only
Vaccination

B

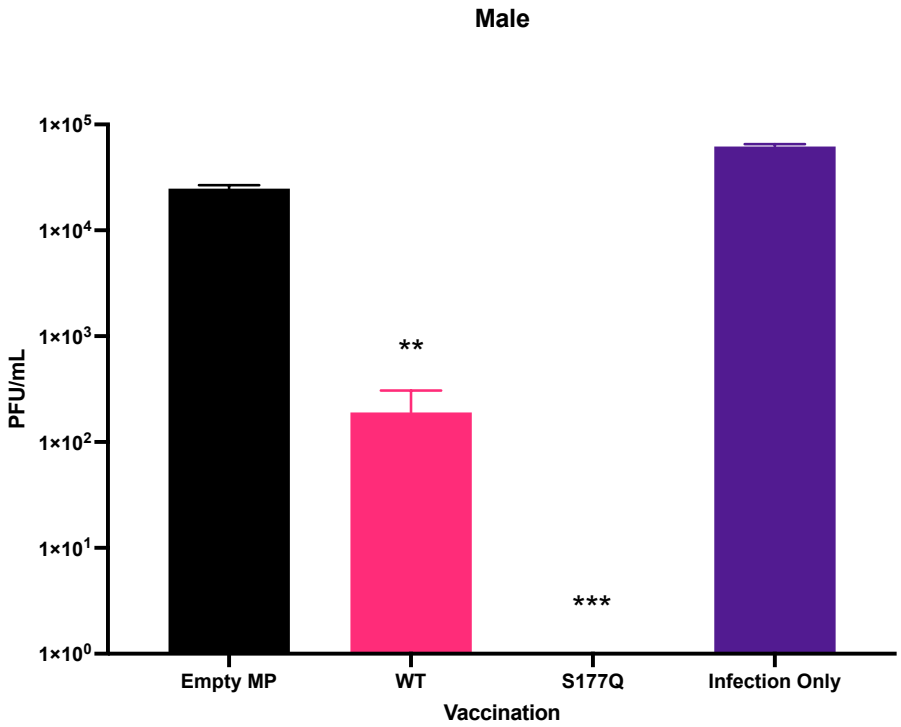
Male
1×10^5
1×10^4
1×10^3
1×10^2
1×10^1
1×10^0
PFU/mL
**
***
Empty MP
WT
S177Q
Infection Only
Vaccination

Figure 2.5 MP vaccination reduces lung RSV titers.

Female (A) and male (B) BALB/c mice were immunized with 10 □g empty MP, WT, or S177Q, all adjuvanted with 10 □g MPLA on days 0 and 21. 14 days post boost mice were i.n. challenged with 106 PFU RSV A2 or unchallenged as naïve control, and on day 5 pi, lungs were removed, and viral titers were determined by plaque assay. Bars represent mean PFU/mL +/- SEM. Data were analyzed by Kruskal-Wallis and compared to infection-only control where * $p<0.05$, ** $p<0.01$, *** $p< 0.001$, and **** $p<0.0001$.

2.5.6 Vaccination modifies the cytokine and chemokine responses to RSV challenge

A potential indicator of RSV disease is distorted cytokine or chemokine responses. To determine this possibility, on day 5 pi, the BALF was collected from vaccinated and challenged mice. The concentrations of cytokines and chemokines were measured by bead-based multiplex cytokine assay. Simultaneously, multiple cytokines and chemokines were evaluated in BALF from vaccinated groups using bead-based multiplex assays (Supplementary Figure 2). The results showed variation between sexes and some vaccination groups. However, for two cytokines, IFNγ and IP-10, there were significant increases in the BALF from female and male mice vaccinated with S177Q (Figure 2.6). IFNγ is a canonical Th1-type cytokine, and IP-10 is a chemokine affected downstream of IFNγ. Both are biomarkers for a Th1-type immune response. While the magnitude differed somewhat, female mice had significant ($p<0.05$) increased IFNγ compared to control groups and a near-significant increase compared to WT BALF ($p = 0.056$) (Figure 2.6A). Male mice had significant ($p<0.05$) increases in BALF IFNγ levels compared to all other groups (Figure 2.6B). IP-10 concentrations in BALF of female mice were significantly increased in S177Q compared to empty MP and infection-only controls (Figure 2.6C). In contrast, male BALF IP-10 was significantly ($p<0.05$) increased compared to WT and the infection-

only control (Figure 2.6D). These data support improved protective Th1-type responses in S177Q vaccinated mice following infection. IgG subtype data (Figure 2.4) suggest these vaccines induce a Th1/2 balanced response that may subtly vary between males and females.

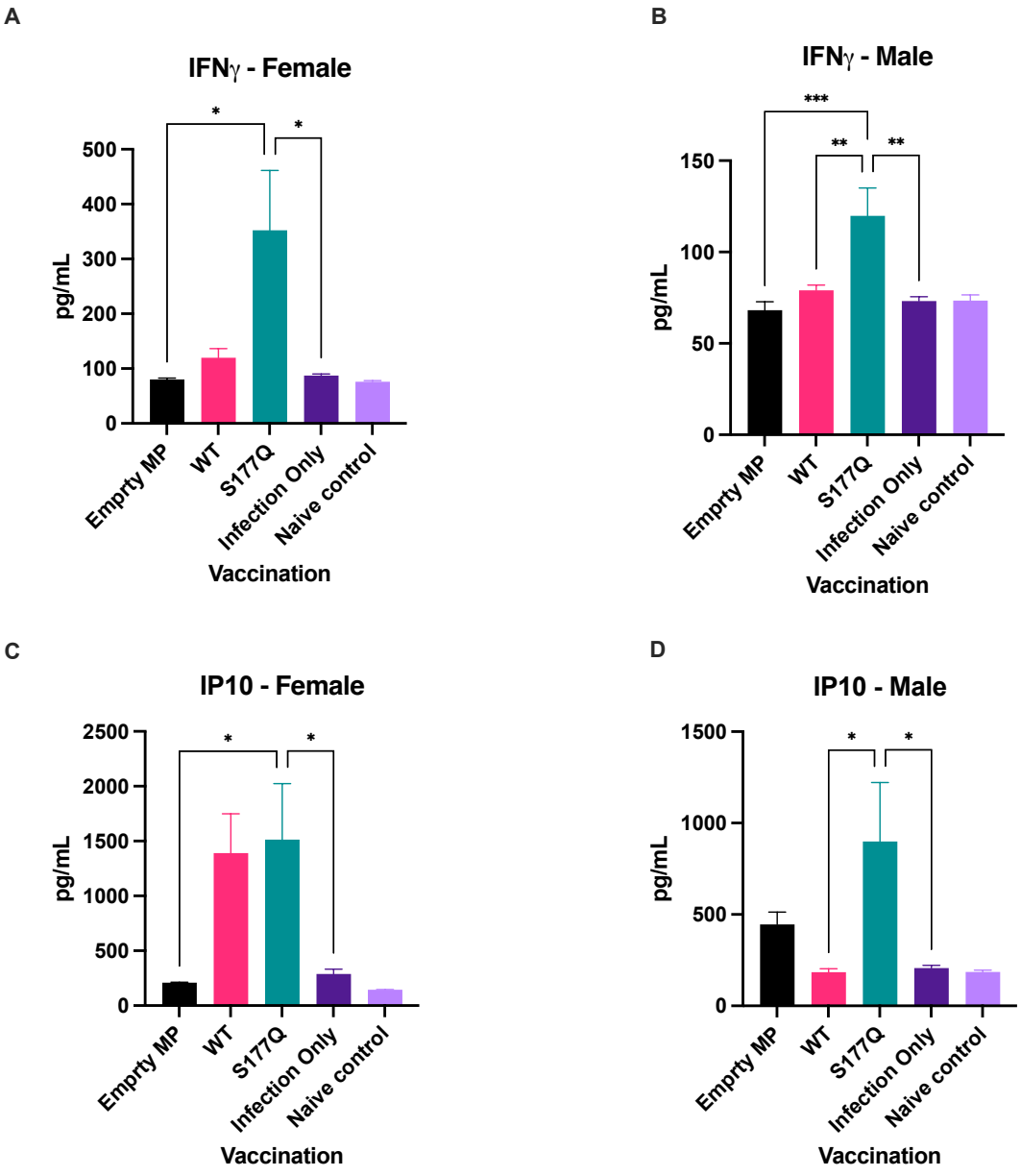

Figure 2.6 Cytokine responses following RSV infection.

Female (A and C) and male (B and D) BALB/c mice were immunized with 10 □g empty MP, WT, or S177Q, all adjuvanted with 10 □g MPLA on days 0 and 21. 14 days post boost mice were i.n. challenged with 106 PFU RSV A2 or unchallenged as naïve control, and on day 5 pi, BALF was collected and analyzed by bead-based cytokine assay. Concentrations of IFNγ (A and C) and IP-10 (B and D) are shown with bars representing mean pg/mL + SEM. Data were analyzed by one-way ANOVA with Dunnett's multiple comparison test where * $p<0.05$, ** $p<0.01$, *** $p<0.001$, and **** $p<0.0001$.

2.5 Discussion

Major advancements in RSV countermeasures have been recently achieved. Two vaccines are available, one for the elderly and one for pregnant women, and a new immune prophylactic is available for all infants (2, 53, 54). Despite these successes, there remains a need for safe and effective RSV vaccines for infants, especially those 2-5 years of age, for whom none of the new countermeasures are approved. We have designed modalities targeting the RSV G protein to address these gaps. During infection, the G protein is responsible for initial virion attachment to host cells via CX3CR1 expressed on airway epithelial cells and interfering with host immunity to infection (24, 26). Therefore, targeting the CX3C motif within the RSV G protein provides two biological mechanisms of protection – reducing initial virion attachment to host cells and preventing immune modulations mediated by G protein. Given the role of the G protein in disease and the history of VERD, there is a major focus on safe countermeasures with low potential reactogenicity, justifying the bias in the field toward developing anti-F protein countermeasures.

We and others have previously described RSV G protein countermeasures that are safe and effective. Specifically, a recent report described a G protein CCD NP vaccine that induced substantial RSV neutralization capability in primary human

airway epithelial cell (hAEC) cultures (55). Similarly, our previous RSV G NP vaccines elicited antibody responses that were neutralizing in vitro with the addition of complement (50). Surprisingly, RSV G MP vaccines noted here neutralize regardless of C', and the S177Q mutation induces improved immunogenicity and neutralization. Another hurdle in developing RSV G protein vaccines is relatively poor immunogenicity. The G protein may prevent sufficient antibody responses, potentially due to infection and re-regulation of neonatal regulatory B cells (nBreg) (56), soluble G protein antigenic decoy (21), or modification of T cell trafficking (57). Given that RSV G appears to leverage its CX3C motif to interact with CX3CR1 and elicit these immune modulating effects, we hypothesized that we could mitigate this issue by mutating residues in the CCD(15, 18). However, to consider the consequences of mutating residues in the CCD that might be important for recognition of neutralizing antibodies, a panel of CCD mutant vaccine candidates were generated by structure guided mutagenesis using high-resolution crystal structures of mAb's 3D3, 2D10, and 3G12(49). Importantly, their epitopes revealed that mAb's 3D3 and 3G12 all use amino acids located on the N-terminal region of the CCD that were not included in our previous CCD-MP vaccine designs(43, 44). Therefore, the new panel of CCD mutant vaccine candidates included a longer range of amino acids in the CCD to fully encompass epitopes recognized by neutralizing antibodies(49). Our investigation into mutated CCDs identified the S177Q mutant, which prevented CX3CR1-mediated chemotaxis similar to the CX4C mutation. However, mice vaccinated with the S177Q mutant had superior antibody responses

with improved Th1-type responses (52). Moreover, despite the mutation, S177Q vaccination still mediated CX3C-blocking antibody responses. Further, human anti-RSV reference sera bind the S177Q mutant with high affinity, similar to binding to WT, and S177Q retains high affinity binding to human and mouse mAbs (49). These previous studies demonstrated the translatable feasibility of the S177Q mutation as an immunogenic and safe antigen, which was recapitulated in the MP platform. Here, S177Q vaccination induced greater IgG responses, including IgG2a, and there were increased concentrations of Th1-type analytes in the BALF on day 5 pi (i.e., IFNγ and IP-10) compared to WT. Finally, this study was performed in male and female BALB/c mice, highlighting subtle inter-sex responses, but broadly, S177Q vaccination was superior in both sexes.

While these studies are promising, we are interested in precision medicine to design the most appropriate vaccine candidate for RSV in infants and young children. We intend to build on the studies shown here to develop LbL-MP RSV G vaccines, as the benefits of this vaccine platform include improved uptake by APCs, resulting in greater immunogenicity.

2.6 Conflict of Interest

Authors declare no conflicts of interest.

2.7 Author Contributions

HB designed and carried out experiments and helped write and edit the manuscript. HB, JM, and MJ were involved in data acquisition. LJ and TJP provided reagents. RD and RT secured funding, guided the project, and wrote and edited the manuscript. All authors contributed to the article and approved the submitted version.

2.8 Funding
Funding was provided by the Georgia Research Alliance (GRA) and from NIH

1R01AI166066.

2.9 Acknowledgment
We gratefully acknowledge Edwin Cardenas, Andrea Jacobs, and Jie Tang for

providing reagents and conducting mouse studies.

2.10 Supplementary

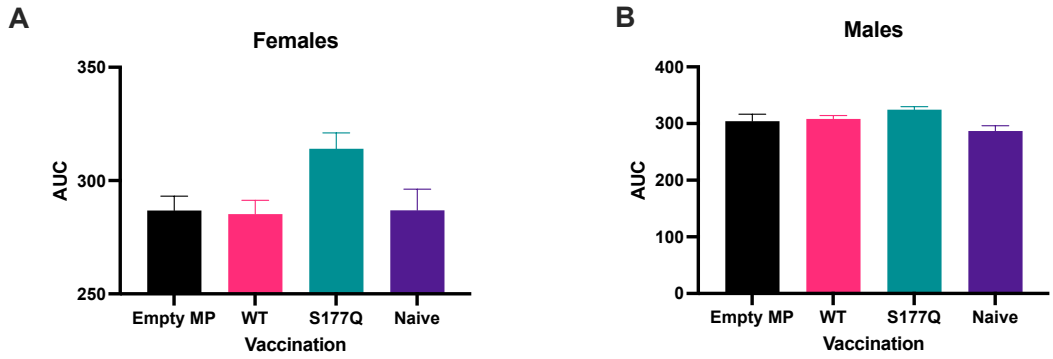

Figure 2.7 Antisera binding to RSV B.

Antisera from (A) female and (B) male mice on day 28 (day 7 post boost) binding to RSV B1. Only antisera generated from S177Q vaccination induced notable binding to RSV B1 compared to naive sera, while empty MP and WT did not. Data were analyzed by one-way ANOVA with Dunnett's multiple comparison test. Compared to naïve sera, empty MP $p > 0.99$ (female) and $p = 0.58$ (male), WT $p>0.99$ (female) and $p=0.42$ (male), and S177Q $p = 0.057$ (male) and S177Q $=0.20$ (female).

A

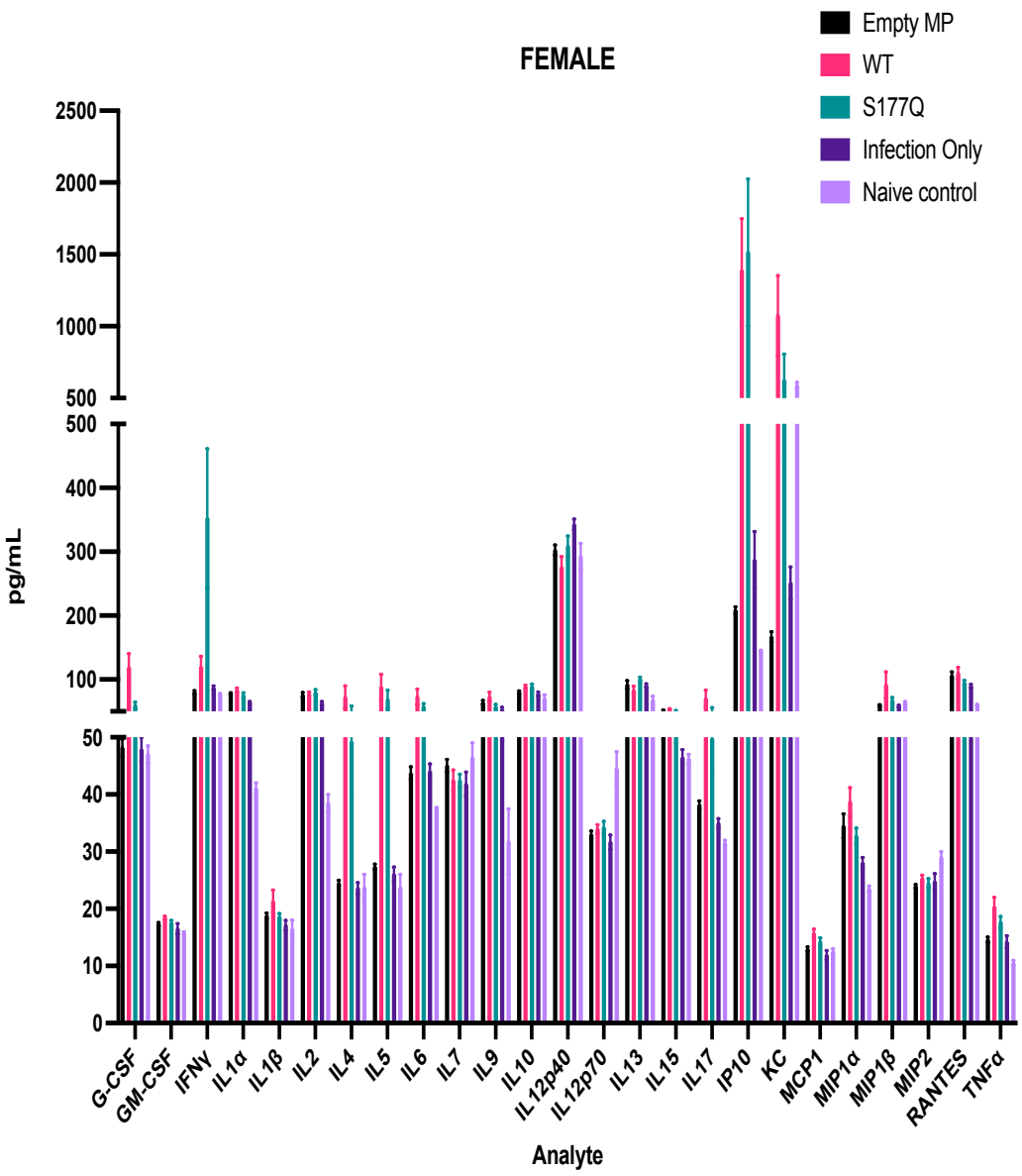
FEMALE
Empty MP
WT
S177Q
Infection Only
Naive control
pg/mL
2500
2000
1500
1000
500
500
400
300
200
100
50
40
30
20
10
0
G-CSF
GM-CSF
IFNγ
IL1α
IL1β
IL2
IL4
IL5
IL6
IL7
IL9
IL10
IL12p40
IL12p70
IL13
IL15
IL17
IP10
KC
MCP1
MIP1α
MIP1β
MIP2
RANTES
TNFα
Analyte

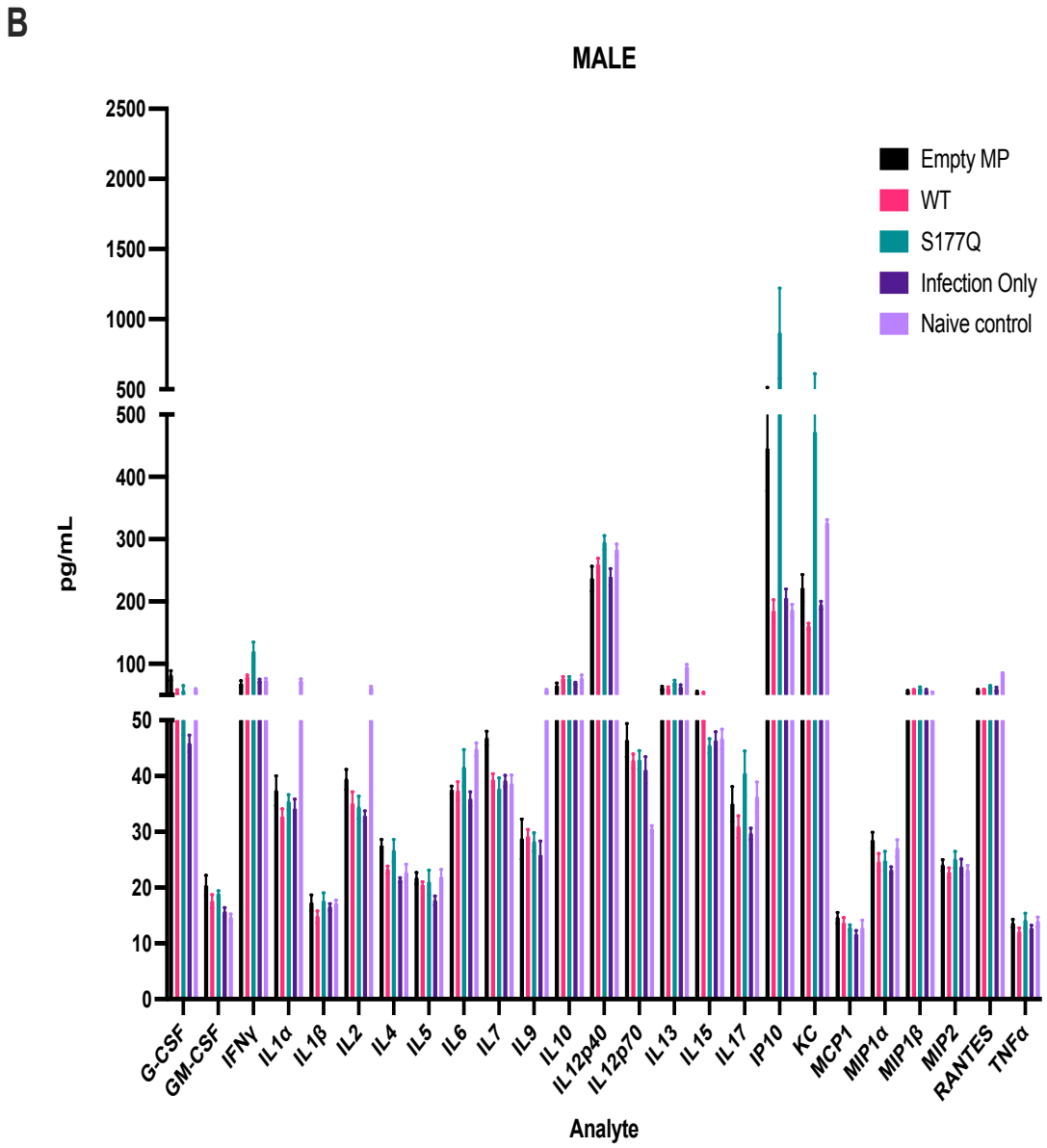

Figure 2.8 25-plex cytokine/chemokine concentrations in the BALF of challenged animals.

BALF was collected on day 5 pi from (A) female and (B) male vaccinated mice and analyzed by 25-plex Luminex (Millipore). Bars represent analytes' mean concentration (pg/mL) +/- SEM.

2.11 References

1. Ruckwardt TJ. The road to approved vaccines for respiratory syncytial virus. NPJ Vaccines. 2023;8(1):138.

2. Kampmann B, Madhi SA, Munjal I, Simoes EAF, Pahud BA, Llapur C, et al. Bivalent Prefusion F Vaccine in Pregnancy to Prevent RSV Illness in Infants. N Engl J Med. 2023;388(16):1451-64.
3. Jorquera PA, Tripp RA. Synthetic Biodegradable Microparticle and Nanoparticle Vaccines against the Respiratory Syncytial Virus. Vaccines (Basel). 2016;4(4).
4. Jorquera PA, Choi Y, Oakley KE, Powell TJ, Boyd JG, Palath N, et al. Nanoparticle vaccines encompassing the respiratory syncytial virus (RSV) G protein CX3C chemokine motif induce robust immunity protecting from challenge and disease. PLoS One. 2013;8(9):e74905.
5. Jorquera PA, Oakley KE, Powell TJ, Palath N, Boyd JG, Tripp RA. Layer-By-Layer Nanoparticle Vaccines Carrying the G Protein CX3C Motif Protect against RSV Infection and Disease. Vaccines (Basel). 2015;3(4):829-49.
6. Powell TJ, Jacobs A, Tang J, Cardenas E, Palath N, Daniels J, et al. Microparticle RSV Vaccines Presenting the G Protein CX3C Chemokine Motif in the Context of TLR Signaling Induce Protective Th1 Immune Responses and Prevent Pulmonary Eosinophilia Post-Challenge. Vaccines (Basel). 2022;10(12).
7. Chatzis O, Darbre S, Pasquier J, Meylan P, Manuel O, Aubert JD, et al. Burden of severe RSV disease among immunocompromised children and adults: a 10 year retrospective study. BMC Infect Dis. 2018;18(1):111.
8. Munro APS, Martinon-Torres F, Drysdale SB, Faust SN. The disease burden of respiratory syncytial virus in Infants. Curr Opin Infect Dis. 2023;36(5):379-84.
9. Jain H, Schweitzer JW, Justice NA. Respiratory Syncytial Virus Infection in Children. StatPearls. Treasure Island (FL)2024.
10. Hall CB. The burgeoning burden of respiratory syncytial virus among children. Infect Disord Drug Targets. 2012;12(2):92-7.
11. Zhaori G. Nirsevimab brings breakthrough in the prevention of respiratory syncytial virus infection in infants - Importance of design. Pediatr Investig. 2023;7(2):144-6.
12. Jorgensen SCJ. Nirsevimab: review of pharmacology, antiviral activity and emerging clinical experience for respiratory syncytial virus infection in infants. J Antimicrob Chemother. 2023;78(5):1143-9.
13. McLellan JS, Ray WC, Peeples ME. Structure and function of respiratory syncytial virus surface glycoproteins. Curr Top Microbiol Immunol. 2013;372:83-104.
14. Bakre AA, Harcourt JL, Haynes LM, Anderson LJ, Tripp RA. The Central Conserved Region (CCR) of Respiratory Syncytial Virus (RSV) G Protein Modulates Host miRNA Expression and Alters the Cellular Response to Infection. Vaccines (Basel). 2017;5(3).
15. Chirkova T, Boyoglu-Barnum S, Gaston KA, Malik FM, Trau SP, Oomens AG, Anderson LJ. Respiratory syncytial virus G protein CX3C motif impairs human airway epithelial and immune cell responses. J Virol. 2013;87(24):13466-79.
16. Anderson LJ, Jadhao SJ, Paden CR, Tong S. Functional Features of the Respiratory Syncytial Virus G Protein. Viruses. 2021;13(7).

17. Zhang L, Peeples ME, Boucher RC, Collins PL, Pickles RJ. Respiratory syncytial virus infection of human airway epithelial cells is polarized, specific to ciliated cells, and without obvious cytopathology. J Virol. 2002;76(11):5654-66.
18. Chirkova T, Lin S, Oomens AGP, Gaston KA, Boyoglu-Barnum S, Meng J, et al. CX3CR1 is an important surface molecule for respiratory syncytial virus infection in human airway epithelial cells. J Gen Virol. 2015;96(9):2543-56.
19. Jeong KI, Piepenhagen PA, Kishko M, DiNapoli JM, Groppo RP, Zhang L, et al. CX3CR1 Is Expressed in Differentiated Human Ciliated Airway Cells and Co-Localizes with Respiratory Syncytial Virus on Cilia in a G Protein-Dependent Manner. PLoS One. 2015;10(6):e0130517.
20. Johnson SM, McNally BA, Ioannidis I, Flano E, Teng MN, Oomens AG, et al. Respiratory Syncytial Virus Uses CX3CR1 as a Receptor on Primary Human Airway Epithelial Cultures. PLoS Pathog. 2015;11(12):e1005318.
21. Bukreyev A, Yang L, Collins PL. The secreted G protein of human respiratory syncytial virus antagonizes antibody-mediated restriction of replication involving macrophages and complement. J Virol. 2012;86(19):10880-4.
22. Shingai M, Azuma M, Ebihara T, Sasai M, Funami K, Ayata M, et al. Soluble G protein of respiratory syncytial virus inhibits Toll-like receptor 3/4-mediated IFN-beta induction. Int Immunol. 2008;20(9):1169-80.
23. Liang B, Kabatova B, Kabat J, Dorward DW, Liu X, Surman S, et al. Effects of Alterations to the CX3C Motif and Secreted Form of Human Respiratory Syncytial Virus (RSV) G Protein on Immune Responses to a Parainfluenza Virus Vector Expressing the RSV G Protein. J Virol. 2019;93(7).
24. Bergeron HC, Tripp RA. Immunopathology of RSV: An Updated Review. Viruses. 2021;13(12).
25. Bergeron HC, Hansen MR, Tripp RA. Interferons-Implications in the Immune Response to Respiratory Viruses. Microorganisms. 2023;11(9).
26. Bergeron HC, Tripp RA. RSV Replication, Transmission, and Disease Are Influenced by the RSV G Protein. Viruses. 2022;14(11).
27. Bergeron HC, Kauvar LM, Tripp RA. Anti-G protein antibodies targeting the RSV G protein CX3C chemokine region improve the interferon response. Ther Adv Infect Dis. 2023;10:20499361231161157.
28. Boyoglu-Barnum S, Todd SO, Chirkova T, Barnum TR, Gaston KA, Haynes LM, et al. An anti-G protein monoclonal antibody treats RSV disease more effectively than an anti-F monoclonal antibody in BALB/c mice. Virology. 2015;483:117-25.
29. Caidi H, Miao C, Thornburg NJ, Tripp RA, Anderson LJ, Haynes LM. Anti-respiratory syncytial virus (RSV) G monoclonal antibodies reduce lung inflammation and viral lung titers when delivered therapeutically in a BALB/c mouse model. Antiviral Res. 2018;154:149-57.
30. Bergeron HC, Murray J, Arora A, Nunez Castrejon AM, DuBois RM, Anderson LJ, et al. Immune Prophylaxis Targeting the Respiratory Syncytial Virus (RSV) G Protein. Viruses. 2023;15(5).

31. Lee Y, Klenow L, Coyle EM, Grubbs G, Golding H, Khurana S. Monoclonal antibodies targeting sites in respiratory syncytial virus attachment G protein provide protection against RSV-A and RSV-B in mice. Nat Commun. 2024;15(1):2900.
32. Boyoglu-Barnum S, Gaston KA, Todd SO, Boyoglu C, Chirkova T, Barnum TR, et al. A respiratory syncytial virus (RSV) anti-G protein F(ab')2 monoclonal antibody suppresses mucous production and breathing effort in RSV rA2-line19F-infected BALB/c mice. J Virol. 2013;87(20):10955-67.
33. Tripp RA, Power UF, Openshaw PJM, Kauvar LM. Respiratory Syncytial Virus: Targeting the G Protein Provides a New Approach for an Old Problem. J Virol. 2018;92(3).
34. Haynes LM, Caidi H, Radu GU, Miao C, Harcourt JL, Tripp RA, Anderson LJ. Therapeutic monoclonal antibody treatment targeting respiratory syncytial virus (RSV) G protein mediates viral clearance and reduces the pathogenesis of RSV infection in BALB/c mice. J Infect Dis. 2009;200(3):439-47.
35. Kim HW, Canchola JG, Brandt CD, Pyles G, Chanock RM, Jensen K, Parrott RH. Respiratory syncytial virus disease in infants despite prior administration of antigenic inactivated vaccine. Am J Epidemiol. 1969;89(4):422-34.
36. Sridhar S, Luedtke A, Langevin E, Zhu M, Bonaparte M, Machabert T, et al. Effect of Dengue Serostatus on Dengue Vaccine Safety and Efficacy. N Engl J Med. 2018;379(4):327-40.
37. Fulginiti VA, Eller JJ, Downie AW, Kempe CH. Altered Reactivity to Measles Virus: Atypical Measles in Children Previously Immunized With Inactivated Measles Virus Vaccines. JAMA. 1967;202(12):1075-80.
38. Murphy BR, Walsh EE. Formalin-inactivated respiratory syncytial virus vaccine induces antibodies to the fusion glycoprotein that are deficient in fusion-inhibiting activity. J Clin Microbiol. 1988;26(8):1595-7.
39. Acosta PL, Caballero MT, Polack FP. Brief History and Characterization of Enhanced Respiratory Syncytial Virus Disease. Clin Vaccine Immunol. 2015;23(3):189-95.
40. Connors M, Giese NA, Kulkarni AB, Firestone CY, Morse HC, 3rd, Murphy BR. Enhanced pulmonary histopathology induced by respiratory syncytial virus (RSV) challenge of formalin-inactivated RSV-immunized BALB/c mice is abrogated by depletion of interleukin-4 (IL-4) and IL-10. J Virol. 1994;68(8):5321-5.
41. Waris ME, Tsou C, Erdman DD, Zaki SR, Anderson LJ. Respiratory synctial virus infection in BALB/c mice previously immunized with formalin-inactivated virus induces enhanced pulmonary inflammatory response with a predominant Th2-like cytokine pattern. J Virol. 1996;70(5):2852-60.
42. Hijano DR, Vu LD, Kauvar LM, Tripp RA, Polack FP, Cormier SA. Role of Type I Interferon (IFN) in the Respiratory Syncytial Virus (RSV) Immune Response and Disease Severity. Front Immunol. 2019;10:566.
43. Fedechkin SO, George NL, Nunez Castrejon AM, Dillen JR, Kauvar LM, DuBois RM. Conformational Flexibility in Respiratory Syncytial Virus G Neutralizing Epitopes. J Virol. 2020;94(6).

44. Fedechkin SO, George NL, Wolff JT, Kauvar LM, DuBois RM. Structures of respiratory syncytial virus G antigen bound to broadly neutralizing antibodies. Sci Immunol. 2018;3(21).
45. Jones HG, Ritschel T, Pascual G, Brakenhoff JPJ, Keogh E, Furmanova-Hollenstein P, et al. Structural basis for recognition of the central conserved region of RSV G by neutralizing human antibodies. PLoS Pathog. 2018;14(3):e1006935.
46. Schulke S, Vogel L, Junker AC, Hanschmann KM, Flaczyk A, Vieths S, Scheurer S. A Fusion Protein Consisting of the Vaccine Adjuvant Monophosphoryl Lipid A and the Allergen Ovalbumin Boosts Allergen-Specific Th1, Th2, and Th17 Responses In Vitro. J Immunol Res. 2016;2016:4156456.
47. Ursin RL, Klein SL. Sex Differences in Respiratory Viral Pathogenesis and Treatments. Annu Rev Virol. 2021;8(1):393-414.
48. Murray J, Bergeron HC, Jones LP, Reener ZB, Martin DE, Sancilio FD, Tripp RA. Probenecid Inhibits Respiratory Syncytial Virus (RSV) Replication. Viruses. 2022;14(5).
49. Nunez Castrejon AM, O'Rourke SM, Kauvar LM, DuBois RM. Structure-Based Design and Antigenic Validation of Respiratory Syncytial Virus G Immunogens. J Virol. 2022;96(7):e0220121.
50. Bergeron HC, Murray J, Juarez MG, Nangle SJ, DuBois RM, Tripp RA. Immunogenicity and protective efficacy of an RSV G S177Q central conserved domain nanoparticle vaccine. Front Immunol. 2023;14:1215323.
51. Harcourt JL, Karron RA, Tripp RA. Anti-G protein antibody responses to respiratory syncytial virus infection or vaccination are associated with inhibition of G protein CX3C-CX3CR1 binding and leukocyte chemotaxis. J Infect Dis. 2004;190(11):1936-40.
52. Bergeron HC, Murray J, Nunez Castrejon AM, DuBois RM, Tripp RA. Respiratory Syncytial Virus (RSV) G Protein Vaccines With Central Conserved Domain Mutations Induce CX3C-CX3CR1 Blocking Antibodies. Viruses. 2021;13(2).
53. Keam SJ. Nirsevimab: First Approval. Drugs. 2023;83(2):181-7.
54. Walsh EE, Perez Marc G, Zareba AM, Falsey AR, Jiang Q, Patton M, et al. Efficacy and Safety of a Bivalent RSV Prefusion F Vaccine in Older Adults. N Engl J Med. 2023;388(16):1465-77.
55. Voorzaat R, Cox F, van Overveld D, Le L, Tettero L, Vaneman J, et al. Design and Preclinical Evaluation of a Nanoparticle Vaccine against Respiratory Syncytial Virus Based on the Attachment Protein G. Vaccines (Basel). 2024;12(3).
56. Zhivaki D, Lemoine S, Lim A, Morva A, Vidalain PO, Schandene L, et al. Respiratory Syncytial Virus Infects Regulatory B Cells in Human Neonates via Chemokine Receptor CX3CR1 and Promotes Lung Disease Severity. Immunity. 2017;46(2):301-14.
57. Harcourt J, Alvarez R, Jones LP, Henderson C, Anderson LJ, Tripp RA. Respiratory syncytial virus G protein and G protein CX3C motif adversely affect CX3CR1+ T cell responses. J Immunol. 2006;176(3):1600-8.

Chapter 3 Structures of a Respiratory Syncytial Virus G Bound to Broadly-Reactive, High-Affinity Antibodies Reveal Novel Epitopes and Vaccine Insights

Maria G. Juarez[a], Sara M. O'Rourke[b,] John V. Dzimianski[b], Delia Gagnon[b], Gabriel Penunuri[b], Russel B. Corbett-Detig[b], Lawrence M. Kauvar[c], and Rebecca M. DuBois[b#]
[a]Department of Molecular, Cell, and Developmental Biology, University of California Santa Cruz, Santa Cruz, California, USA
[b]Department of Biomolecular Engineering, University of California Santa Cruz, Santa Cruz, California, USA
[c]Trellis Bioscience LLC, Redwood City, CA, USA
[#]Correspondence to: rmdubois@ucsc.edu

3.1 Abstract

Respiratory syncytial virus (RSV) is a leading cause of severe lower respiratory tract disease in children, immunocompromised populations, and the elderly. Newly available prophylactics involving the fusion glycoprotein (RSV F) demonstrate efficacy in preventing severe lower respiratory tract disease, however new formulations may be required to prevent upper-respiratory infections and reduce transmission. Thus, it is important to exploit other sites of vulnerability on the RSV virion. The RSV attachment glycoprotein G binds to the CX3CR1 chemokine receptor to promote viral entry into human airway epithelial cells and to modulate host immunity characterized by a dampened Th1/favored Th2 cytokine profile. Antibodies against RSV G are a known correlate of protection, however, RSV G itself has been overlooked as a vaccine immunogen due to its highly O-glycosylated and variable regions and low immunogenicity. Previously, several broadly-reactive, high-affinity anti-RSV G human monoclonal antibodies were isolated from RSV-experienced individuals and were shown to be broadly protective *in vitro* and *in vivo*.

In this study, we investigated three high-affinity antibodies from this panel. Using X-ray crystallography, we solved the structures of these antibodies in complex with an RSV G antigen and defined three novel conformational epitopes comprised of highly conserved RSV G residues on its central conserved domain (CCD). Binding competition studies and cryoelectron microscopic structural studies demonstrated that the CCD, while only 40 amino acids in length, can display two antigenic sites simultaneously. Analyses of anti-RSV G antibody germ line lineages in the context of antibody-CCD complex structures reveal strategies for the elicitation of lineage-diverse, broadly-reactive, high-affinity antibodies targeting RSV G. Specifically, we think developing vaccine designs that maintain RSV G CCD flexibility is key towards stimulating high-affinity antibodies with high sequence identity to their genomic precursors. Antigen flexibility might circumvent the need for antibodies to undergo prolonged affinity maturation that might be necessary to gain high affinity for more rigid antigens. Together, these findings support the synergistic potential of targeting the RSV G CCD in next-generation prophylactics.

3.2 Author Summary

Respiratory syncytial virus (RSV) utilizes two glycoproteins for efficient viral entry into airway epithelial cells: G and F. Virus attachment is mediated by the G glycoprotein and membrane-fusion is mediated by the F glycoprotein. Approved intervention strategies target RSV F alone. However, antibodies that target RSV G are also correlated to protection against severe RSV disease, and the development of strategies that target RSV G may synergize with current RSV F-targeted strategies to

provide more robust protection. Here, we investigated how antibodies target RSV G. We used biophysical methods to map the three-dimensional structures of tightly binding antibodies bound to RSV G to identify amino acids in the G protein that are important for vaccine design. We found that all antibodies bind a small region of RSV G that is highly conserved across RSV strains, termed the central conserved domain (CCD), and that this small region can bind up to two antibodies simultaneously. Additionally, the antibodies bind unique conformations, potentially resulting in resistance to virus mutations. Together, our findings serve as a blueprint for how we can use RSV G as an immunogen target.

3.3 Introduction

Lower respiratory infections are the leading cause of infant mortality worldwide with Respiratory Syncytial Virus (RSV) as the primary causative agent (1, 2). RSV induced lower respiratory disease also significantly impacts children under 5, immunocompromised individuals, and the elderly (3-7). Current FDA approved prophylactic strategies include two monoclonal antibodies, palivizumab (Synagis) and nirsevimab (Beyfortus), and three vaccines, Abrysvo (Pfizer), Arexvy (GSK), and mRESVIA (Moderna), all of which target only one of two major surface glycoproteins required by RSV for efficient infectivity (8-11). While these prophylactics are effective at reducing severe lower respiratory symptoms, upper respiratory infections are still prevalent and may contribute to RSV shedding and transmission in the community (12-16).

RSV is a filamentous, enveloped, negative sense, single stranded RNA virus with a 15 kilobase genome coding for 11 proteins (17). RSV belongs to the

pneumoviridae family of viruses which rely on their G and F glycoproteins to mediate attachment and membrane-fusion, respectively, to airway epithelial cells (17, 18). RSV F is a type I integral membrane protein and it facilitates fusion between the viral envelope and the host cell plasma membrane by undergoing a series of conformational changes taking it from a pre-fusion to a post-fusion state (18-20). Antibodies that target the pre-fusion state of RSV F are highly correlated to lower disease severity. In fact, Nirsevimab, Abryso, Arexvy and mRESVIA were all designed to target antigenic sites Ø and V which are only accessible in this conformation (21-23). However, known variability localized in these sites highlight the potential for the generation of escape against current prophylactics (20, 24, 25). This limitation materialized during a phase 3 clinical trial for Suptavumab, an anti-preF neutralizing antibody that failed to meet its efficacy endpoint due to the emergence of an RSV B strain yielding two key mutations in its binding epitope (26, 27). Escape mutations to Nirsevimab have already been identified in circulation, albeit in low abundance (28). Nevertheless, these escape mutants do not restrict viral fitness *in vitro*, making it possible for one to emerge as the dominant strain in the future (29).

To improve the protective breadth of RSV prophylactics, it is important to consider all correlates of protection which not only includes antibodies targeting pre-fusion RSV F, but also those targeting RSV G (23, 30). Antibodies that target RSV G are correlated with lower disease severity even while being present at $1/30^{th}$ the abundance of those that target the pre-fusion RSV F (23). Mechanistically, anti-RSV

G antibodies impede RSV G interaction with the human CX3CR1 receptor and are shown to directly neutralize virus infection *in vitro* using primary human airway (HAE) and bronchial epithelial cells (31-33). In one study using primary HAE's, anti-RSV G antibodies targeting the CCD reach up to 92% RSV neutralization where mAb 131-2G, a well-studied protective antibody *in vivo*, reaches complete neutralization (33-35). These antibodies also mediate opsonization, antibody dependent cellular cytotoxicity (ADCC), and antibody dependent cellular phagocytosis (ADCP) to promote viral clearance (31-33, 36). Moreover, anti-RSV G antibodies mitigate the immune modulating activities of RSV G, and using PBMC's, A549 cells, and a two-chamber transwell *in-vitro* system, anti-RSV G antibodies were found to restore type I and III interferon levels that are normally suppressed by RSV G-CX3CR1 interactions (37). *In vivo*, anti-RSV G antibodies work prophylactically and therapeutically to restore the Th1/Th2 cytokine profile, decrease mucus production, and relieve pulmonary inflammation using both mouse and cotton rat models (31, 34, 35, 38, 39). Notably, the broadly-reactive human monoclonal antibody 3D3 was superior to palivizumab (Synagis), a commercially available anti-RSV F monoclonal antibody, in reducing viral load in mice in both prophylactic and post-infection treatment models (39). Considering the crucial role of RSV G in viral entry and disease, it is a promising target for the development of improved prophylactic strategies that could be used alone and/or in combination with those that target RSV F.

RSV G is a ~300 amino acid type II membrane protein. Its extracellular region is composed of two highly-O-glycosylated mucin-like domains flanking a ~40 amino acid region known as the central conserved domain (CCD) (Fig1a). The CCD contains four cysteines that form two disulfide bonds with 1-4 and 2-3 connectivity. The CCD interacts with CX3CR1 to promote virus attachment and modulate immune responses (32, 36, 40). In previous studies, five high-resolution crystal structures of human monoclonal antibodies (mAbs) in complex with the RSV G CCD were elucidated (31, 41, 42). Unexpectedly, these structures revealed that these mAbs bind to conformational epitopes on the CCD, with additional interactions in the CCD beyond their linear epitopes. However, it is unclear how many conformational epitopes on the CCD exist, if multiple mAbs can bind to the CCD simultaneously, or how anti-RSV G human mAb sequences compare to their germlines and to each other.

To broaden our understanding of RSV G's epitope landscape and to understand the basis for elicitation of broadly-reactive high-affinity anti-RSV G antibodies from germline lineages, we investigated three broadly-reactive high-affinity anti-RSV G human mAbs 1G1, 2B11, and 1G8, which were previously isolated from RSV-experienced individuals (39). We solved the crystal structures of these antibodies in complex with the CCD and found that each mAb recognizes a unique conformational epitope, distinct from those characterized previously. Moreover, we found that while some mAbs bind to nearly identical CCD amino acids, each antibody makes unique combinations of hydrophobic, electrostatic, and

hydrogen bond interactions with either the backbone or sidechain to stabilize contact with the CCD(Fig1C). Epitope binning assays and cryoelectron microscopic studies reveal that the CCD can accommodate binding of two broadly-reactive monoclonal antibodies simultaneously, supporting the potential for combination anti-RSV G monoclonal antibody therapeutics. Finally, mAb sequence analyses of known broadly-reactive anti-RSV G human antibodies reveal that they are derived from several different germline lineages, and that they are of modest divergence from their germline genes. Altogether, these studies reveal the potential for the RSV G CCD to elicit diverse polyclonal antibody responses that resist virus mutational escape. This work serves to inform the development of next-generation RSV vaccines and antibody therapeutics.

3.4 Results

3.4.1 mAb 1G1, 2B11, and 1G8 bind RSV G with high affinity

Previously, a panel of broadly-reactive high-affinity human monoclonal antibodies (mAbs) was isolated from RSV-experienced individuals, and several mAbs were shown to be protective in prophylactic and post-infection mouse models (31, 35, 38, 39, 43-45). Here, we investigated mAbs 1G1, 1G8, and 2B11 from this panel. We selected mAb 1G1 because linear epitope mapping studies had shown no binding to any RSV G linear peptide, suggesting it has a conformational epitope. Additionally, we selected mAbs 1G8 and 2B11 due to their high affinity binding for RSV. All three mAbs are broadly-reactive and bind RSV G from both A and B subtypes (39).We first generated the recombinant mAbs 1G1, 1G8, and 2B11 and subjected them to kinetics

binding experiments with recombinant RSV G ectodomain (RSV G^{ecto}) using biolayer interferometry (Figure 3.1). We found that mAb 1G1 binds RSV G^{ecto} with nanomolar affinity (4.54 nM) while mAb 1G8 and mAb 2B11 bind RSV G^{ecto} with picomolar affinity (52.6 pM and 31.9 pM, respectively), consistent with published results (39)(Figure 3.1).

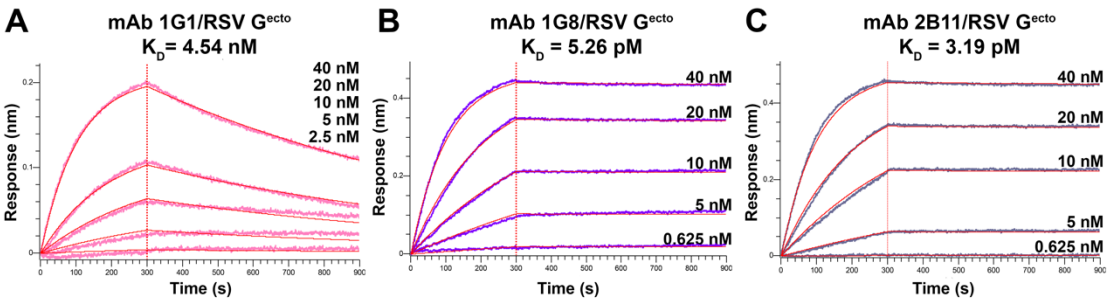

Figure 3.1 Biolayer interferometry binding studies show that mAbs 1G1, 1G8, and 2B11 bind to RSV Gecto with high affinity.

Biolayer interferometry traces for (A) mAb 1G1 (pink traces), (B) mAb 1G8 (purple traces), and (C) mAb 2B11 (slate gray traces) binding to RSV G^{ecto}. Concentrations of RSV G^{ecto} used for each trace are shown. The vertical red line indicates the transition of the biosensors from the association step to the dissociation step. Curve fits using a 1:1 global binding model are colored red. K_D values were determined using the average of two technical replicates.

3.4.2 High-resolution structures of Fabs 1G1, 1G8, and 2B11 bound to RSV G CCD

To understand the molecular basis for the high-affinity and broad-reactivity of these mAbs, we used X-ray crystallography to determine the high-resolution structures of the 1G1, 1G8, and 2B11 antigen binding fragments (Fabs) in complex with the RSV G CCD (Figure 3.2, Table 1). All three mAbs recognize novel conformational epitopes on the CCD formed by varying conformations of the CCD's N-terminal region (CCD amino acids 161-171) along with one face of the cysteine loop (CCD amino acids 172-187). These conformational epitopes explain the lack of linear

epitope binding for mAb 1G1 and unveil additional epitope amino acids beyond the linear epitopes for mAbs 1G8 and 2B11.

The 1G1-CCD complex structure reveals a 1,083-Å^2 interface of which 849-Å^2 is contributed by the heavy chain and 235-Å^2 is contributed by the light chain (Figure 3.2A). Major hydrophobic contacts are mediated by F103, Y54, P53, A30, T31, and T28 in the heavy chain complementarity-determining region (HCDR) loops HCDR2 and HCDR3 (Figure 3.2D). The N-terminal tail of the CCD is comprised of both polar and non-polar residues that are tucked into a pocket created by the 1G1 heavy and light chain. F170 and F163 in the CCD form pi-pi stacking interactions with Y104 in HCDR3 while F164 and H165 in the CCD rest inside a hydrophobic pocket formed by Y113 in HCDR3 and Y43, Y48, P54, and L55 in the light chain CDR (LCDR) loop LCDR2. A salt bridge is mediated by K49 in LCDR2 interacting with D162 in the CCD. Eleven hydrogen bond interactions, the most seen among the three crystal structures in this study, are predominantly mediated by HCDR2 and HCDR3 with the CCD backbone, a pattern observed previously in the antibody 3G12-CCD interface (42).

The 1G8-CCD complex structure reveals a 1040-Å^2 interface of which 845-Å^2 is contributed by the heavy chain and 196-Å^2 is contributed by the light chain (Figure 3.2B). The N-terminal tail of the CCD, which includes the linear epitope amino acids 164-172, wraps around the heavy and light chain, predominantly interacting with HCDR3, HCDR2, and LCDR3. Heavy chain residues V107, L104, L102, Y60, T59, and Y35 and light chain residue W94 form major and minor hydrophobic pockets

wherein lie the CCD amino acids F163, F165, V167, F168, and I175 (Figure 3.2E). Five out of six hydrogen bond interactions are found between antibody 1G8 and the CCD backbone.

The 2B11-CCD complex structure reveals a 1130-Å^2 interface of which 820-Å^2 is contributed by the heavy chain and 310-Å^2 is contributed by the light chain (Figure 3.2C). This interface is the largest out of the three in this study. Similar to what was observed in the structures with antibodies 1G1 and 1G8, the N-terminal tail of the CCD, which includes the linear epitope amino acids 162-172, forms intimate interactions with antibody 2B11 using both hydrogen bond and hydrophobic interactions (Figure 3.2F). In particular, HCDR2 amino acids I51, I52, P55, P56, A58, I60, and A72 form a hydrophobic interface to interact with the CCD. Interestingly, K74 in the 2B11 heavy chain forms a tunnel with P56 from HCDR2 where the CCD amino acid F165 neatly tucks into. Beyond the linear epitope amino acids, one face of the CCD's cysteine loop lays flat over 2B11, making prominent interactions with HCDR3, LCDR1, and LCDR3. Specifically, amino acids K23 and L101 in HCDR3 and H34, L99, I98, and T96 in LCDR1 and LCDR3 create a hydrophobic environment that interacts with CCD amino acids P180, T181, and I185 located at the apex of the cysteine loop. In addition, N179 in the CCD forms a hydrogen bond with H34 in LCDR2.

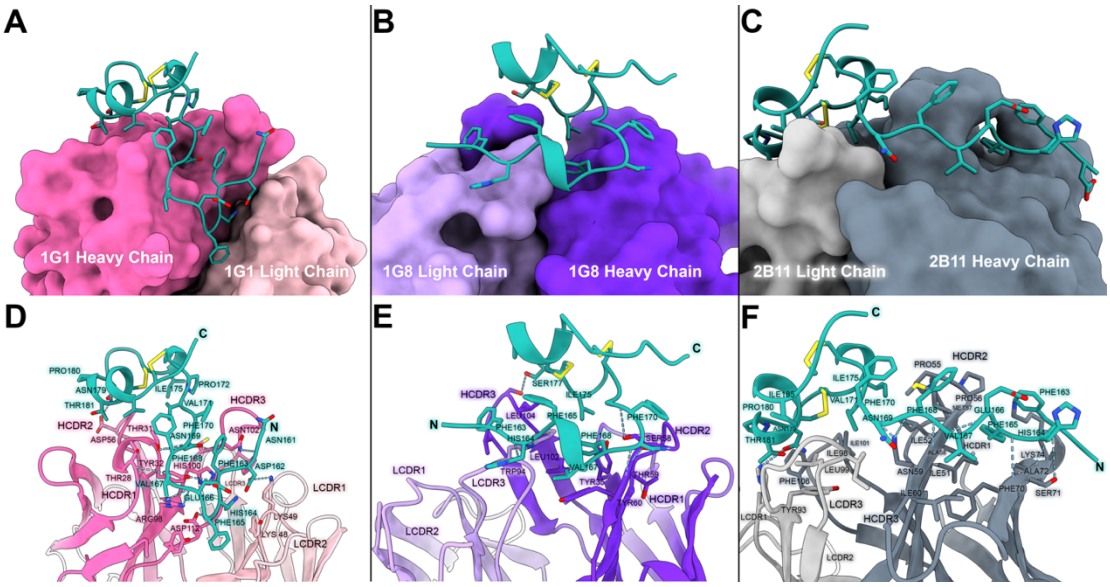

Figure 3.2 Crystal structures of antibody - RSV G CCD complexes reveal novel conformational epitopes.

A-C) Overall surface views of Fab 1G1 (pink), Fab 1G8 (purple), and Fab 2B11 (slate gray) bound to RSV G CCD (cyan). The CCD is shown as stick-and-ribbon view with disulfide bonds colored yellow. (D-F) Detailed stick-and-ribbon models depicting the molecular interactions between Fab 1G1, Fab 1G8, and Fab 2B11 and the CCD. Blue dotted lines indicate hydrogen bonds.

	Fab1G1-RSV G CCD	Fab 1G8-RSV G CCD	Fab 2B11-RSV G CCD
PDB Code	9CQA	9CQB	9CQD
Data collection			
Space group	P 21 21 21	P 31 2 1	P 1 21 1
Cell dimensions			
a, *b*, *c* (Å)	76.2,80.75, 175.18	67.39, 67.39, 286.34	74.65, 184.33, 161.23
α, β, © (°)	90, 90, 90	90, 90, 120	90, 96.87, 90
Resolution (Å)	47.32-1.74 (1.80-1.74)*	286.35-2.50 (2.54-2.50)	92.17-3.10 (3.15-3.10)
R_{merge}	0.100 (2.346)	0.171 (1.385)	0.412 (1.884)
R_{pim}			
$I / \sigma I$	14.6 (1.0)	12.7 (1.0)	3.3 (0.4)
CC(1/2)	0.999 (0.457)	0.997 (0.553)	0.984 (0.348)

Completeness (%)	99.2 (92.0)	100.0 (100.0)	100.0 (99.1)
Redundancy	13.2 (9.6)	18.9 (19.6)	13.2 (10.3)
Refinement			
Resolution (Å)	47.32-1.74 (1.80-1.74)	58.36-2.5 (2.59-2.50)	79.88-3.1 (3.21-3.10)
No. reflections	110821 (10422)	27222 (2663)	78360 (7747)
R_{work} / R_{free}	0.211/0.226	0.226/0.263	0.293/0.292
No. atoms			
Protein	7451	3578	25773
Ligand/ion	20	0	0
Water	393	16	0
B-factors			
Protein	34.79	54.45	74.50
Ligand/ion	30.0		
Water	39.08	44.81	
R.m.s. deviations			
Bond lengths (Å)	0.008	0.009	0.006
Bond angles (°)	0.97	1.09	0.88
Ramachandran statistics	98.56	93.07	93.55
Favored (%)	1.44	6.93	6.45
Allowed (%)	0.00	0.00	0.00
Outliers (%)			

Table 3.1 Data Collection and Refinement Statistics

*Values in parentheses are for highest-resolution shell.

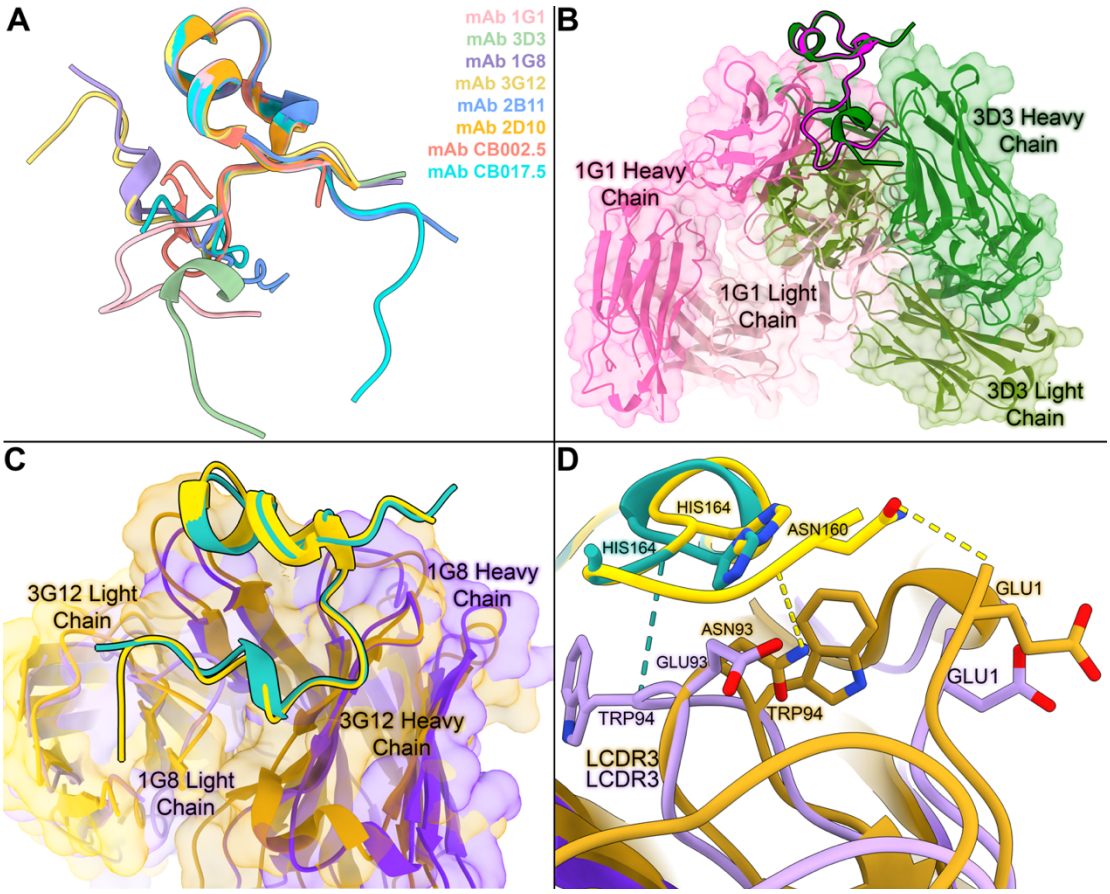

Figure 3.3 Comparative structural analyses of mAbs bound to similar RSV G CCD conformations reveal distinct interactions.

A) Overlay of RSV G CCD structures when bound to antibodies 1G1 (pink, PDB code 9CQA), 3D3 (pale green, PDB code 5WNA), 1G8 (periwinkle, PDB code 9CQB), 3G12 (yellow, PDB code 6UVO), 2B11 (blue, PDB code 9CQD), 2D10 (orange, PDB code 5WN9), CB002.5 (salmon pink, PDB code 6BLI), and CB017.5 (turquoise PDB code 6BLH). (B) Overlay of the structures Fab 1G1 (pink surface and ribbon model) and Fab 3D3 (green surface and ribbon model) bound to RSV G CCD (ribbon model in magenta when bound to Fab 1G1 and forest green when bound to Fab 3D3) (C,D) Overview and zoom-in of the overlay of the structures of Fab 1G8 (purple) and Fab 3G12 (goldenrod) bound to RSV G CCD (ribbon model in sea green when bound to Fab 1G8 and gold when bound to Fab 3G12). In panel C, sea green dotted lines represent hydrogen bonds between Fab 1G8 and RSV G CCD and gold dotted lines represent hydrogen bonds between Fab 3G12 and RSV G CCD.

3.4.3 Antibodies bound to similar RSV G CCD conformations and epitope amino acids utilize distinct molecular interactions

Alignment of the CCDs from the three antibody-CCD structures reported here and the five antibody-CCD structures determined previously reveal that the CCD can adopt several different conformations (Figure 3.3A)(32, 42, 43). However, two of the structures reported here appear to bind a conformation of CCD that is similar to that in another structure. For example, the RSV G CCD conformation and the epitope amino acids of Fab 1G1 resemble those of Fab 3D3 (42)(Figure 3.3B, 3.4C). However, a closer inspection reveals distinct angles of approach and distinct molecular interactions. Specifically, overlayed Fab 1G1-RSV G CCD and Fab 3D3-RSV G CCD structures reveal a 23.9° angle difference in approach by these antibodies for binding to the CCD (Figure 3.3B). At the molecular level, Fab 1G1 relies on an extensive hydrogen bond network with the CCD backbone whereas Fab 3D3 relies on sidechain-sidechain interactions (Figure 3.4C). Overall, while antibodies 1G1 and 3D3 bind to nearly identical amino acids on the CCD, their different angles of binding result in different contributions by each CCD amino acid to the epitope (Figure 3.4C).

In contrast, Fab 1G8 and Fab 3G12, which are from the same antibody germline (described further below), have similar angles of approach, capture RSV G CCD in a nearly identical conformation, and bind to nearly identical amino acids on the CCD (Figure 3.3C, 3.4C). Despite this, molecular nuances exist in their mode of binding to the CCD. Most notably, W94 from the Fab 1G8 LCDR2 is flipped over and positioned on the opposite side of the RSV G CCD N-terminal tail compared to

W94 from the Fab 3G12 LCDR2 (Figure 3.3D). This difference allows W94 to create a hydrogen bond with RSV G CCD amino acid H164, an interaction not seen in the Fab 3G12-RSV G CCD interface (Figure 3.3D, 3.4C). Also, N93 from the Fab 3G12 LCDR2 acts as a hydrogen bond donor to the carboxy group of RSV G CCD amino acid N160. At this same position, Fab 1G8 LCDR2 bares E93 which is negatively charged and is unable to act as a hydrogen bond donor.

Overall, comparative analyses of the epitopes for all six human mAbs from our panel for which we have high-resolution structures is shown in Figure 3.4. Although several of these mAbs bind to the same RSV G amino acids, each mAb displays a unique pattern and type of interaction, resulting in a unique epitope. Notably, analysis of approximately 6000 publicly available RSV G sequences reveals that the CCD is extraordinarily conserved (Figure 3.4A,B). This conservation explains the broad reactivity of these mAbs to both RSV A and B subtypes and further validates the RSV G CCD as a target for vaccines and therapeutics.

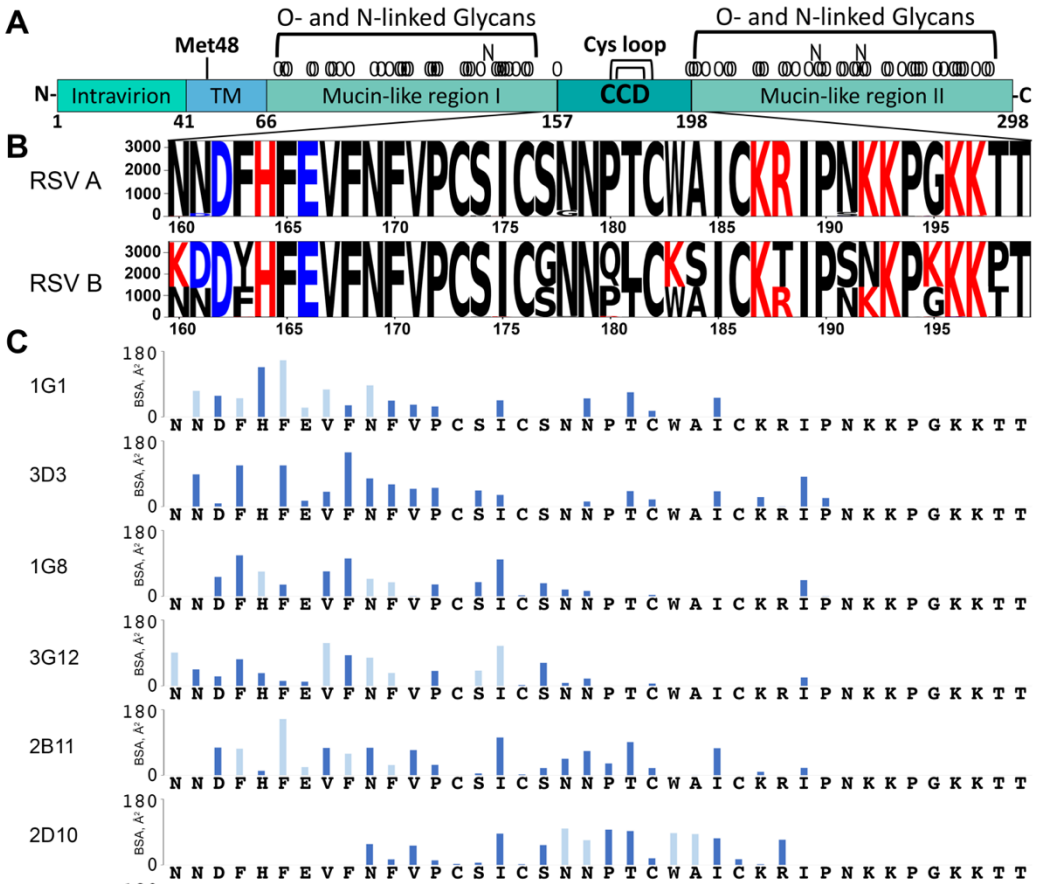

Figure 3.4 Broadly-reactive human mAbs use distinct interactions to bind to RSV G amino acids that are conserved across thousands of RSV genotypes

(A) Schematic of the RSV G gene. (B) RSV G CCD sequence conservation analysis using the National Center for Biotechnology Information (NCBI) database. (C) Buried surface area (BSA) quantitation for each antibody-CCD interface across each CCD amino acid using PDBePISA. Light blue bars indicate antibodies making a hydrogen bond with the CCD peptide backbone. Dark blue bars indicate other hydrophilic or hydrophobic interactions.

3.4.4 RSV G CCD has to two non-overlapping antigenic sites

To determine if the RSV G CCD, which is only ~40 amino acids, has more than one antigenic site, we conducted an epitope binning assay with the six human mAbs from our panel for which we have structural information. Biolayer interferometry biosensors coated with recombinant RSV G glycoprotein were used to

evaluate competitive binding by each mAb against the other, allowing the generation of a competitive binding matrix (Figure 3.5A,B). Antibodies 1G1, 3D3, 1G8, 3G12, and 2B11 all competed against each other for binding to RSV G, confirming that they share the same antigenic site, termed γ1, consistent with their structures and overlapping epitopes (Figure 3.5B). In contrast, antibody 2D10 was the only antibody in our panel that did not compete for binding to RSV G, supporting that it binds to a distinct antigenic site, termed γ2. Interestingly, antibody 2B11 appears to compete intermediately with antibody 2D10 for binding to RSV G when it is introduced in the second association step. This can be explained through its slight overlap with antibody 2D10 when viewing the overlaid structures (Figure 3.5C). No competition was observed when antibody 2B11 was introduced in the first association step, likely due to the higher affinity of antibody 2D10 (K_D < 1pM) compared to antibody 2B11 (K_D = 4.5 nM) (42).

Taking structural data and epitope binning data together, we propose antigenic site γ1 at residues N160-P172 and antigenic site γ2 at residues C173-R188. To further support this antigenic model, we incubated non-competing Fabs 2D10 and 3D3 with recombinant RSV G glycoprotein and used this sample to collect cryoelectron microscopy (cryo-EM) data (Figure 3.5E). A ~6.9 Å-resolution 3D volume shows the relative shape of two Fabs bound at one focal point (RSV G CCD)(Figure 3.5E). Unfortunately, the RSV G mucin-like domains are highly flexible and were not seen in both our raw and processed data and might also explain the low resolution. Nevertheless, we created an overlay of the crystal structures of Fabs 2B11 and 3D3

bound to RSV G CCD and modeled this into our 3D volume (Figure 3.5E). This data serves to corroborate the existence of two antigenic sites and is the first time that RSV G bound to two antibodies simultaneously has been visualized.

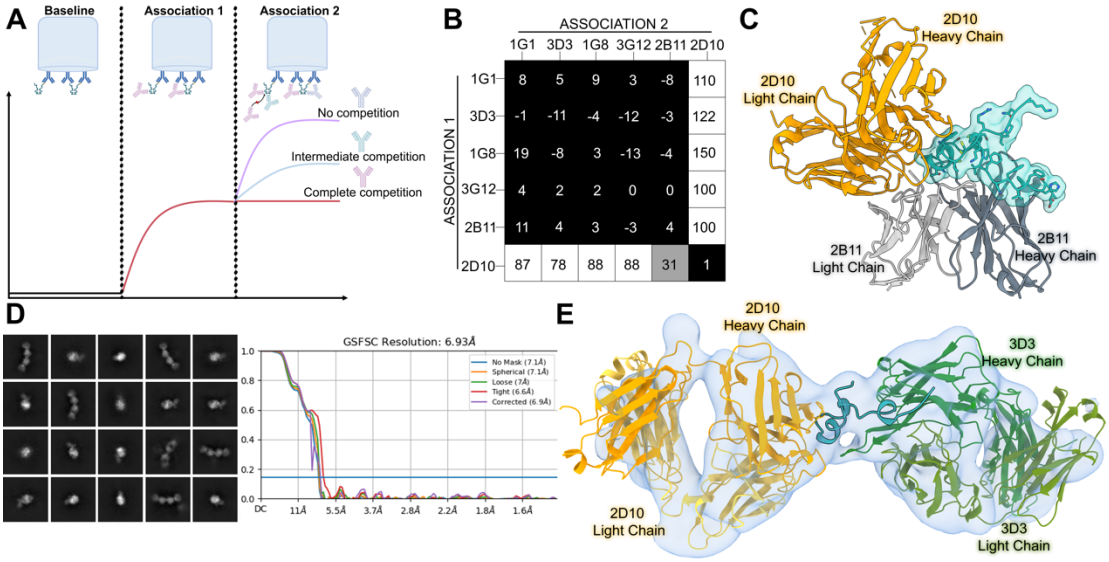

Figure 3.5 Biolayer interferometry epitope binning and cryo-EM reveal two non-overlapping antigenic sites on the RSV G CCD.

(A) Graphical description of the epitope binning experimental design using biolayer interferometry. RSV G^{ecto} coated on biosensors (Baseline) is incubated with one mAb to saturation (Association 1) and then incubated with a second mAb to evaluate binding (Association 2). (B) Epitope binning data showing the extent of competition between the mAbs in the Association 1 and 2 steps. Higher numbers indicate strong reactivity of the mAb in Association 2 in the presence of the mAb in Association 1 (no competition) and lower numbers indicate complete competition. Data represent the average of two technical replicates. (C) Overlay of the crystal structures Fab 2B11 (slate gray) and antibody scFv 2D10 (orange) bound to RSV G CCD (cyan). (D) Approximately 6.9 Å-resolution cryo-EM map and model of Fab 2D10 and Fab 3D3 bound to RSV G^{ecto}. The model was generated using the overlaid crystal structures of the scFv 2D10 - RSV G CCD and Fab 3D3 - RSV G CCD complexes, which and the model was then fit into the map using ChimeraX Isolde. (E) Representative 2D classes and gold standard Fourier shell correlation (GSFSC) graph.

3.4.5 Anti-RSV G antibodies have modest divergence from genomic precursors

B-cell precursors undergo a process called VDJ recombination where selected variable (V), diversity (D), and joining (J) genes are rearranged as the B-cell matures and migrates to secondary lymph nodes. These naïve B-cells reside in the secondary lymph organs until they are activated, at which point, they are instructed to enter the light zone of the germinal center and undergo affinity maturation, the process of purposely creating nucleotide substitutions or insertions in CDR1 and CDR2 (coded by the V gene) and CDR3 (coded by the D and J gene in the heavy chain and the V and J genes in the light chain). To understand the genetic basis for the elicitation of broadly-reactive high-affinity anti-RSV G antibodies, we analyzed variable heavy chain (VH) and variable light chain (VL) germline gene usage for each antibody from our panel of 13 mAbs and nine other anti-RSV G human mAbs with publicly available sequences(32, 40, 47). We found 10 distinct VH gene precursors and 12 distinct VL gene precursors across these twenty-two anti-RSV G mAbs. Surprisingly, these mAbs show relatively high sequence identity to their germline genes (77.6%-95.9% in VH and 81.1%-97.9% in VL) indicating moderate levels of somatic hypermutation (Table 2). Additionally, we find HCDR3 lengths to be 8-18 amino acids long. Each antibody uses a unique set of heavy and light chains except for antibodies 1G8, 3G12, and 1A5.

mAb	VH Gene	VH% Identity	CDRH3 Length	CDRH3 Sequence	VL Gene	VL% Identity
1G1	IGHV1-18*01	81.6	9	CARNHCNFYHDFW	IGLV3-25*02	91.7
3D3	IGHV3-9*01	80.4	15	CAIMVATTKNDFHYYKDVW	IGKV3-11*01	90.5
1G8	IGHV4-39*01	82.8	10	CAKQQLSLSPVENW	IGKV3-15*01	81.1

3G12	IGHV4-39*01	93.9	11	CARHLVWFGELRNNW	IGKV3-15*01	96.8
2B11	IGHV1-69*02	84.7	12	CAREILQSPPFAVDVW	IGLV2-14*01	83.8
2D10	IGHV1-18*01	86.7	15	CGRDMLGVVQAVAGPFDSW	IGKV1-12*01	90.5
6A12	IGVH3-74*03	95.9	9	CVRVLGAAMFDIW	IGKV3-11*01	97.9
10C6	IGHV3-30*03	90.8	17	CVRPDVIAVAGTALSNPFDLW	IGKV3-15*01	91.6
5D8	IGHV3-30-3*02	87.8	16	CAKDGLDYGGDLVYYGMDVW	IGVL3-25*02	77
3F9	IGHV1-18*01	84.7	15	CARLPLLGYSSGWYAFDMW	IGVL2-8*01	96
1A5	IGHV4-39*01	83.8	10	CARQQLSLSPVENW	IGKV3-15*01	81.1
1D4	IGHV1-46*01	81.6	8	CARVHKGRAEQW	IGKV4-1*01	95
1F12	IGHV1-46*02	79.6	8	CVRGSNLLPHLW	IGKV3-20*01	86.5
CB017.5	IGHV3-33*01	92.8	13	CARDPIVGHTRDGLDVW	IGLV3-25*02	89.5
CB002.5	IGHV4-4*08	89.6	14	CARSGFCSDDACYRRGSW	IGKV1-39*01	93.6
AT34	IGHV3-30*03	90.7	17	CASQGAKGGHELSFYCALDVW	IGKV1-5*01	90.5
AT50	IGHV1-18*01	88.7	17	CARGGAQEMVRIHYYYYGMDW	IGKV1-9*01	87.4
AT42	IGHV4-38-2*02	85.6	9	CARHWAGLYFDSW	IGKV3-20*01	88.5
AT51	IGHV1-18*01	84.7	18	CARPATSYDDLRSGYLNYCDYW	IGKV1-9*01	90.5
AT32	IGHV1-24*01	83.7	16	CAAEARYCDNSRCSPNFDHW	IGKV4-1*01	93.9
AT33	IGHV1-69*01	81.6	14	CARDAEWAAGSDYFFDYW	IGLV3-25*02	87.2
AT40	IGHV3-30*01	77.6	17	CARGRALDDFADYGGYYFDYW	IGKV1-12*01	87.4

Table 3.2 Germline Gene Sequence Identity

3.5 Discussion

Here, we defined three novel highly conserved conformational epitopes on the RSV G CCD using X-ray crystallography, and we visualized two non-competing antigenic sites (γ1 and γ2) using cryo-EM. We find that the CCD, while only 40 amino acids in length, can adopt multiple conformations that are recognized by

diverse antibody paratopes. For mAb 1G1, a linear epitope could not be mapped(40), and now we understand that its reactivity with RSV G can be explained via a unique conformational epitope. Of note, antibody 1G1's extensive hydrogen bond network with the RSV G CCD N-terminal tail is largely composed of peptide backbone amino and carbonyl groups, leaving open the possibility that it may be more resistant to mutations in the CCD compared to other antibodies, although its affinity is not as strong as other mAbs in the panel. For antibodies 1G8 and 2B11, we find that these antibodies also recognize conformational epitopes, which include amino acids beyond their linear epitopes(40). Epitope binning studies reveal that five out of the six mAbs investigated are able to compete with each other for binding, termed antigenic site γ1, whereas mAb 2D10 binds to a distinct epitope, termed antigenic site γ2. Interestingly, mAb 2B11 showed partial competition with mAb 2D10, which can be explained by a partial overlap of their epitopes on opposite faces of the CCD's cysteine loop.

It is well known that extensive genomic divergence via somatic hypermutation (SHM) is a common feature of broadly-neutralizing high-affinity antibodies, such as those targeting HIV and influenza virus(46-48). The broadly neutralizing anti-HIV-1 antibody VRC01 variable heavy chain has a sequence identity of 58.2% to its germline gene IGVH1-2*02. In a similar vein, broadly-neutralizing anti-influenza antibody C05 possesses a 24 amino acid long HCDR3 which it utilizes to insert into the HA receptor binding site. In contrast, broadly-neutralizing high-affinity antibodies targeting RSV G diverge modestly from their germline sequences, with the lowest sequence identity being 77.6% and with the longest HCDR3 at 18 amino acids in

length across 22 monoclonal antibodies. While the VRC01 antibody has an HCDR3 length of only 12 amino acids, it relies more heavily on its HCDR2 to form the highest surface area interface with the HIV gp120 protein and takes advantage of its LCDR1 to make important contacts with an HIV gp120 N-linked glycan(48). Similarly, Fab 2B11 and Fab 1G8 appear to rely more heavily on their HCDR2 and light chain residues, and possess only 12 and 10 amino acid long HCDR3s, respectively. However, antibody 1G1 uses its CDRH3 to a higher degree, making its length an important factor when we consider how divergent it might be from its germline gene. It is important to consider the role that RSV G's flexibility has in the generation of the high affinities (KDs from nM to pM) observed in these antibodies. It is possible that the CCD's flexibility allows it to conform to bind to germline-like antibodies, circumventing their need to undergo high SHM to achieve high affinity, something that could make the CCD an optimal target for vaccines.

Another feature of some broadly-neutralizing antibodies is that they can be restricted in their antibody germline usage. For example, the highly potent anti-influenza HA mAb CR6261 belongs to a panel of thirteen antibodies, all of which use the same VH gene (IGHV1-69), making it evident that mAb diversity is severely restricted for this antigenic site. In stark contrast, our analysis of 22 anti-RSV G antibodies use 10 unique VH genes in combination with 12 unique VL genes. Elicitation of diverse anti-RSV G antibodies might be the result of the CCD's ability to display a wide range of conformational epitopes via highly flexible N- and C-

termini. The ability to elicit diverse antibodies with different modes of binding would make it difficult for virus escape, further supporting the CCD as a target for vaccines.

Altogether, our studies reveal the RSV G CCD as an ideal vaccine target due to its high sequence conservation and its high flexibility that promotes the elicitation of diverse, high-affinity, and broadly-neutralizing antibodies. These features are especially notable for such a small antigenic target of ~40 amino acids. Moreover, the existence of two non-competing antigenic sites, γ1 and γ2, on the CCD further supports its potential to elicit antibody responses that resist virus escape. However, we acknowledge that there has been little selective pressure for the RSV G CCD to mutate due to its naturally low immunogenicity. Thus, it is unclear if selective pressure from a CCD-focused vaccine would result in RSV mutational escape, and future studies focused on this area would be informative. A limitation to performing escape studies *in vitro* is that anti-G antibodies are directly RSV-neutralizing only in primary airway epithelial cells, making such studies technically challenging(32-34, 40).

Overall, this study broadens our understanding of the RSV G epitope landscape and serves as a blueprint for structure-guided vaccine design and therapeutic antibody strategies.

3.6 Materials and Methods

3.6.1 Production of bnmAbs 1G1, 3D3, 1G8, 2B11, 2D10, and 3G12

Genes encoding bnmAbs 1G1, 3D3, 1G8, 2B11, 2D10, and 3G12 were identified using CellSpot single cell phenotyping from clonal populations of B-cells derived from PBMC's of RSV experienced individuals and sequenced using RT-PCR as

previously described by (Collarini et al. 2009 Trellis Bioscience). For this study, recombinant bnmAbs were expressed by transient transfection of suspension adapted Chinese Hamster Ovary Cells (CHO-S), (Thermo Fisher, Life Technologies, Carlsbad, CA) with plasmids expressing full length human light and IgG1 heavy chains. Expression cassettes comprising a CMV promotor, a secretory peptide, variable domain sequences from the RSV antibody panel, human constant domains and poly A tail were assembled by Gibson cloning into the appropriate VRCO1 backbone sequences in pCMVR (Xu et al., PMD 2061), previously obtained from the NIH AIDS Reagent program. Sanger sequencing was used to verify seamless re-construction of all plasmids. Prior to transfection, CHO-S cells were maintained at a density of 0.3-2.0e6/mL in CD-CHO medium supplemented with 8 mM GlutaMax, 100 μM hypoxanthine and 16 μM thymidine in shake flask cultures at 37 °C, 8% CO2, 85% humidity, rotating at 135 rpm in an ISF1-X shaker incubator (Kuhner, Birsfelden, Switzerland). For protein production, cells were transfected using an STX electroporation system (MaxCyte Inc., Gaithersburg, MD) according to the manufacturer's protocol using endotoxin free DNA. Following transfection, cells were maintained at a density of 1.0 e7/mL in CD OptiCHO supplemented with 0.1% pluronic acid, 2 mM GlutaMax, 100 μM hypoxanthine and 16 μM thymidine. At 24 hours post electroporation, protein expression was enhanced by adding sodium butyrate (1mM final concentration) and lowering the temperature to 32°C. Cultures were fed daily with CHO Growth A, 0.5% Yeastolate (BD, Franklin Lakes, NJ, US), 2.5% CHO-CD Efficient Feed A, and 0.25 mM GlutaMax, 2 g/L Glucose (Sigma-

Aldrich St. Louis, MO, US) and harvested when cell viability dropped to below 50% (usually following 8-14 days in culture). All media and supplements were purchased from Thermo Fisher, Life Technologies, Carlsbad, CA unless stated otherwise. Secreted mAbs were purified from conditioned media by affinity chromatography using a HiTrap Protein G column (Cytiva) in PBS buffer [pH7.4]. Bound antibody was eluted with 0.1 M glycine•HCl [pH2.8] and immediately neutralized with 1M tris pH 9 100ul/ mL eluted. Purified mAbs were verified by Coomassie stained SDS-PAGE with both reducing and non-reducing (no DTT) loading buffer, dialyzed into PBS [pH7.4] and flash frozen for long term storage.

3.6.2 Antibody Germline Gene Sequence Identity Analysis

We began with protein sequences for the variable region of each heavy and light chain. Using the IgBlast tool on the National Center for Biotechnology Information (NCBI) website, we input each sequence, selecting the top hit for each variable (V) gene and allele to include in our table. Additionally, we included the CDRH3 sequences using the Martin (Enhanced Chothia) numbering scheme as a guide to set consistent boundaries around each CDRH3.

3.6.3 Expression and Purification of Fabs 3D3, 2D10, 1G1, 1G8, and 2B11

Fabs 3D3 and 2D10 were generated by incubation of full length mAb with immobilized papain, followed by removal of the Fc fragment with protein A using a Pierce™ Fab Preparation Kit (Thermo Fisher, Life Technologies, Carlsbad, CA). Fabs were further purified by Superdex 200 size-exclusion chromatography in 10 mM Tris-HCl pH 8.0 and 150 mM NaCl. Purified Fabs were dialyzed into PBS, pH [7.4], and flash frozen for long term storage. Full length mAb 1G1, 2B11, and 1G8 plasmids were linearized using primers flanking the CH2 and CH3 domains so as to exclude

them during PCR to generate the Fab fragment sequence. A synthetic geneblock encoding a 2xStreptactin-Tag (for heavy chain only) was then cloned C-terminal to the Fab sequence using Gibson assembly. Sanger sequencing was used to verify these plasmids. Fabs were expressed in an identical manner to mAbs, in CHO-S culture. Secreted Fabs were affinity purified from media adjusted to 50mM Tris [pH8], 1mM EDTA, supplemented with 27 mg/ L Biolock (IBA life sciences), using a StrepTrap HP column (Cytiva) in 50mM Tris [pH8], 150mM NaCl and 1mM EDTA wash buffer, eluting with wash buffer containing 2.5 mM d-Desthiobiotin. Purified Fabs were verified by Coomassie stained SDS-PAGE with both reducing and non-reducing (no DTT) loading buffer and dialyzed into 1xPBS, pH7.4 and flash frozen for long term storage.

3.6.4 Expression and Purification of RSV Gecto

A synthetic gene encoding RSV strain A2 (RSV/A2) G protein (RSV Gecto) spanning amino acids 64-298 (UniProtKB entry P03423) was codon optimized for human codon usage and cloned into a CMV driven expression derived from pcDNA3.1 (https://doi.org/10.1371/journal.pone.0197656) C-terminal to a CCR5 secretion signal sequence and N-Terminal to a 6xHistidine-Tag followed by a 2xStreptactin-Tag. Sanger sequencing was used to verify this plasmid. Recombinant RSV Gecto was produced by transient transfection of CHO-S cells and secreted RSV Gecto was purified from CHO media adjusted to pH[8] by the addition of Tris buffer to a final concentration of 50mM, supplemented with 1mM EDTA and Biolock (IBA life sciences) at 27mg/L . Protein was recovered by affinity purification using a StrepTrap HP column (Cytiva). Wash buffer comprising 50mM Tris [pH8], 150 mM

NaCl, 1mM EDTA, and elution buffer 2.5 mM d-Desthiobiotin). Purified RSV Gecto was verified by SDS-PAGE in both reducing and non-reducing (no DTT) loading buffer and dialyzed into 1xPBS, pH7.4 and flash frozen for long term storage. A biotinylated version of RSV Gecto was produced in an identical manner to RSV Gecto with the exception of the addition of carboxy terminal AviTag recognition sequence, and replacement of the 2xStreptactin-Tag with a 10XHis tag in the expression cassette. Purification was accomplished on a Ni Sepharose Hi Trap excel column (Cytiva) equilibrated with 20mM sodium phosphate pH7.4, 0.5M NaCl, pH7.4. Conditioned CHO media was adjusted to pH7.4, 0.5M NaCl prior to column loading. Wash buffer included 20mM imidazole, and an imidazole gradient from 20mM to 500mM was applied using an ACTA Pure protein purification system (Cytiva), to elute bound protein. Eluted fractions were analyzed by SDS-PAGE prior to pooling. RSV Gecto AviTag was then dialyzed into PBS pH[7.4], and biotinylated using GST-BirA ligase as described by Fairhaed and Howath (2015). Briefly,100uM of RSV Gecto AviTag was incubated with 1uM GST-BirA in the presence of 20mM MgCl2, 2mM ATP, 0.15mM D-Biotin for 1 hour at room temperature with rocking. The same amount of fresh biotin and GST-BirA were added again prior to incubating overnight. GST-BirA was removed by incubation of the sample with a 50% (V/V) slurry of glutathione-HiCap resin in PBS for 30 minutes at room temperature, followed by centrifugation and collection of the supernatant which was extensively dialyzed against PBS pH 7.4 prior to flash freezing. RSV Gecto with a GALNT3 restricted o-linked glycosylation pattern was generated specifically

for structural studies by expression of RSV Gecto in Simple Cell (SC) ZFN192 GALNT3 suspension adapted CHOK1, a gift from H Clausen (Yang et al 2014). Stable pools RSV Gecto SC ZFN192 GALNT3_ were generated by transfection followed by selection in 0.8mg/mL G418. For protein expression, a pool of G418 resistant RSV Gecto _SC ZFN192 GALNT3 cells was grown to a density of 5e6/mL in BalanCD CHO Growth A - Irvine Scientific (FujiFilm) supplemented with 2mM GlutaMax, 100 μM hypoxanthine and 16 μM thymidine and 0.1 % pluronic in standard shake flask culture. The temperature was then dropped to 32°C, and sodium butyrate added to a final concentration of 1mM. The cultures supplemented as described for transient CHO-S expression, excepting on a 3 day schedule. Cultures were harvested when cell viability dropped <50% by trypan blue exclusion, and protein purified on a StrepTactin Sepharose HP column (as previously described for CHO-S produced RSV Gecto) followed by size exclusion chromatography on a Superose 6 increase 10/300 column (Cytiva) in 50mM Tris [pH8], 300 mM NaCl, 1mM EDTA and verified by Coomassie stained SDS-PAGE. The protein was then dialyzed into TBS (50 mM Tris-Cl, pH 7.5 150 mM NaCl) before flash freezing.

3.6.5 Binding Kinetics

Binding kinetics were assessed using biolayer interferometry on an Octet Red384 instrument. Anti-Human Fc-Capture AHC biosensors (Sartorius, REF 18-0015) were equilibrated in kinetics buffer (.1% BSA, .02% Tween20, 1xPBS [pH7.4]). Biosensors were then dipped into wells containing kinetics buffer for 60 seconds to record a baseline measurement. Next, biosensors were loaded with either mAb 1G1, mAb 1G8, or mAb 2B11 at a concentration of 2 ug/ml for 60 seconds followed by

another baseline step for 60 seconds. Loaded biosensors were then dipped into wells containing two-fold serial dilutions of purified RSV Gecto for 300 seconds with the highest concentration being 40 nM and the lowest being .625 nM. The last biosensor was dipped into kinetics buffer which served as a control and to subtract non-specific upward or downward drift from our measurements. A dissociation step was measured for 600 seconds after moving biosensors into wells containing kinetics buffer. All steps were done with a shakespeed of 1000 rpm and at room temperature. Two technical replicates were done per antibody. KD's were calculated using the Data Analysis HT software version 11.1 with a 1:1 binding model and dilutions fitted globally per assay.

3.6.6 Epitope Binning

Epitope binning was done using biolayer interferometry on an Octet Red384 instrument and following suggestions from "Epitope binning of monoclonal and polyclonal antibodies by biolayer interferometry" by Kaito Nagashima and Jarrod J. Mousa. Anti-penta histidine HIS1K biosensors (Sartorius, REF 18-0038) were equilibrated in kinetics buffer (.1% BSA, .02% Tween20, 1xPBS [pH7.4]). Biosensors were then dipped into wells containing kinetics buffer for 60 seconds to record a baseline measurement. Next, biosensors were loaded with RSV Gecto at a concentration of 4 ug/ml for 150 seconds followed by another baseline step for 60 seconds. Loaded biosensors were then dipped into wells containing either mAb 1G1, mAb 2D10, mAb 3G12, mAb 3D3, mAb 2B11, or mAb 1G8 at concentration of 100 ug/ml for 300 seconds in the first association step. The second association step was done by dipping into either mAb 1G1, mAb 2D10, mAb 3G12, mAb 3D3, mAb 2B11, or mAb 1G8 at

a concentration of 100 ug/ml for 300 seconds so that every antibody got a chance to compete with all other antibodies in addition to itself. Antibodies in the first association step were also tested in the second association step to test antibodies in both directions and observe the effect of steric hindrance which might occur after the first association step. A dissociation step was measured for 600 seconds after moving biosensors into wells containing kinetics buffer. A no load control (kinetics buffer) was used to assess antibody binding to the biosensor itself and a 0 ug/ml concentration of antibody (kinetics buffer) was used in another control to verify complete saturation of the first antibody to its corresponding RSV G epitope. A dissociation step was measured for 600 seconds after moving biosensors into wells containing kinetics buffer. Two technical replicates were done per antibody and order of association. mAb 2B11 was assessed using anti-streptavidin SA biosensors (Sartorius, REF 18-0009) and biotinylated RSV Gecto due to its apparent affinity for anti-penta histidine HIS1K biosensors in the no load control assay despite the absence of a his- or strep-tag. All assays were done with a shakespeed of 400 rpm. To generate a value for competition between two mAbs, the signal of mAb B (second association step) in the presence of mAb A (first association step) was divided by the saturated signal of mAb A and then multiplied by 100 for a percentage value per this formula:

$$\%\ \text{Competition} = \frac{\text{Signal mAb A with mAb B}}{\text{Signal mAb A}} \times 100\%$$

3.6.7 Expression and Purification of RSV G157-197

A synthetic gene encoding RSV strain A2 (RSV/A2) G protein amino acids 157 to 197 (UniProtKB entry P03423) was codon optimized for E. coli and cloned into

pRSFDuet-1 in frame with an N-terminal methionine and a C-terminal 6xHistidine-Tag. Sanger sequencing was used to verify this plasmid. Two methods were used to express and purify recombinant RSV G157-197 as a result of optimization. (1) Recombinant RSV G157-197 was expressed in T7Express Escherichia coli cells overnight at 18°C. Cells were lysed by ultrasonication in wash buffer (20 mM Tris-HCl [pH 8], 25 mM imidazole, 150 mM NaCl) containing 1 mM MgCl2, protease inhibitors, and benzonase. E. coli lysates were clarified by centrifugation and filtration using a .22 um vacuum filter. RSV G157-197 was purified from clarified lysates by affinity chromatography using a HiTrap TALON Crude column (GE Healthcare, REF 28-9537-66) and washed with wash buffer containing 6M urea. Protein was eluted in wash buffer containing 500 mM imidazole. (2) Recombinant RSV G157-197 was expressed in SHuffle T7 Competent E. coli cells (New England Bioslabs, REF C3026J) overnight at 18°C. Cells were lysed by ultrasonication in wash buffer (20 mM Tris-HCl [pH 8], 25 mM imidazole, 300 mM NaCl) containing 1mM MgCl2, protease inhibitors, and benzonase. E. coli lysates were clarified by centrifugation and filtration using a .22 um vacuum filter. Clarified lysates were mixed with 1 ml of packed HisPur Cobalt Resin (Thermo Scientific, REF 89965) and rotated for 1 hour at 4C. Recombinant RSV G157-197 was eluted on a centrifuge column (Pierce, REF 89898) using wash buffer containing 500 mM imidazole and verified on Coomassie stained SDS-PAGE with both reducing and non-reducing (no DTT) loading buffer.

3.6.8 Production and Structure Determination of Fab 1G1-RSV G157-197 Complex

A 5 molar excess of recombinant RSV G157-197 at .1 mg/ml was mixed with Fab 1G1 at 1.5 mg/ml and concentrated to 2.8 mg/ml. This sample was size exclusion purified using an S75 10/300 size exclusion chromatography (SEC) column with 50 mM Tris-HCl (pH 8) and 150 mM NaCl. Size exclusion purified material was verified by Coomassie stained SDS-PAGE and was concentrated to 5 mg/ml. Crystals were grown by hanging drop vapor diffusion at 22°C with well solution containing .1M BIS-TRIS (pH 6.5), 0.2M Ammonium Sulfate, and 24.5% PEG 3350. Crystals were dipped into a cryoprotectant (well solution containing 25% PEG400) and flash frozen in liquid nitrogen. Frozen crystals were shipped to the Advanced Photon Source (APS) and diffraction data was collected at beamline 23-ID-B using an x-ray wavelength of 1.033167 Å (12 keV). Diffraction data from one crystal were integrated and scaled using XDS where cc1/2 was used to determine the cutoff resolution(50). Phases were solved using molecular replacement on PHENIX.phaser. The molecular replacement model for the variable domain of Fab 1G1 was generated using SWISS model while the constant domain model came from the crystal structure of VRC01 (PDB code: 3NGB). The molecular replacement model for RSV G157-197 came from the crystal structure of RSV G bound to Fab 3D3 (PDB code: 5WNA) using residues 171-186. The electron density map and model were refined using PHENIX.refine while manual assignment and fitting of amino acid side chains into electron density were done using COOT. Visualization of final structural features were done in Pymol.

3.6.9 Production and Structure Determination of Fab 1G8-RSV G157-197 Complex

A 4 molar excess of recombinant RSV G157-197 at .3 mg/ml was mixed with Fab 1G8 at .5 mg/ml, concentrated to .6 mg/ml, dialyzed into 10mM Tris-HCl (pH 8) and 150 mM NaCl. This sample was size exclusion purified using an S75 10/300 size exclusion chromatography (SEC) column with 50 mM Tris-HCl (pH 8) and 150 mM NaCl. Size exclusion purified material was verified by Coomassie stained SDS-PAGE and was concentrated to 5 mg/ml. Crystals were grown by hanging drop vapor diffusion at 22°C with well solution containing .15M Sodium Thiocyanate and 16% PEG 3350. Crystals were dipped into a cryoprotectant (well solution containing 25% glycerol) and flash frozen in liquid nitrogen. Frozen crystals were shipped to the Advanced Light Source (ALS) and diffraction data was collected at beamline 5.0.1 using an x-ray wavelength of .97Å (12.4 keV). Diffraction data from one crystal were integrated and scaled using DIALS where cc1/2 was used to determine the cutoff resolution. Phases were solved using molecular replacement on PHENIX.phaser. The molecular replacement model for the variable domain of Fab 1G8 was generated using SWISS model while the constant domain model came from the crystal structure of VRC01 (PDB code: 3NGB). The molecular replacement model for RSV G157-197 came from the crystal structure of RSV G bound to Fab 3D3 (PDB code: 5WNA) using residues 171-186. The electron density map and model were refined using PHENIX.refine while manual assignment and fitting of amino acid side chains into electron density were done using COOT. Visualization of final structural features were done in Pymol.

3.6.10 Production and Structure Determination of Fab 2B11-RSV G157-197 Complex

A 4 molar excess of recombinant RSV G157-197 at .3 mg/ml was mixed with Fab 2B11 at .6 mg/ml, concentrated to 1 mg/ml, dialyzed into 10mM Tris-HCl (pH 8) and 150 mM NaCl. This sample was size exclusion purified using an S75 10/300 size exclusion chromatography (SEC) column with 50 mM Tris-HCl (pH 8) and 150 mM NaCl. Size exclusion purified material was verified by Coomassie stained SDS-PAGE and was concentrated to 3.1 mg/ml. Crystals were grown by hanging drop vapor diffusion at 22°C with well solution containing .22M Ammonium Citrate Dibasic and 15% PEG 3350. Crystals were dipped into a cryoprotectant (well solution containing 25% PEG400) and flash frozen in liquid nitrogen. Frozen crystals were shipped to the Advanced Light Source (ALS) and diffraction data was collected at beamline 5.0.1 using an x-ray wavelength of .97Å (12.4 keV). Two diffraction datasets from one crystal were integrated and scaled using DIALS where cc1/2 was used to determine the cutoff resolution. Phases were solved using molecular replacement on PHENIX.phaser. The molecular replacement model for the variable domain of Fab 2B11 was generated using SWISS model while the constant domain model came from the crystal structure of VRC01 (PDB code: 3NGB). The molecular replacement model for RSV G157-197 came from the crystal structure of RSV G bound to Fab 3D3 (PDB code: 5WNA) using residues 171-186. The electron density map and model were refined using PHENIX.refine while manual assignment and fitting of amino acid side chains into electron density were done using COOT. Visualization of final structural features were done in Pymol.

3.6.11 Production and CryoEM Grid preparation of Fab 3D3-RSV Gecto-Fab 2D10 Complex

Equimolar ratios of size exclusion purified GALNT3 restricted RSV Gecto and 2D10 Fab were incubated with gentle mixing at 4°C for one hour before adding a second molar equivalent of 3D3 Fab and a further one hour incubation. The complex was then purified away from free Fab using a Superose 6 increase 10/300 column (Cytiva) in 50mM Tris [pH7.5], 150 mM NaCl and verified on Coomassie stained SDS-PAGE. Purified Fab 3D3-RSV Gecto-Fab 2D10 complex was used at 1.4 mg/ml (approximately 10.5 uM). 3 µl of sample were fast incubated with 0.5 µL of octyl-D-glucoside and deposited onto a glow-discharged UltrAuFoil R 2/2 200 gold mesh grid using a ThermoFisher Scientific Vitrobot Mark VI and blotted at 4 °C, 100% humidity for 1.5 seconds before plunge-frozen in liquid ethane. CryoEM Data Collection of Fab 3D3-RSVGecto-Fab 2D10 Complex Images were collected using a ThermoFisher Scientific Glacios-cryoTwin transmission electron microscope operating at 200 kV using a Gatan K2 Summit direct electron detection and pixel size of 0.69 Å (57,000x) and total dose of 38 e-/Å2 with defocus range between -0.8 and 3.0 µm. A total of 6,605 movies were collected across all grids and processing using cryoSPARC v4.1. Stage drift and beam-induced anisotropic motion during data collection were corrected using patch-based motion correction. Defocus variation was determined using patch-based CTF estimation. Exposures were manually inspected and curated to remove poor-quality micrographs by setting thresholds for CTF fit resolution (< 10 Å), motion distance, and astigmatism.

3.6.12 CryoEM Data Processing

Curated exposures were subjected to automated blob picking using a box size of 40-80 Å resulting in a total of 9,716,771 particles. Picked particles were manually inspected and pruned using a low pass filter, normalized cross-correlation (NCC), and power thresholds to select the highest quality particles. Particles were extracted using a box size of 320 pixels, resulting in a total of 3,159,582 particles and 3,152 movies. Subsequent rounds of 2D classification were performed in order to obtain a suitable set of references for the template picking using a particle diameter of 320 Å, followed by manual inspection of picked particles, particle extraction using a box size of 320 pixels, and 2D classification. Selected 2D classes underwent Ab Initio (67 classes were picked), followed by 3D-classification and the selected set of particles and volume underwent to cycles of non-uniform refinement. The final polishment was performed using local CTF refinement using 50,831 particles. The best 3D reconstructed map was visualized on UCSF-ChimeraX and overlayed crystal structures of Fab 3D3-RSV G157-197 (PDB code: 5WNB) and ScFv 2D10-RSV G157-197(PDB Code: 5WN9).

3.7 Acknowledgements

We thank Trellis biosciences for the discovery of the anti-G antibody panel which laid the foundation of this work. We thank Stanislav Fedechkin and Ana Maria Nuñez Castrejon for pioneering the structural studies of Fab 3D3, ScFv 2D10, and Fab 3G12 in complex with the CCD. The electron microscopy work was guided by Vitor Serrão and we thank him for his support in grid preparation and data processing. We thank the Advanced Light Source and the Advanced Photon source for allotting us

beamtime to shoot our crystals and collect vital datasets for this work. We also thank the crystallography core at the University of California, Santa Cruz, specifically Seth Rubin, Sarvind, Tripathi, and Vanessa Mariscal, for help with instrumentation and reagent access. Finally, we thank David Boyd for his insight on antibody germline gene analysis.

3.8 References

1. Lozano R, Naghavi M, Foreman K, Lim S, Shibuya K, Aboyans V, et al. Global and regional mortality from 235 causes of death for 20 age groups in 1990 and 2010: a systematic analysis for the Global Burden of Disease Study 2010. Lancet. 2012;380(9859):2095-128.
2. Shi T, McAllister DA, O'Brien KL, Simoes EAF, Madhi SA, Gessner BD, et al. Global, regional, and national disease burden estimates of acute lower respiratory infections due to respiratory syncytial virus in young children in 2015: a systematic review and modelling study. Lancet. 2017;390(10098):946-58.
3. Branche AR, Falsey AR. Respiratory syncytial virus infection in older adults: an under-recognized problem. Drugs Aging. 2015;32(4):261-9.
4. Falsey AR, Hennessey PA, Formica MA, Cox C, Walsh EE. Respiratory syncytial virus infection in elderly and high-risk adults. N Engl J Med. 2005;352(17):1749-59.
5. Falsey AR, Walsh EE. Respiratory syncytial virus infection in elderly adults. Drugs Aging. 2005;22(7):577-87.
6. Widmer K, Griffin MR, Zhu Y, Williams JV, Talbot HK. Respiratory syncytial virus- and human metapneumovirus-associated emergency department and hospital burden in adults. Influenza Other Respir Viruses. 2014;8(3):347-52.
7. McLaughlin JM, Khan F, Begier E, Swerdlow DL, Jodar L, Falsey AR. Rates of Medically Attended RSV Among US Adults: A Systematic Review and Meta-analysis. Open Forum Infect Dis. 2022;9(7):ofac300.
8. Palivizumab, a Humanized Respiratory Syncytial Virus Monoclonal Antibody, Reduces Hospitalization From Respiratory Syncytial Virus Infection in High-risk Infants. Pediatrics. 1998;102(3):531-7.
9. Griffin MP, Yuan Y, Takas T, Domachowske JB, Madhi SA, Manzoni P, et al. Single-Dose Nirsevimab for Prevention of RSV in Preterm Infants. N Engl J Med. 2020;383(5):415-25.
10. Topalidou X, Kalergis AM, Papazisis G. Respiratory Syncytial Virus Vaccines: A Review of the Candidates and the Approved Vaccines. Pathogens. 2023;12(10).
11. Wilson E, Goswami J, Baqui AH, Doreski PA, Perez-Marc G, Zaman K, et al. Efficacy and Safety of an mRNA-Based RSV PreF Vaccine in Older Adults. N Engl J Med. 2023;389(24):2233-44.

12. Resch B. Product review on the monoclonal antibody palivizumab for prevention of respiratory syncytial virus infection. Hum Vaccin Immunother. 2017;13(9):2138-49.
13. Olchanski N, Hansen RN, Pope E, D'Cruz B, Fergie J, Goldstein M, et al. Palivizumab Prophylaxis for Respiratory Syncytial Virus: Examining the Evidence Around Value. Open Forum Infect Dis. 2018;5(3):ofy031.
14. Suss RJ, Simoes EAF. Respiratory Syncytial Virus Hospital-Based Burden of Disease in Children Younger Than 5 Years, 2015-2022. JAMA Netw Open. 2024;7(4):e247125.
15. McMorrow ML, Moline HL, Toepfer AP, Halasa NB, Schuster JE, Staat MA, et al. Respiratory Syncytial Virus-Associated Hospitalizations in Children <5 Years: 2016-2022. Pediatrics. 2024.
16. Walsh EE, Peterson DR, Kalkanoglu AE, Lee FE, Falsey AR. Viral shedding and immune responses to respiratory syncytial virus infection in older adults. J Infect Dis. 2013;207(9):1424-32.
17. Battles MB, McLellan JS. Respiratory syncytial virus entry and how to block it. Nat Rev Microbiol. 2019;17(4):233-45.
18. McLellan JS, Ray WC, Peeples ME. Structure and function of respiratory syncytial virus surface glycoproteins. Curr Top Microbiol Immunol. 2013;372:83-104.
19. McLellan JS, Chen M, Joyce MG, Sastry M, Stewart-Jones GB, Yang Y, et al. Structure-based design of a fusion glycoprotein vaccine for respiratory syncytial virus. Science. 2013;342(6158):592-8.
20. McLellan JS, Chen M, Leung S, Graepel KW, Du X, Yang Y, et al. Structure of RSV fusion glycoprotein trimer bound to a prefusion-specific neutralizing antibody. Science. 2013;340(6136):1113-7.
21. Walsh EE, Wang L, Falsey AR, Qiu X, Corbett A, Holden-Wiltse J, et al. Virus-Specific Antibody, Viral Load, and Disease Severity in Respiratory Syncytial Virus Infection. J Infect Dis. 2018;218(2):208-17.
22. Graham BS, Modjarrad K, McLellan JS. Novel antigens for RSV vaccines. Curr Opin Immunol. 2015;35:30-8.
23. Capella C, Chaiwatpongsakorn S, Gorrell E, Risch ZA, Ye F, Mertz SE, et al. Prefusion F, Postfusion F, G Antibodies, and Disease Severity in Infants and Young Children With Acute Respiratory Syncytial Virus Infection. J Infect Dis. 2017;216(11):1398-406.
24. Hause AM, Henke DM, Avadhanula V, Shaw CA, Tapia LI, Piedra PA. Sequence variability of the respiratory syncytial virus (RSV) fusion gene among contemporary and historical genotypes of RSV/A and RSV/B. PLoS One. 2017;12(4):e0175792.
25. Mas V, Nair H, Campbell H, Melero JA, Williams TC. Antigenic and sequence variability of the human respiratory syncytial virus F glycoprotein compared to related viruses in a comprehensive dataset. Vaccine. 2018;36(45):6660-73.

26. Simoes EAF, Forleo-Neto E, Geba GP, Kamal M, Yang F, Cicirello H, et al. Suptavumab for the Prevention of Medically Attended Respiratory Syncytial Virus Infection in Preterm Infants. Clin Infect Dis. 2021;73(11):e4400-e8.
27. Langedijk AC, Harding ER, Konya B, Vrancken B, Lebbink RJ, Evers A, et al. A systematic review on global RSV genetic data: Identification of knowledge gaps. Rev Med Virol. 2022;32(3):e2284.
28. Wilkins D, Langedijk AC, Lebbink RJ, Morehouse C, Abram ME, Ahani B, et al. Nirsevimab binding-site conservation in respiratory syncytial virus fusion glycoprotein worldwide between 1956 and 2021: an analysis of observational study sequencing data. Lancet Infect Dis. 2023;23(7):856-66.
29. Zhu Q, Lu B, McTamney P, Palaszynski S, Diallo S, Ren K, et al. Prevalence and Significance of Substitutions in the Fusion Protein of Respiratory Syncytial Virus Resulting in Neutralization Escape From Antibody MEDI8897. J Infect Dis. 2018;218(4):572-80.
30. Nziza N, Jung W, Mendu M, Chen T, Julg B, Graham B, et al. Longitudinal humoral analysis in RSV-infected infants identifies pre-existing RSV strain-specific G and evolving cross-reactive F antibodies. Immunity. 2024.
31. Nziza N, Jung W, Mendu M, Chen T, Julg B, Graham B, et al. Longitudinal humoral analysis in RSV-infected infants identifies pre-existing RSV strain-specific G and evolving cross-reactive F antibodies. Immunity. 2024;57(7):1681-95 e4.
32. Jones HG, Ritschel T, Pascual G, Brakenhoff JPJ, Keogh E, Furmanova-Hollenstein P, et al. Structural basis for recognition of the central conserved region of RSV G by neutralizing human antibodies. PLoS Pathog. 2018;14(3):e1006935.
33. Johnson SM, McNally BA, Ioannidis I, Flano E, Teng MN, Oomens AG, et al. Respiratory Syncytial Virus Uses CX3CR1 as a Receptor on Primary Human Airway Epithelial Cultures. PLoS Pathog. 2015;11(12):e1005318.
34. Cortjens B, Yasuda E, Yu X, Wagner K, Claassen YB, Bakker AQ, et al. Broadly Reactive Anti-Respiratory Syncytial Virus G Antibodies from Exposed Individuals Effectively Inhibit Infection of Primary Airway Epithelial Cells. J Virol. 2017;91(10).
35. Caidi H, Miao C, Thornburg NJ, Tripp RA, Anderson LJ, Haynes LM. Anti-respiratory syncytial virus (RSV) G monoclonal antibodies reduce lung inflammation and viral lung titers when delivered therapeutically in a BALB/c mouse model. Antiviral Res. 2018;154:149-57.
36. Boyoglu-Barnum S, Gaston KA, Todd SO, Boyoglu C, Chirkova T, Barnum TR, et al. A respiratory syncytial virus (RSV) anti-G protein F(ab')2 monoclonal antibody suppresses mucous production and breathing effort in RSV rA2-line19F-infected BALB/c mice. J Virol. 2013;87(20):10955-67.
37. Jeong KI, Piepenhagen PA, Kishko M, DiNapoli JM, Groppo RP, Zhang L, et al. CX3CR1 Is Expressed in Differentiated Human Ciliated Airway Cells and Co-Localizes with Respiratory Syncytial Virus on Cilia in a G Protein-Dependent Manner. PLoS One. 2015;10(6):e0130517.

38. Chirkova T, Boyoglu-Barnum S, Gaston KA, Malik FM, Trau SP, Oomens AG, Anderson LJ. Respiratory syncytial virus G protein CX3C motif impairs human airway epithelial and immune cell responses. J Virol. 2013;87(24):13466-79.
39. Boyoglu-Barnum S, Chirkova T, Todd SO, Barnum TR, Gaston KA, Jorquera P, et al. Prophylaxis with a respiratory syncytial virus (RSV) anti-G protein monoclonal antibody shifts the adaptive immune response to RSV rA2-line19F infection from Th2 to Th1 in BALB/c mice. J Virol. 2014;88(18):10569-83.
40. Collarini EJ, Lee FE, Foord O, Park M, Sperinde G, Wu H, et al. Potent high-affinity antibodies for treatment and prophylaxis of respiratory syncytial virus derived from B cells of infected patients. J Immunol. 2009;183(10):6338-45.
41. Chirkova T, Lin S, Oomens AGP, Gaston KA, Boyoglu-Barnum S, Meng J, et al. CX3CR1 is an important surface molecule for respiratory syncytial virus infection in human airway epithelial cells. J Gen Virol. 2015;96(9):2543-56.
42. Fedechkin SO, George NL, Wolff JT, Kauvar LM, DuBois RM. Structures of respiratory syncytial virus G antigen bound to broadly neutralizing antibodies. Sci Immunol. 2018;3(21).
43. Fedechkin SO, George NL, Nunez Castrejon AM, Dillen JR, Kauvar LM, DuBois RM. Conformational Flexibility in Respiratory Syncytial Virus G Neutralizing Epitopes. J Virol. 2020;94(6).
44. Lee Y, Klenow L, Coyle EM, Grubbs G, Golding H, Khurana S. Monoclonal antibodies targeting sites in respiratory syncytial virus attachment G protein provide protection against RSV-A and RSV-B in mice. Nat Commun. 2024;15(1):2900.
45. Haynes LM, Caidi H, Radu GU, Miao C, Harcourt JL, Tripp RA, Anderson LJ. Therapeutic monoclonal antibody treatment targeting respiratory syncytial virus (RSV) G protein mediates viral clearance and reduces the pathogenesis of RSV infection in BALB/c mice. J Infect Dis. 2009;200(3):439-47.
46. Boyoglu-Barnum S, Todd SO, Chirkova T, Barnum TR, Gaston KA, Haynes LM, et al. An anti-G protein monoclonal antibody treats RSV disease more effectively than an anti-F monoclonal antibody in BALB/c mice. Virology. 2015;483:117-25.
47. Tim Beaumont EY, inventor; AIMM Therapeutics BV, assignee. RSV G PROTEIN SPECIFIC ANTIBODIES. United States2017 June 30, 2017.
48. Zhou T, Georgiev I, Wu X, Yang ZY, Dai K, Finzi A, et al. Structural basis for broad and potent neutralization of HIV-1 by antibody VRC01. Science. 2010;329(5993):811-7.
49. Kabsch W. XDS. Acta Cryst. 2010.

Chapter 4 Implications for Respiratory Syncytial Virus G glycoprotein-based vaccines and monoclonal antibody prophylaxis: A Brief Review.

4.1 Review

Lower respiratory infections are the leading cause of infant mortality worldwide with Respiratory Syncytial Virus (RSV) as the primary causative agent(1, 2). By age 2 nearly all children have had an RSV infection with the most severe cases in those who have a related pre-existing condition such as pulmonary complications, immunodeficiency, and exposure to nicotine or maternal inflammation(3-5). RSV induced lower respiratory disease also significantly impacts children under 5, immunocompromised individuals, and the elderly(6-10). It causes 33.1 million cases of lower respiratory tract infection worldwide and in the US alone, it causes 6,000-10,000 deaths among adults above age 65 and 100-300 deaths in children under 5(2, 11). Current FDA approved prophylactic strategies include two monoclonal antibodies, palivizumab (Synagis) and nirsevimab (Beyfortus), and three vaccines, Abrysvo (Pfizer), Arexvy (GSK), and mRESVIA (Moderna); all of which target only one of two major surface glycoproteins required by RSV for efficient infectivity(12-15). While these prophylactics are effective at reducing severe lower respiratory symptoms, upper respiratory infection is still prevalent and compounded by co-infection with other respiratory disease such as SARS-CoV2(16-19). Additionally, even mild upper respiratory symptoms contribute towards RSV shedding and transmission especially when considering the general proximity of vulnerable populations localized in hospital settings(20).

RSV is a filamentous, enveloped, negative sense, single stranded RNA virus with a 15 kilobase genome coding for 11 proteins(21). It belongs to the pneumoviridae family of viruses which rely on their G and F glycoproteins to mediate attachment and fusion, respectively, to airway epithelial cells(21, 22). RSV F is a type I integral membrane protein and it facilitates fusion between the viral envelope and the host cell plasma membrane by undergoing a series of conformational changes taking it from a pre-fusion to a post-fusion state(22-24). Antibodies that target the pre-fusion state of RSV F are highly correlated to lower disease severity, in fact, Nirsevimab, Abryso, Arexvy and mRESVIA were all designed to target antigenic sites Ø and V which are only accessible in this conformation(25-27). These prophylactics, which debuted after over 60 years since RSV was first isolated, have overcome challenges that dozens of other candidates have failed to achieve in clinical trials: eliciting robust correlates of protection against RSV, lengthening the window of protection, and maintaining protection across RSV A and RSV B strains(14, 28-31). These elements confer significant reduction of at least two or three symptoms of severe lower respiratory symptoms and are available for the elderly (Arexvy, Abrysvo, mRESVIA), pregnant mothers (Abrysvo), and infants (Nirsevimab)(13, 32, 33). These efficacy endpoints were met in 50.3-75.7% of infants (Abrysvo and Nirsevimab), leaving behind an unmet need for one-half to one-fourth of remaining infants experiencing severe lower respiratory symptoms(34, 35). Additionally, upper respiratory infection and acute RSV disease (defined as onset of at least 10 days, decreased appetite, wheezing, shortness of breath, and sporadic cessation of breathing

for more than 10 seconds) were not included as efficacy endpoints in Nirsevimab and Abrysvo clinical trials(34-36). These symptoms are problematic because they serve as avenues for transmission, disrupt infant health and childcare(37-40). Additionally, the correlation between early childhood RSV infection to developing asthma later in life implies that reducing symptoms of RSV alone is only the first step towards addressing the apparent two-part pathogenic process: short-term infection and long-term destabilization of host immunity(39, 40).

The RSV F glycoprotein has historically been the focal point for RSV prophylactic and therapeutic studies in part due to its high sequence conservation between RSV A and RSV B subtypes, however, known variability localized in sites V and O serve as a platform for the generation of escape mutants(24, 41, 42). This limitation materialized during a phase 3 clinical trial for Suptavumab, an anti-preF neutralizing antibody that failed to meet its efficacy endpoint due to the emergence of an RSV B strain yielding two key mutations in its binding epitope(30, 43). Nirsevimab, Arexvy, and Abrysvo were all designed to target sites Ø or V and, unlike palivizumab, are intended for broad use among the patient population, escalating selective pressure against RSV F for the first time(14, 44). Escape mutations to Nirsevimab have already been identified in circulation, albeit in low abundance(45). Nevertheless, these escape mutants do not restrict viral fitness *in vitro*, making it possible for one to emerge as the dominant strain in the future(46).

To achieve sterilizing immunity or improve the protective breadth of prophylactics that are currently available, it is important to consider all correlates of

protection which not only target RSV F, but RSV G as well(27, 47). Antibodies that target RSV G are correlated to lower disease severity even while being present at $1/30^{th}$ the abundance of those that target the pre-fusion conformation of RSV F(27). This observation aligns well with RSV G's significant role during infection: using recombinant RSV VLP's expressing a C-terminally truncated G glycoprotein or removing it altogether severely decreases viral entry in primary human airway epithelial cells(48-50). Additionally, it is well understood that apart from RSV G's role in attachment, it can also modulate host immunity characterized by a dampened Th1/favored Th2 cytokine profile. Considering RSV G's role in viral entry and modulation of host immunity, it is a lucrative target for the development of improved, well-rounded prophylactic strategies that could be used alone and/or in combination with those that target RSV F.

RSV G has historically been held back as a vaccine immunogen compared to RSV F. This is largely due to its connection to the first attempt to develop an RSV vaccine in the 1960's. Patients who received a formalin inactivated whole RSV vaccine and subsequently acquired natural RSV infections experienced unusually severe respiratory symptoms as opposed to protection and was fatal in two cases(51). Similar vaccine enhanced respiratory symptoms were reproduced in mice vaccinated with RSV G purified from cell lysates, resulting in a paucity of studies involving G as a target for prophylaxis(52). However, investigation into the pathogenesis concomitant to vaccine-enhanced disease, specifically type 2 cytokines and pulmonary eosinophilia, between FI-RSV and recombinant RSV with G gene

deletions showed similar infection profiles and served to uncouple RSV G from vaccine enhanced respiratory disease observed in the 1960's(53, 54). Since then, research groups have focused on understanding RSV G's precise role during infection to inform safe vaccine strategies.

Studies have suggested a role for RSV G in the dampened Th1/favored Th2 cytokine profile during RSV infection. The presence of a methionine at position 48 functions as a secondary translation initiation site producing a truncated version of RSV G that lacks the signal peptide for membrane trafficking, resulting in its secretion into the extracellular matrix(22). It has been proposed that the membrane bound version of RSV G (Gm) carries out attachment while the soluble version (Gs) is what predominantly mediates the apparent deleterious immune response(55). RSV G is composed of ~300 amino acids, most of which are highly glycosylated and highly variable across RSV strains. These regions can be divided into two mucin-like domains flanking a 40 amino acid region known as the central conserved domain (CCD) (Fig1a). The central conserved domain contains four cysteines in a CX3C configuration which all together form two disulfide bonds. It is thought that this structural motif competes with CX3CL1 (the endogenous ligand, fractalkine) for binding to CX3CR1 to potentiate disease. CX3CR1 is expressed on a myriad of innate and adaptive immune cells including neonatal B-cells, pDCs, CD8+ T-cells, eosinophils, neutrophils, and CD4+ memory T-cells. RSV G operates antagonistically to Fractalkine, diminishing host antiviral immune responses by impeding activation of cytotoxic T-cells, reducing IFN levels, trafficking eosinophils and neutrophils into

the lung, and stimulating the production of type Π cytokines(56-61). RSV G might also have an aberrant downstream effect with its interaction with TLR-4 which results in lower levels of type I interferons thereby suppressing the antiviral activity of ISG15, a clinical marker for increased disease severity in infants(62-65). Additionally, the CCD is recognized by a special subset of T-cells bearing use of the $V\beta14^{+}$ gene resulting in type Π cytokine release that mediates migration of eosinophils into the lung(66). These properties of RSV G allow RSV to evade the antiviral immune response altogether while potentiating disease characterized by an unbalanced Th1/Th2 cytokine profile and substantial pulmonary inflammation.

Together, these studies suggest that RSV G plays a unique and complex role in pathogenesis involving both attachment and modulation of host immunity which might explain why antibodies targeting this protein are a strong correlate for lower disease severity(27, 47). Anti-RSV G antibodies impede viral replication through direct neutralization *in vitro* using primary human airway and bronchial epithelial cells. They also mediate opsonization, antibody dependent cellular cytotoxicity (ADCC), and antibody dependent cellular phagocytosis (ADCP) to promote viral clearance and mitigate RSV G's deleterious immune response(49, 50, 67, 68). Using PBMC's, A549 cells, and a two-chamber transwell *in-vitro* system, anti-G antibodies were found to restore type I and 3 IFN levels that are normally suppressed by RSV G-CX3CR1 interactions(61). Moreover, they work prophylactically and therapeutically to restore the Th1/Th2 cytokine profile, decrease mucus production blocking the airways, and relieve pulmonary inflammation *in vivo* using mouse and cotton rat

models(67, 69-72). Finally, among a panel of twelve protective and broadly reactive antibodies isolated from RSV experienced individuals is mAb 3D3. It has demonstrated 100-fold higher efficiency than palivizumab (Synagis), a commercially available anti-F monoclonal antibody, in clearing RSV infection in mice and is currently undergoing pre-clinical trial evaluation(72). Despite the potential and logic behind targeting RSV G with prophylactic and therapeutic strategies, there are no FDA approved RSV G-based vaccines or anti-G monoclonal antibodies commercially available at this time.

A clear obstacle towards an RSV G-based vaccine is strategically removing its aberrant interaction with CX3CR1 while maintaining its immunogenicity. Using protein x-ray crystallography and linear epitope mapping, work from multiple groups found that broadly-reactive and protective mAbs bind distinct conformational epitopes on the CCD(67, 68, 73, 74). One group used three of these structures to generate a blueprint for teasing apart amino acids that make up important epitopes and amino acids that can be modified to abrogate CX3CR1 binding and were used in structure guided mutagenesis to rationally produce an S177Q mutant in the RSV G CCD(75). Importantly, a recombinant RSV G construct bearing the proposed S177Q mutant was used to vaccinate mice and results from this study revealed higher IgG2a titers, a well characterized marker for a Th1 type response(76). This study was important because it showed for the first time that a vaccine using RSV G could be modified to mitigate the effects is has upon binding to CX3CR1 *in vivo*. This mutant was subsequently included in multimerized vaccine designs to improve the apparent

low immunogenicity observed in vaccine studies using monomeric RSV G(77). While results from this study showed increased anti-RSV G IgG titers, the Th1/Th2 cytokine profile resembled that of a natural infection despite the presence of the S177Q mutant(77). Additionally, IgG titers between the S177Q CCD bearing nanoparticles and previously obtained data vaccinating with monomeric RSV G were not markedly different(76, 77). Of note, these nanoparticles were insoluble, likely due to the inherent hydrophobicity of the CCD itself with nearly half of its amino acids being non-polar(77). Whether this construct is incompatible with the nanoparticle platform to elicit a more balanced Th1/Th2 response or if the S177Q mutant needs further investigation is unclear. In a newer study, the nanoparticle platform was altered to include glycosylation sites between each CCD at the protomer interface to prevent aggregation(78). Another strategy used in this paper was to include a negatively charged linker (made from fusing negatively charged amino acids to the N- or C-terminus of the CCD) to add a repulsive charge between neighboring CCD's(78). Results from this study showed greatly improved solubility and induction of IgG titers. A limitation from this study is that markers of immune modulation (cytokine and IgG subclass profiling) were not assessed and mutants designed to abrogate CX3CR1 binding were not investigated. Additionally, characterization of mAb binding to RSV G CCD bearing nanoparticles were not included, an experiment that might help assess disulfide bridge dependent conformational epitopes. However, these preliminary studies serve as a proof-of-principle to address long-standing issues preventing RSV G based vaccines from entering human clinical trials. Until all safety,

immunogenicity, and solubility issues are met in one cohesive solution for RSV G based vaccines, they might require further optimization and innovative design.

4.2 References

1. Lozano R, Naghavi M, Foreman K, Lim S, Shibuya K, Aboyans V, et al. Global and regional mortality from 235 causes of death for 20 age groups in 1990 and 2010: a systematic analysis for the Global Burden of Disease Study 2010. Lancet. 2012;380(9859):2095-128.
2. Shi T, McAllister DA, O'Brien KL, Simoes EAF, Madhi SA, Gessner BD, et al. Global, regional, and national disease burden estimates of acute lower respiratory infections due to respiratory syncytial virus in young children in 2015: a systematic review and modelling study. Lancet. 2017;390(10098):946-58.
3. Glezen WP, Taber LH, Frank AL, Kasel JA. Risk of primary infection and reinfection with respiratory syncytial virus. Am J Dis Child. 1986;140(6):543-6.
4. Shi T, Balsells E, Wastnedge E, Singleton R, Rasmussen ZA, Zar HJ, et al. Risk factors for respiratory syncytial virus associated with acute lower respiratory infection in children under five years: Systematic review and meta-analysis. J Glob Health. 2015;5(2):020416.
5. Wheeler SM, Dotters-Katz S, Heine RP, Grotegut CA, Swamy GK. Maternal Effects of Respiratory Syncytial Virus Infection during Pregnancy. Emerg Infect Dis. 2015;21(11):1951-5.
6. Branche AR, Falsey AR. Respiratory syncytial virus infection in older adults: an under-recognized problem. Drugs Aging. 2015;32(4):261-9.
7. Falsey AR, Hennessey PA, Formica MA, Cox C, Walsh EE. Respiratory syncytial virus infection in elderly and high-risk adults. N Engl J Med. 2005;352(17):1749-59.
8. Falsey AR, Walsh EE. Respiratory syncytial virus infection in elderly adults. Drugs Aging. 2005;22(7):577-87.
9. Widmer K, Griffin MR, Zhu Y, Williams JV, Talbot HK. Respiratory syncytial virus- and human metapneumovirus-associated emergency department and hospital burden in adults. Influenza Other Respir Viruses. 2014;8(3):347-52.
10. McLaughlin JM, Khan F, Begier E, Swerdlow DL, Jodar L, Falsey AR. Rates of Medically Attended RSV Among US Adults: A Systematic Review and Meta-analysis. Open Forum Infect Dis. 2022;9(7):ofac300.
11. Matias G, Taylor R, Haguinet F, Schuck-Paim C, Lustig R, Shinde V. Estimates of mortality attributable to influenza and RSV in the United States during 1997-2009 by influenza type or subtype, age, cause of death, and risk status. Influenza Other Respir Viruses. 2014;8(5):507-15.
12. Palivizumab, a Humanized Respiratory Syncytial Virus Monoclonal Antibody, Reduces Hospitalization From Respiratory Syncytial Virus Infection in High-risk Infants. Pediatrics. 1998;102(3):531-7.

13. Griffin MP, Yuan Y, Takas T, Domachowske JB, Madhi SA, Manzoni P, et al. Single-Dose Nirsevimab for Prevention of RSV in Preterm Infants. N Engl J Med. 2020;383(5):415-25.
14. Topalidou X, Kalergis AM, Papazisis G. Respiratory Syncytial Virus Vaccines: A Review of the Candidates and the Approved Vaccines. Pathogens. 2023;12(10).
15. Wilson E, Goswami J, Baqui AH, Doreski PA, Perez-Marc G, Zaman K, et al. Efficacy and Safety of an mRNA-Based RSV PreF Vaccine in Older Adults. N Engl J Med. 2023;389(24):2233-44.
16. Resch B. Product review on the monoclonal antibody palivizumab for prevention of respiratory syncytial virus infection. Hum Vaccin Immunother. 2017;13(9):2138-49.
17. Olchanski N, Hansen RN, Pope E, D'Cruz B, Fergie J, Goldstein M, et al. Palivizumab Prophylaxis for Respiratory Syncytial Virus: Examining the Evidence Around Value. Open Forum Infect Dis. 2018;5(3):ofy031.
18. Suss RJ, Simoes EAF. Respiratory Syncytial Virus Hospital-Based Burden of Disease in Children Younger Than 5 Years, 2015-2022. JAMA Netw Open. 2024;7(4):e247125.
19. McMorrow ML, Moline HL, Toepfer AP, Halasa NB, Schuster JE, Staat MA, et al. Respiratory Syncytial Virus-Associated Hospitalizations in Children <5 Years: 2016-2022. Pediatrics. 2024.
20. Walsh EE, Peterson DR, Kalkanoglu AE, Lee FE, Falsey AR. Viral shedding and immune responses to respiratory syncytial virus infection in older adults. J Infect Dis. 2013;207(9):1424-32.
21. Battles MB, McLellan JS. Respiratory syncytial virus entry and how to block it. Nat Rev Microbiol. 2019;17(4):233-45.
22. McLellan JS, Ray WC, Peeples ME. Structure and function of respiratory syncytial virus surface glycoproteins. Curr Top Microbiol Immunol. 2013;372:83-104.
23. McLellan JS, Chen M, Joyce MG, Sastry M, Stewart-Jones GB, Yang Y, et al. Structure-based design of a fusion glycoprotein vaccine for respiratory syncytial virus. Science. 2013;342(6158):592-8.
24. McLellan JS, Chen M, Leung S, Graepel KW, Du X, Yang Y, et al. Structure of RSV fusion glycoprotein trimer bound to a prefusion-specific neutralizing antibody. Science. 2013;340(6136):1113-7.
25. Walsh EE, Wang L, Falsey AR, Qiu X, Corbett A, Holden-Wiltse J, et al. Virus-Specific Antibody, Viral Load, and Disease Severity in Respiratory Syncytial Virus Infection. J Infect Dis. 2018;218(2):208-17.
26. Graham BS, Modjarrad K, McLellan JS. Novel antigens for RSV vaccines. Curr Opin Immunol. 2015;35:30-8.
27. Capella C, Chaiwatpongsakorn S, Gorrell E, Risch ZA, Ye F, Mertz SE, et al. Prefusion F, Postfusion F, G Antibodies, and Disease Severity in Infants and Young Children With Acute Respiratory Syncytial Virus Infection. J Infect Dis. 2017;216(11):1398-406.

28. Ruckwardt TJ. The road to approved vaccines for respiratory syncytial virus. NPJ Vaccines. 2023;8(1):138.
29. Jorgensen SCJ. Nirsevimab: review of pharmacology, antiviral activity and emerging clinical experience for respiratory syncytial virus infection in infants. J Antimicrob Chemother. 2023;78(5):1143-9.
30. Simoes EAF, Forleo-Neto E, Geba GP, Kamal M, Yang F, Cicirello H, et al. Suptavumab for the Prevention of Medically Attended Respiratory Syncytial Virus Infection in Preterm Infants. Clin Infect Dis. 2021;73(11):e4400-e8.
31. Domachowske JB, Chang Y, Atanasova V, Cabanas F, Furuno K, Nguyen KA, et al. Safety of Re-dosing Nirsevimab Prior to RSV Season 2 in Children With Heart or Lung Disease. J Pediatric Infect Dis Soc. 2023;12(8):477-80.
32. Rasmussen SA, Jamieson DJ. Maternal RSV Vaccine - Weighing Benefits and Risks. N Engl J Med. 2024;390(11):1050-1.
33. Papi A, Ison MG, Langley JM, Lee DG, Leroux-Roels I, Martinon-Torres F, et al. Respiratory Syncytial Virus Prefusion F Protein Vaccine in Older Adults. N Engl J Med. 2023;388(7):595-608.
34. Fleming-Dutra KE, Jones JM, Roper LE, Prill MM, Ortega-Sanchez IR, Moulia DL, et al. Use of the Pfizer Respiratory Syncytial Virus Vaccine During Pregnancy for the Prevention of Respiratory Syncytial Virus-Associated Lower Respiratory Tract Disease in Infants: Recommendations of the Advisory Committee on Immunization Practices - United States, 2023. MMWR Morb Mortal Wkly Rep. 2023;72(41):1115-22.
35. Drysdale SB, Cathie K, Flamein F, Knuf M, Collins AM, Hill HC, et al. Nirsevimab for Prevention of Hospitalizations Due to RSV in Infants. N Engl J Med. 2023;389(26):2425-35.
36. Kampmann B, Madhi SA, Munjal I, Simoes EAF, Pahud BA, Llapur C, et al. Bivalent Prefusion F Vaccine in Pregnancy to Prevent RSV Illness in Infants. N Engl J Med. 2023;388(16):1451-64.
37. Chu HY, Kuypers J, Renaud C, Wald A, Martin E, Fairchok M, et al. Molecular epidemiology of respiratory syncytial virus transmission in childcare. J Clin Virol. 2013;57(4):343-50.
38. Wahl I, Wardemann H. Sterilizing immunity: Understanding COVID-19. Immunity. 2022;55(12):2231-5.
39. Sigurs N, Gustafsson PM, Bjarnason R, Lundberg F, Schmidt S, Sigurbergsson F, Kjellman B. Severe respiratory syncytial virus bronchiolitis in infancy and asthma and allergy at age 13. Am J Respir Crit Care Med. 2005;171(2):137-41.
40. Stein RT, Sherrill D, Morgan WJ, Holberg CJ, Halonen M, Taussig LM, et al. Respiratory syncytial virus in early life and risk of wheeze and allergy by age 13 years. Lancet. 1999;354(9178):541-5.
41. Hause AM, Henke DM, Avadhanula V, Shaw CA, Tapia LI, Piedra PA. Sequence variability of the respiratory syncytial virus (RSV) fusion gene among contemporary and historical genotypes of RSV/A and RSV/B. PLoS One. 2017;12(4):e0175792.

42. Mas V, Nair H, Campbell H, Melero JA, Williams TC. Antigenic and sequence variability of the human respiratory syncytial virus F glycoprotein compared to related viruses in a comprehensive dataset. Vaccine. 2018;36(45):6660-73.
43. Langedijk AC, Harding ER, Konya B, Vrancken B, Lebbink RJ, Evers A, et al. A systematic review on global RSV genetic data: Identification of knowledge gaps. Rev Med Virol. 2022;32(3):e2284.
44. Rogovik AL, Carleton B, Solimano A, Goldman RD. Palivizumab for the prevention of respiratory syncytial virus infection. Can Fam Physician. 2010;56(8):769-72.
45. Wilkins D, Langedijk AC, Lebbink RJ, Morehouse C, Abram ME, Ahani B, et al. Nirsevimab binding-site conservation in respiratory syncytial virus fusion glycoprotein worldwide between 1956 and 2021: an analysis of observational study sequencing data. Lancet Infect Dis. 2023;23(7):856-66.
46. Zhu Q, Lu B, McTamney P, Palaszynski S, Diallo S, Ren K, et al. Prevalence and Significance of Substitutions in the Fusion Protein of Respiratory Syncytial Virus Resulting in Neutralization Escape From Antibody MEDI8897. J Infect Dis. 2018;218(4):572-80.
47. Nziza N, Jung W, Mendu M, Chen T, Julg B, Graham B, et al. Longitudinal humoral analysis in RSV-infected infants identifies pre-existing RSV strain-specific G and evolving cross-reactive F antibodies. Immunity. 2024.
48. Chirkova T, Lin S, Oomens AGP, Gaston KA, Boyoglu-Barnum S, Meng J, et al. CX3CR1 is an important surface molecule for respiratory syncytial virus infection in human airway epithelial cells. J Gen Virol. 2015;96(9):2543-56.
49. Jeong KI, Piepenhagen PA, Kishko M, DiNapoli JM, Groppo RP, Zhang L, et al. CX3CR1 Is Expressed in Differentiated Human Ciliated Airway Cells and Co-Localizes with Respiratory Syncytial Virus on Cilia in a G Protein-Dependent Manner. PLoS One. 2015;10(6):e0130517.
50. Johnson SM, McNally BA, Ioannidis I, Flano E, Teng MN, Oomens AG, et al. Respiratory Syncytial Virus Uses CX3CR1 as a Receptor on Primary Human Airway Epithelial Cultures. PLoS Pathog. 2015;11(12):e1005318.
51. Kim HW, Canchola JG, Brandt CD, Pyles G, Chanock RM, Jensen K, Parrott RH. Respiratory syncytial virus disease in infants despite prior administration of antigenic inactivated vaccine. Am J Epidemiol. 1969;89(4):422-34.
52. Hancock GE, Speelman DJ, Heers K, Bortell E, Smith J, Cosco C. Generation of atypical pulmonary inflammatory responses in BALB/c mice after immunization with the native attachment (G) glycoprotein of respiratory syncytial virus. J Virol. 1996;70(11):7783-91.
53. Johnson TR, Teng MN, Collins PL, Graham BS. Respiratory syncytial virus (RSV) G glycoprotein is not necessary for vaccine-enhanced disease induced by immunization with formalin-inactivated RSV. J Virol. 2004;78(11):6024-32.
54. Johnson TR, Varga SM, Braciale TJ, Graham BS. Vbeta14(+) T cells mediate the vaccine-enhanced disease induced by immunization with respiratory syncytial

virus (RSV) G glycoprotein but not with formalin-inactivated RSV. J Virol. 2004;78(16):8753-60.
55. Johnson TR, Johnson JE, Roberts SR, Wertz GW, Parker RA, Graham BS. Priming with secreted glycoprotein G of respiratory syncytial virus (RSV) augments interleukin-5 production and tissue eosinophilia after RSV challenge. J Virol. 1998;72(4):2871-80.
56. Imai T, Hieshima K, Haskell C, Baba M, Nagira M, Nishimura M, et al. Identification and molecular characterization of fractalkine receptor CX3CR1, which mediates both leukocyte migration and adhesion. Cell. 1997;91(4):521-30.
57. Harcourt J, Alvarez R, Jones LP, Henderson C, Anderson LJ, Tripp RA. Respiratory syncytial virus G protein and G protein CX3C motif adversely affect CX3CR1+ T cell responses. J Immunol. 2006;176(3):1600-8.
58. Zhivaki D, Lemoine S, Lim A, Morva A, Vidalain PO, Schandene L, et al. Respiratory Syncytial Virus Infects Regulatory B Cells in Human Neonates via Chemokine Receptor CX3CR1 and Promotes Lung Disease Severity. Immunity. 2017;46(2):301-14.
59. Hussell T, Openshaw PJ. Intracellular IFN-gamma expression in natural killer cells precedes lung CD8+ T cell recruitment during respiratory syncytial virus infection. J Gen Virol. 1998;79 (Pt 11):2593-601.
60. Bergeron HC, Kauvar LM, Tripp RA. Anti-G protein antibodies targeting the RSV G protein CX3C chemokine region improve the interferon response. Ther Adv Infect Dis. 2023;10:20499361231161157.
61. Chirkova T, Boyoglu-Barnum S, Gaston KA, Malik FM, Trau SP, Oomens AG, Anderson LJ. Respiratory syncytial virus G protein CX3C motif impairs human airway epithelial and immune cell responses. J Virol. 2013;87(24):13466-79.
62. Oshansky CM, Krunkosky TM, Barber J, Jones LP, Tripp RA. Respiratory syncytial virus proteins modulate suppressors of cytokine signaling 1 and 3 and the type I interferon response to infection by a toll-like receptor pathway. Viral Immunol. 2009;22(3):147-61.
63. Shingai M, Azuma M, Ebihara T, Sasai M, Funami K, Ayata M, et al. Soluble G protein of respiratory syncytial virus inhibits Toll-like receptor 3/4-mediated IFN-beta induction. Int Immunol. 2008;20(9):1169-80.
64. Heinonen S, Velazquez VM, Ye F, Mertz S, Acero-Bedoya S, Smith B, et al. Immune profiles provide insights into respiratory syncytial virus disease severity in young children. Sci Transl Med. 2020;12(540).
65. Thwaites RS, Coates M, Ito K, Ghazaly M, Feather C, Abdulla F, et al. Reduced Nasal Viral Load and IFN Responses in Infants with Respiratory Syncytial Virus Bronchiolitis and Respiratory Failure. Am J Respir Crit Care Med. 2018;198(8):1074-84.
66. Varga SM, Wang X, Welsh RM, Braciale TJ. Immunopathology in RSV infection is mediated by a discrete oligoclonal subset of antigen-specific CD4(+) T cells. Immunity. 2001;15(4):637-46.

67. Jones HG, Ritschel T, Pascual G, Brakenhoff JPJ, Keogh E, Furmanova-Hollenstein P, et al. Structural basis for recognition of the central conserved region of RSV G by neutralizing human antibodies. PLoS Pathog. 2018;14(3):e1006935.
68. Cortjens B, Yasuda E, Yu X, Wagner K, Claassen YB, Bakker AQ, et al. Broadly Reactive Anti-Respiratory Syncytial Virus G Antibodies from Exposed Individuals Effectively Inhibit Infection of Primary Airway Epithelial Cells. J Virol. 2017;91(10).
69. Boyoglu-Barnum S, Chirkova T, Todd SO, Barnum TR, Gaston KA, Jorquera P, et al. Prophylaxis with a respiratory syncytial virus (RSV) anti-G protein monoclonal antibody shifts the adaptive immune response to RSV rA2-line19F infection from Th2 to Th1 in BALB/c mice. J Virol. 2014;88(18):10569-83.
70. Boyoglu-Barnum S, Gaston KA, Todd SO, Boyoglu C, Chirkova T, Barnum TR, et al. A respiratory syncytial virus (RSV) anti-G protein F(ab')2 monoclonal antibody suppresses mucous production and breathing effort in RSV rA2-line19F-infected BALB/c mice. J Virol. 2013;87(20):10955-67.
71. Caidi H, Miao C, Thornburg NJ, Tripp RA, Anderson LJ, Haynes LM. Anti-respiratory syncytial virus (RSV) G monoclonal antibodies reduce lung inflammation and viral lung titers when delivered therapeutically in a BALB/c mouse model. Antiviral Res. 2018;154:149-57.
72. Collarini EJ, Lee FE, Foord O, Park M, Sperinde G, Wu H, et al. Potent high-affinity antibodies for treatment and prophylaxis of respiratory syncytial virus derived from B cells of infected patients. J Immunol. 2009;183(10):6338-45.
73. Fedechkin SO, George NL, Wolff JT, Kauvar LM, DuBois RM. Structures of respiratory syncytial virus G antigen bound to broadly neutralizing antibodies. Sci Immunol. 2018;3(21).
74. Fedechkin SO, George NL, Nunez Castrejon AM, Dillen JR, Kauvar LM, DuBois RM. Conformational Flexibility in Respiratory Syncytial Virus G Neutralizing Epitopes. J Virol. 2020;94(6).
75. Nunez Castrejon AM, O'Rourke SM, Kauvar LM, DuBois RM. Structure-Based Design and Antigenic Validation of Respiratory Syncytial Virus G Immunogens. J Virol. 2022;96(7):e0220121.
76. Bergeron HC, Murray J, Nunez Castrejon AM, DuBois RM, Tripp RA. Respiratory Syncytial Virus (RSV) G Protein Vaccines With Central Conserved Domain Mutations Induce CX3C-CX3CR1 Blocking Antibodies. Viruses. 2021;13(2).
77. Bergeron HC, Murray J, Juarez MG, Nangle SJ, DuBois RM, Tripp RA. Immunogenicity and protective efficacy of an RSV G S177Q central conserved domain nanoparticle vaccine. Front Immunol. 2023;14:1215323.
78. Voorzaat R, Cox F, van Overveld D, Le L, Tettero L, Vaneman J, et al. Design and Preclinical Evaluation of a Nanoparticle Vaccine against Respiratory Syncytial Virus Based on the Attachment Protein G. Vaccines (Basel). 2024;12(3).

Appendix 1 Crystal hits that yielded datasets for deposited structures

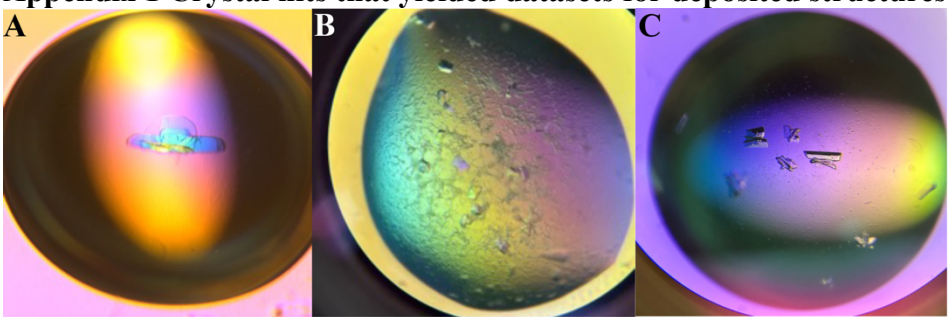

Figure 5.1 Pictures of Crystal Hits

(A) Fab 1G1-RSV G CCD (B) Fab 1G8-RSV G CCD (C) Fab 2B11-RSV G CCD.